Titre: Title:	Étude de l'interface béton-composite pour un composite laminé directement sur le béton
Auteur: Author:	Katayoun Soulati
Date:	2001
Type:	Mémoire ou thèse / Dissertation or Thesis
Référence: Citation:	Soulati, K. (2001). Étude de l'interface béton-composite pour un composite laminé directement sur le béton [Ph.D. thesis, École Polytechnique de Montréal]. PolyPublie. https://publications.polymtl.ca/7071/

UNIVERSITÉ DE MONTRÉAL

ÉTUDE DE L'INTERFACE BÉTON-COMPOSITE POUR UN COMPOSITE LAMINÉ DIRECTEMENT SUR LE BÉTON

KATAYOUN SOULATI

DÉPARTEMENT DE GÉNIE MÉCANIQUE

ÉCOLE POLYTECHNIQUE DE MONTRÉAL

THÈSE PRÉSENTÉE EN VUE DE L'OBTENTION

DU DIPLÔME DE PHILOSOPHIAE DOCTOR

(GÉNIE MÉCANIQUE)

DÉCEMBRE 2001

UNIVERSITÉ DE MONTRÉAL

ÉCOLE POLYTECHNIQUE DE MONTRÉAL

Cette thèse intitulée :

ÉTUDE DE L'INTERFACE BÉTON-COMPOSITE POUR UN COMPOSITE LAMINÉ DIRECTEMENT SUR LE BÉTON

Présentée par : SOULATI Katayoun

en vue de l'obtention du diplôme de : Philosophiae Doctor

a été dûment acceptée par le jury d'examen constitué de :

B. Fisa, Ph.D., président
R. Gauvin, D.Sc. A., membre et directeur de recherche
B. Massicotte, Ph.D., membre
B. Benmokrane, Ph.D., membre

À mon fils Sam,

qui m'a donné le courage de tenir bon jusqu'à la fin.

J'espère que tu auras toi aussi le courage et la persérvérance d'aller

jusqu'au bout de tes rêves.

REMERCIEMENTS

Je tiens à remercier mon directeur, monsieur Raymond Gauvin, pour la confiance qu'il m'a accordée, le support et les conseils qu'il m'a donnés et pour son appui financier. Les connaissances et l'expérience que j'ai acquises en sa compagnie me seront un atout précieux.

Je tiens à remercier les professeurs du département de génie mécanique à l'École Polytechnique, madame Marie Bernard et messieurs Bo Fisa, François Trochu, Bernard Sanschagrin, Rachid Boukhili et aussi les professeurs Bruno Massicotte et Richard Roux de département de génies civil, géologique et des mines.

Je remercie le personnel du laboratoire de Structure du département de génie civil à l'École Polytechnique ainsi que monsieur Mario Desroche, de Sika Canada, pour le support technique qu'ils m'ont donné.

Mes remerciement s'adressent également à tous les membres du CRASP ainsi qu'au personnel du département de génie mécanique. Je pense également à tous mes collègues qui ont étudié avec moi, qui m'ont permis d'évoluer dans un milieu stimulant et multiculturel. Ils m'ont beaucoup appris.

Je remercie Renée Bourgeois pour son amitié dans les moments essentiels et le support qu'elle m'a donné pour compléter ce travail.

Finalement, je tiens à remercier tout particulièrement mes parents qui m'ont donné le support et le courage de poursuivre mes études jusqu'à la fin. Malgré la distance, ils ont toujours été là quand j'avais besoin d'eux et je m'estime extrêmement chanceuse. Je pense également aux membres de ma famille, sans exception, qui m'ont toujours supportée. Je les remercie.

RÉSUMÉ

Des matériaux composites sont collés à la surface en flexion de poutres en béton armé pour les renforcer et les raidir. Quand la poutre renforcée est conçue pour la flexion, on s'attend à ce que sa rupture se produise par rupture en compression du béton dans la zone de compression ou la rupture en traction du composite sur la partie composée, ainsi que l'écoulement interne de l'acier. En pratique, cependant, dans la majorité des cas, il a été observé que les poutres renforcées par cette méthode rompent par le délaminage du composite de la surface de béton avant l'atteinte de la capacité uniaxiale de conception. Le mode de rupture de délaminage est théoriquement imprévisible. À cause de sa nature fragile, il devrait être prévu.

Le but principal de cette recherche est une meilleure compréhension du mode de rupture par délaminage en mettant l'emphase sur l'effet des propriétés des matériaux composites sur le comportement structurel complet et le comportement du lien béton-composite. La recherche est divisée en deux sections. La première comporte des essais structurels et l'analyse de poutres en béton armé renforcées par un composite et la deuxième partie se concentre sur les propriétés d'interfaces béton-composite. Cette thèse est principalement de nature expérimentale, le but étant d'améliorer la compréhension de l'effet des matériaux composites et de concevoir des poutres renforcées pour prévenir le mode de rupture par délaminage par le choix approprié du composite.

Dans le chapitre 3, nous examinons la résistance et le mode de rupture de poutres en béton armé renforcées avec des couches verre/époxy et carbone/époxy laminées, directement sur la surface de la poutre. Les poutres sont chargées en flexion quatre points. La position du chargement et l'épaisseur du composite sont variées pour les poutres renforcées avec carbone/époxy. Les résultats expérimentaux montrent que la rigidité et la résistance des poutres sont augmentées en utilisant le composite comme renfort externe. Ils montrent aussi que la force et le mode de rupture des poutres hybrides dépendent du type de matériaux composites et de sa quantité. Il a été trouvé que la poutre renforcée par carbone/époxy se brise par délaminage de composite. La rigidité du composite a une influence importante sur la résistance de la poutre renforcée et le mode de rupture. La position à laquelle le délaminage arrive dépend de la quantité du composite utilisée et de l'état de contraintes à l'interface.

Le chapitre 4 examine le comportement en flexion des poutres de béton armé endommagées, renforcées extérieurement avec un matériau composite laminé directement sur le côté en traction des poutres. Dans le programme expérimental, les essais ont été effectués sur neuf poutres. Certaines des poutres ont été rechargées à 30% et 60 % de leur résistance ultime avant l'application du composite verre/époxy et carbon/époxy. Le comportement des poutres est étudié et comparé en termes du patron de fissuration du béton, des déformations, du seuil de plastification de l'acier et de la charge limite. Les poutres pré-chargées, quand renforcées par des composites, ont montré plus de déformation à une capacité d'absorption d'énergie de déformation plus

haute en comparaison aux poutres non endommagées. Les matériaux composites avaient peu d'effet sur l'initiation de fissures de flexion dans le béton, mais ils ont vraiment fourni une résistance tant à la propagation qu'à l'ouverture des fissures. Quand le composite est collé sur la surface de béton en traction, nous pouvons profiter de la rigidité de flexion supplémentaire fournie par le béton en traction et la rigidité de flexion supplémentaire fournie par le béton entre les fissures. Malgré la grande fissuration avant l'application du composite, la poutre réparée a préservé son intégrité structurelle, confirmant l'efficacité de cette technique de réparation. Nous avons observé que le mode de rupture par délaminage peut commencer au bout d'une fissure de flexion présente à l'interface béton-composite.

Pour comprendre le mécanisme de délaminage, l'étude du comportement de l'interface composite-béton est réalisée sous plusieurs modes de chargement dans le chapitre 5. La méthodologie analytique-expérimentale combinée présentée dans ce chapitre représente une application de la mécanique de la rupture pour concevoir deux spécimens de sandwich pour la caractérisation de l'interface béton-composite. Ces spécimens, un spécimen de disque sandwich Brésilien et un spécimen de poutre en flexion pur, contiennent une couche mince de composite serré entre deux pièces de béton. Le spécimen de poutre est utilisé pour réaliser le mode I d'ouverture de fissure alors que le spécimen de disque Brésilien est chargé sous plusieurs angles de chargement pour obtenir différentes proportions de mode I et mode II d'ouverture de

fissure. Cette approche nous a permis d'obtenir la ténacité de l'interface béton-composite en fonction du module d'élasticité du composite et du béton.

Finalement, le chapitre 6 examine l'effet des propriétés mécaniques du composite sur la résistance de l'interface béton-composite. Le spécimen de disque Brésilien et le spécimen de poutre proposé dans le chapitre précédent sont utilisés pour obtenir les courbes de ténacité de l'interface béton-verre/époxy et l'interface béton-carbone/époxy.

Les résultats d'essais montrent que la résistance de l'interface dépend des propriétés mécanique du composite et de l'angle de chargement. Pour le même béton et le même angle de chargement, la ténacité de l'interface est différente pour les deux composites, ceci indique que la fissure d'interface est affectée par les propriétés mécaniques du composite et confirme l'efficacité des spécimens sandwichs pour évaluer les propriétés de l'interface.

La résistance de l'interface obtenue par la méthode expérimentale présentée dans cette étude a une application directe pour l'interprétation et la prédiction des propriétés de l'interface. La valeur de l'énergie critique de la rupture obtenue de ce modèle expérimental peut être utilisée avec l'analyse structurelle pour concevoir des éléments de béton armé renforcés par un composite pour empêcher le mode de rupture par délaminage.

ABSTRACT

Composite materials are bonded to the tension face of reinforced concrete beams under flexural loading to strengthen and stiffen them. When the strengthened beam is designed for flexure, it is expected to fail by compression failure of the concrete in the compression side or tension failure of composite on the tension side, after internal steel yielding. In practice, however, in the majority of cases, it was observed that the RC beams strengthened by this method failed by delamination of the composite from the concrete surface before reaching the maximum designed capacity. The debonding mode of failure is theoretically unpredictable. Because of its brittle nature, it should be prevented.

The main goal of this research is a better understanding of the debonding mode of failure with an emphasis on the effect of the composite material properties on the overall structural behaviour and the composite-concrete bond behaviour. The research is divided in two portions. The first one is an experimental and theoretical analysis of RC beams reinforced with composites. The second part examine the composite-concrete interface behaviour based on fracture mechanics and specimen testing. This thesis is therefore mainly experimental in nature. The goal is to get a better understanding of the effect of composite materials properties in order to design RC beams to prevent the debonding mode of failure through proper selection of composite reinforcement.

In the chapter3, we study the behaviour of composite strengthened RC beams under four point bending. This type of loading has the advantage of creating both constant and variable moment regions along the beam span. In order to study the effect of composite materials on the overall structural behaviour of the reinforced concrete beams under flexure, carbon epoxy and glass epoxy composites were laminated directly on the concrete surface using hand layup technique. The concrete surface was sandblasted to quality suggested in the litterature and practically applied in the field. The RC beams were designed under-reinforced by steel to avoid over strengthening after application of the composite and to obtain a failure after the internal steel yielding point. This was done to achieve an extensive cracking and deflection at the point of failure and second to investigate the effectiveness of the external composite reinforcement method after the steel yielding point where composite mostly effective. In the design process, precautions were taken to avoid the debonding mode of failure starting at the composite curtailment zone as well as shear failure of concrete.

In chapter 4 we investigate the effect of composite material stiffness on the structural response of strengthened beam. Experimental results show that the strength and mode of failure of hybrid beam depend on composite material properties and its reinforcement ratio. It is shown that the strength of the beam is less sensitive to the increase in composite rigidity since a more rigid composite favours a debonding mode of failure. It was shown that the rigidity and thickness of the composite have an important influence on the failure by delamination.

In chapter 3 the effect of the level of damage is investigated by loading RC beams to two level of damage before composite strengthening. The beams were strengthened by two types of composite. The study shows that the final mode of failure is not affected by the level of damage, however, pre-loaded RC beams when strengthened by composite showed higher strain and higher strain energy absorption capacity compared to undamaged strengthened beams. Taking rigidity of the strengthened beam, EI, as the principal member property, it is shown that the moment of inertia of the beam is influenced by the extend of flexural cracking. The pattern and the extend of the flexural cracks depend on the composite material property. The pattern and extend of the flexural cracks depend on the composite material property. The examination of the cracks indicates that the size and density of the cracks were less in strengthened beam than in the un-strengthened control beams. In spite of pre- cracking before strengthening the repaired beam preserved its structural integrity during loading, confirming the effectiveness of this repair technique.

In chapter 5 the debond crack was traced to originate at the location of concrete tensile crack opening at the interface. Bond failure most probably starts at the location of a flexural crack, because the crack tip at the interface is the place where the local stress concentration is superimposed on the shear stress produced by loading. An interface crack originated at the composite-concrete interface can be conducted in the direction of already existing shear crack or to be arrested at the position of an aggregate, enter into the concrete, following the aggregate paste interface and separate a thin layer of

concrete while delaminating the composite. Debonding mode of failure is further studied by looking closer at the composite-concrete interface. Principles of fracture mechanics is applied to design two sandwich specimen, Brazilian sandwich disk specimen and pure bending sandwich beam specimen. In these specimens one layer of composite is sandwiched between two pieces of bulk concrete and they are particularly designed and calibrated to measure the fracture toughness of composite-concrete interface under mixed mode of loading. Using Brazilian disk specimen fracture toughness of the interface is obtained for wide range of mixed mode of loading by changing the loading angle. The results of mixed mode (mode I/mode II) crack opening obtained from Brazilian disk specimen and the mode I crack opening obtained using pure bending sandwich specimen can be used to trace the fracture toughness curve representing the composite-concrete interface fracture properties.

In chapter 6, the effect of composite material mechanical properties on the composite-concrete interface properties is investigated using the developed sandwich specimens. In general it was observed that the fracture toughness of the interface is dependent on the phase angle of loading and composite material mechanical properties. It was observed that for the same concrete and angle of loading the interfacial fracture toughness is different for the two composite-concrete systems, which demonstrates the effectiveness of this testing method in evaluation of interface properties.

Development of bond crack at the composite-concrete interface plays a significant role in debonding mode of failure. The final failure occurs through the formation of continuous crack bridging the already existing cracks. The approach developed by this study led to some useful information with respect to understanding the global composite-concrete interface behaviour as affected by bond cracking.

The fracture resistance measurements conducted in this study have direct applicability to the interpretation and prediction of composite-concrete interface resistance. The value of critical fracture energy release rate obtained from sandwich specimen can be used in conjunction with structural analysis to design composite strengthened reinforced concrete elements against debonding mode of failure.

TABLE DES MATIÈRES

LISTE DES TABLEAUX

LISTE DES FIGURES

LISTE DES SIGLES ET ABRÉVIATIONS

A_s	Area of steel
A_{frp}	Area of composite
$2a$	Crack length
α	Dundru's Parameters
α_1	Coefficient
b	Beam width
β	Dundru's Parameters
β_1	Coefficient
c	Distance from extreme compression face to the neutral axis
C_c	Compression force in concrete
d	Distance from the extreme compression face to the centroid of the tension steel
E_{frp}	Modulus of elasticity of compoaite
E_1	Modulus of elasticity of material 1
E_2	Modulus of elasticity of material 2
E_c	Modulus of elasticity of concrete
ε	Concrete strain
ε_s	Steel strain
ε	Composite strain
ε_{com}	Composite strain
ε_{con}	Concrete strain

f_c'	Concrete compressive strength
f_{frp}	Composite tensile stress
f_y	Steel yielding point
f_s	Steel tensile stress
f_r	The modulus rupture of concrete
φ	curvature
ϕ	Phase angle of the bulk material
G	Strain energy release rate
G_1	Shear modulus of material 1
G_I	Opening mode interfacial fracture energy
G_{II}	Sliding mode interfacial fracture energy
G_2	Shear modulus of material 2
h	The overall depth of the beam
I_e	Effective moment of inertia
I_g	Moment of inertia of gross concrete section
I_{cr}	The moment of inertia of complete cracked section
K	Real stress intensity factor
K_1	Real mode 1 stress intensity factors of the interface
K_2	Real mode 2 stress intensity factors of the interface
K_I	Mode I stress intensity factor of the bulk material
K_{II}	Mode II stress intensity factor of the bulk material

K^{∞}	Stress intensity factor of the bulk material
N_I	Non-dimensional calibration factors
N_{II}	Non-dimensional calibration factors
M_n	Nominal moment capacity of the beam
M_{cr}	Cracking moment
M_u	Ultimate moment
P	load
R	Brazilian disk radius
r	Distance ahead of crack tip
t	Specimen thickness
T_s	Internal force due to tension in steel
T_{frp}	Internal force due to tension in composite
y_t	The distance from the centroid of transformed section
σ_{22}	Stress at crack tip
σ_{12}	Stress at crack tip
ψ	Real angle of complex quantity
$\hat{\psi}$	Real phase angle
ν_1	Poisson's ratio of material 1
ν_2	Poisson's ratio of material 2

INTRODUCTION

En raison de la croissante dégradation des infrastructures de béton, fréquemment combinée avec le besoin de mise à niveau des structures afin qu'elles puissent rencontrer les nouvelles exigences , les aspects de renouvellement structurel et de réparation ont suscité un intérêt considérable durant les dernières années. Le vieillissement et la détérioration des éléments d'infrastructure actuels comme les ponts et les constructions sont un problème de plusieurs milliards de dollars au vingt et unième siècle. Le renforcement externe d'éléments en béton armé et précontraint à l'aide de plaques en composite collées est devenu une technologie confirmée. Les techniques d'attachement des plaques de renforcement ont varié du collage, en utilisant des adhésifs, à l'ancrage ou la combinaison des deux. La plaque augmente la rigidité et la capacité de charge des poutres précédemment déficientes, pourvu que la méthode d'attachement permette le transfert des contraintes entre la surface de béton et la plaque. La méthode de renforcement par collage de plaque a l'avantage de causer une variation minimale des dimensions de la poutre et une interruption minimale de l'utilisation normale de la structure pendant l'application.

La réparation d'ouvrages en béton armé à l'aide de plaques d'acier collées utilisant la résine d'époxy est une technique fréquemment employée. Bien que pratique, cette méthode a montré les inconvénients suivants : (a) détérioration de l'interface acier-béton causée par la corrosion de l'acier; (b) difficulté de manipuler les plaques en

chantier, (c) présence de nombreux joints, en raison de la longueur limitée de plaque d'acier. Dans ce contexte, l'utilisation de matériaux composites représente une alternative intéressante puisque le problème de la corrosion ne se pose plus et que les plaques peuvent être beaucoup plus longues ou même continues. Ces plaques sont appliquées sur la face en traction ou dans les zones de compression ou de cisaillement. En plus d'être très légères et d'un ratio résistance/ poids élevé, elles peuvent être fabriquées sous forme de rouleaux continus de grandes longueurs laminés sur place, ce qui élimine les joints.

Les matériaux composites sont collés à la surface de béton à l'aide d'adhésif structurel. Le composite utilisé comme matériel fortifiant est typiquement fait de fibres continues de carbone, aramid ou de fibres de verre dans une ou deux directions, collées ensemble avec des résines comme le polyester, le vinylester ou l'époxy. Les matériaux composites pour le renforcement des structures sont disponibles généralement sous forme de laminés rigides, ou de tissus à imprégner sur place. Ces avantages principaux des tissus sont qu'ils sont imprégnés avec la résine in-situ et qu'ils sont appliqués directement sur la surface de béton. Quand cette méthode est utilisée, la résine joue aussi le rôle de l'adhésif. Cette méthode nous permet de créer un joint composite et béton, sans une phase intermédiaire d'adhésif au milieu. Cependant la combinaison de ces matériaux, le béton et le composite, crée un joint rigide dont la performance structurelle est plus difficile à déterminer.

Un mode de rupture généralement observé sur poutres renforcées avec des matériaux composites est la rupture par délaminage de composite. Ce mode de rupture est souvent soudain et catastrophique. La méthode d'analyse basée sur la compatibilité des déformations et l'équilibre des forces est efficace dans la prévision du comportement des poutres renforcées en flexion quand la rupture finale est une rupture en flexion. La rupture en flexion est définie soit par la rupture en compression de béton sur la face comprimée en compression de la poutre ou par la rupture en traction du composite sur la face tendue de la poutre, après l'écoulement de l'acier. Le mode de rupture prématuré par délaminage réduit la ductilité dans le sens de la diminution de la flèche maximale de la structure. Le mode de rupture par délaminage est théoriquement imprévisible, c'est pourquoi la technique d'application est souvent combinée avec le boulonnage ou tout autre ancrage approprié pour prévenir le décollage.

Pour les poutres renforcées par cette méthode, l'uniformité de la section est conservée par le transfert des contraintes de cisaillement à travers l'interface. La fissuration continue du béton en traction vient créer un état de contraintes complexe à l'interface béton-composite au bout des fissures. L'interface doit résister aussi bien aux contraintes normales qu'aux contraintes de cisaillement. Donc, les caractéristiques de l'interface béton-composite sont des facteurs significatifs influençant le comportement structurel et les mécanismes de transfert de charge à travers l'interface. Pour prévoir le comportement des poutres ainsi renforcées, une caractérisation de l'interface béton-composite est donc indispensable.

Pour analyser le joint, il y a fondamentalement deux options disponibles. La première consiste à analyser le joint en utilisant la méthode des éléments finis. La deuxième option consiste à évaluer le joint dans des conditions qui correspondent le mieux à celles rencontrées en usage. Le comportement et la résistance de l'interface ont fait l'objet de plusieurs études utilisant une variété de techniques comme par exemple le joint à simple recouvrement (single lap joint), le joint à double recouvrement (double lap joint) ou par pelage (peel spécimens). Bien que ces approches aient mené à des informations très utiles quant à la compréhension du comportement global du lien affecté par les propriétés mécaniques des adhérents et dans l'évaluation de la longueur efficace de collage, le calcul des contraintes basé sur la charge ultime provenant de ces données expérimentales doit être appliqué avec soin puisqu'il est sensible aux paramètres comme la géométrie ou dans le cas de 'peel test', ils ne représentent pas l'état actuel de contraintes présent à l'interface.

Parce que la rupture de l'interface est une caractéristique de lien, il faut exprimer la résistance de l'interface en termes de paramètres qui atteignent une valeur critique pour la rupture catastrophique. Une méthodologie pour déterminer les caractéristiques d'interface béton - composite devrait prendre en considération des concepts de mécanique de la rupture. Au meilleur de notre connaissance, aucune méthodologie n'a encore été présentée à partir de laquelle nous pouvons obtenir les propriétés de rupture de l'interface.

Cette recherche est un effort pour répondre à ce problème. Elle vise aussi à déterminer si le type de matériau composite qui agit comme un paramètre dans la conception structurelle peut être modifié pour empêcher le mode de rupture par délaminage et aussi permettre une augmentation de la ductilité de la structure. Le but de cette étude est tout d'abord de permette une meilleure compréhension du mode du rupture par délaminage tout en soulignant l'effet des propriétés du matériau composite sur le comportement structurel complet et ensuite de mieux comprendre l'effet des propriétés mécaniques des composites sur les propriétés mécaniques de l'interface. Pour réaliser ces objectifs, la procédure expérimentale et l'analyse ont été faites sur des poutres de béton armé renforcé. Les poutres de béton armé neuves et endommagées sont renforcées extérieurement avec deux types de fibres imprégnées avec la même résine. Le composite est laminé directement sur la surface du béton. Le mode de rupture par délaminage observé dans certains de ces essais était analysé pour développer une nouvelle méthodologie d'essais expérimentaux pour évaluer la performance de l'interface et pour déterminer les propriétés mécaniques de l'interface béton-composite. Cette méthode expérimentale est basée sur l'approche de la mécanique de la rupture et des essais expérimentaux utilisant de nouveaux échantillons qui sont inspirés de ceux utilisés pour étudier la rupture du béton entre autres. Ces travaux font l'objet des quatre articles scientifiques de cette thèse. Deux touchant la rupture sur les poutres et deux touchant la mécanique de la rupture et les essais en propagation de fissure.

CHAPITRE 1

ANALYSE BIBLIOGRAPHIQUE

Les sujets traités dans cette thèse peuvent être regroupés en 3 domaines :

- le comportement des poutres renforcées
- l'effet de différents paramètres sur le mode de rupture par délaminage
- l'étude des propriétés de l'interface et du mécanisme de transfert de charge à travers l'interface.

Ce chapitre présente une revue de la bibliographie existante sur ces sujets, en portant un intérêt tout particulier au comportement de l'interface puisqu'il s'agit de l'aspect traité dans cette thèse. Dans chacun des articles, nous présentons également une analyse bibliographique spécifique au sujet traité. Nous faisons ensuite une synthèse de ces analyses et l'accompagnons de renseignements complémentaires et de références non encore disponibles au moment de la rédaction des articles ou qui les complètent.

1.1 Comportement des poutres renforcées

Le comportement des poutres en béton armé renforcées par des matériaux composites a été étudié par plusieurs chercheurs. Bonacci et Maalej (2001), ont effectué une revue

complète des résultats expérimentaux et des paramètres influant sur le comportement structurel de la poutre renforcée.

On a montré que les poutres en béton armé renforcées par des matériaux composites peuvent créer trois régions distinctes dans la courbe charge - flèche de la structure hybride, correspondant à la section non fissurée de la poutre, à la section fissurée avant l'écoulement d'acier interne et, finalement, à la partie avec écoulement d'acier dans la poutre insuffisamment renforcée suivi par la rupture finale de la poutre (Meier, 1992). Le comportement structurel de la poutre renforcée par des composites dépend des propriétés mécaniques du composite et du béton et de l'interaction de ces deux matériaux à travers leur interface (Karbhari, 2001).

Contrairement à la technique de renforcement de la poutre par collage de plaques d'acier, le renfort externe ne peut être considéré comme une augmentation équivalente du renfort interne puisque les composites ne manifestent pas le comportement plastique élastique de l'acier et qu'on ne peut déceler aucun point d'écoulement. La courbe contrainte - déformation est une ligne droite jusqu'à la rupture (Bhutta and Qadi, 1993).

Les première études théoriques (Wei *et al.*, 1991; Triantafillou et Plevris, 1992) se sont cependant concentrées sur la rupture du béton en compression ou la rupture des composites en traction. Les procédés de design sont basés sur la méthode de

compatibilité des déformations en supposant un lien parfait entre le composite et le béton (ISIS Canada, 2000).

Des études théoriques sur les différents paramètres montrent que les paramètres les plus significatifs influant sur la résistance ultime en flexion sont la résistance en compression du béton, le pourcentage de l'acier, le module d'élasticité du matériau composite et l'épaisseur de la plaque de composite (Picard *et al.*, 1995). Cette méthode de renforcement est particulièrement efficace pour des poutres où la proportion de renforcement en acier est relativement basse (An *et al.*, 1991, Ross *et al.*, 1999). Le modèle analytique de Bhutta and Qadi (1994) basé sur les théories de la poutre de béton armé et de la poutre laminée de composites est capable de prévoir la rigidité, la résistance et la flèche de la poutre hybride en présumant un lien parfait entre le composite et le béton. El-attar et El-bar (1994) ont effectué des études analytiques qui prenaient en considération le comportement non linéaire de la relation traction - allongement et la fissuration du béton. La comparaison des résultats théoriques et expérimentaux révèle leur concordance étroite, mais la différence devient considérable quand la déformation de la poutre hybride augmente. Triantafillou et Plevris (1981) (1992) présentent des équations décrivant les différents modes de rupture. Triantafillou et Deskovic (1991) (1992) présentent des diagrammes de rupture pour des poutres ayant des proportions de renfort différentes. En prenant la quantité du renfort FRP externe comme une variable, ils présentent des diagrammes de rupture pour trois types de composites unidirectionnels : carbone FRP, Kevlar FRP et verre

FRP. Lorsque la déformation à la rupture est la même, plus la rigidité du composite est grande, plus haute est la capacité de moment. Cependant, il n'est pas avantageux d'utiliser un renfort de carbone plutôt que de verre parce que, bien qu'il ait un module d'élasticité plus grand, il diminue la déformation à la rupture et, par le fait même, la ductilité de toute la structure.

En général, les modèles analytiques négligent le comportement non linéaire du béton en traction. Les applications basées sur ces modèles se limitent aux structures dont la géométrie et les conditions de chargement sont assez simples. L'analyse détaillée de la structure renforcée est réalisée par simulation numérique en considérant les comportements non linéaires des matériaux. Nitereka et Neale (1999) ont mené une simulation numérique pour analyser le comportement de la poutre hybride en utilisant un modèle d'élément fini non linéaire. Ces modèles analytiques et théoriques ne peuvent pas prévoir le mode de rupture par délaminage. La recherche expérimentale montre cependant que lorsque les poutres renforcées par des composites collés sont chargées sous flexion, la rupture finale est souvent associée au délaminage du composite (Ritchie *et al.*, 1991).

1.2 Effet des propriétés des matériaux

Une augmentation de la résistance du béton en compression augmente le moment ultime et la ductilité de la poutre renforcée. Les matériaux composites sont plus

efficaces quand la résistance de compression du béton est plus grande. Avec du béton plus résistant, la rupture de composite peut survenir si le module d'élasticité du matériau composite est trop faible. Les résultats des essais expérimentaux indiquent que la rigidité, la résistance et la ductilité de la poutre renforcée varient selon le type de composite utilisé (Swamy *et al.*, 1996; Hutchinson et Rahimi, 1996; Limberger *et al.*, 1996; Demers *et al.*, 1996). La capacité en flexion augmente quand l'épaisseur des composites augmente (de 8 à 20 mm). Cependant, la contrainte développée dans le matériau composite lors de la rupture est plus élevée dans les couches plus minces. Le matériau composite est donc plus efficace dans les couches plus minces.

De nombreux chercheurs ont utilisé les composites à base de fibres de carbone en raison de leurs grandes résistances en traction et rigidité comparativement à d'autres composites. Cependant, la fibre de verre a aussi été largement étudiée (Saadatmanesh et Ehsani, 1991, Deblois *et al.*, 1992), peut-être en partie en raison de son prix réduit. Le module élastique des composites de fibres de verre est relativement faible, ce qui peut entraîner des flèches plus élevées et, par conséquent, limiter leur utilisation dans les éléments en béton. L'effet du type de composite et de l'épaisseur a été étudié par Bhutta et Qadi (1994). Ce travail montre que le pourcentage d'augmentation de la capacité de moment de la poutre est plus haut pour le Kevlar/époxy, bien que son module d'élasticité soit presque la moitié de celui du composite carbone/époxy.

Sharif *et al.*(1994) ont étudié l'influence de l'épaisseur du composite sur la capacité ultime en flexion des poutres renforcées par des matériaux composites. Il a été observé

qu'une épaisseur importante réduisait la flèche de l'élément et retardait l'écoulement d'acier. Lorsque l'épaisseur augmente, ces contraintes sont fortes et une rupture prématurée par délaminage se produit, accompagnée de rupture locale en cisaillement (Hoa *et al.*, 1996; Arduini *et al.*, 1996). Ces résultats sont corroborés par Triantafillou et Plevris (1992).

Le type de colle a également été étudié (Saadatmanesh *et al.*, 1995). Afin de réaliser un bon collage, ce qui conditionne le succès de l'opération, il faut choisir une colle de type époxy ayant une résistance et une rigidité suffisantes pour assurer la transmission des efforts entre le composite et le béton. Elle doit également être suffisamment résistante pour éviter une rupture fragile de l'interface suite à la fissuration du béton. Swamy *et al.* (1987) ont étudié l'influence de l'épaisseur de la couche de colle avec des plaques en acier. Il a été établi que la fissuration et les déformations étaient réduites lorsque l'épaisseur de colle augmentait, mais dans une moindre mesure que lorsque l'épaisseur de la plaque est le paramètre étudié.

1.3 Comportement des poutres pré-fissurées

Les données publiées sur la performance de cette technique de réparation lorsqu'on l'utilise pour réparer des poutres de béton armé structurellement endommagées sont limitées. L'application de la technique de collage par plaque d'acier pour renforcer des poutres de béton armé structurellement endommagées a été étudiée par Swamy *et al.*

(1989) et Basunbul *et al.* (1990). Ils ont renforcé des poutres endommagées alors qu'elles étaient déchargées et aussi quand elles étaient toujours sous charge. Leurs résultats expérimentaux montrent que le renforcement de poutres de béton armé endommagées par collage de plaques d'acier est efficace et que ces poutres ont fait preuve d'une rigidité et d'une résistance supérieures à celles de la poutre originale non renforcée. Hussain *et al.* (1995) ont étudié l'effet de l'épaisseur de la plaque d'acier, avec des épaisseurs variant de 1 à 3 mm, sur le comportement et le mode de rupture des poutres renforcées endommagées. Ils ont observé la rupture prématurée par délaminage à la zone de raccourcissement de la plaque quand l'épaisseur de la plaque augmentait. Ils ont aussi déclaré que même l'application d'ancrage a l'extrémité au moyen de boulons d'ancrage ne pouvait pas empêcher la rupture prématurée des plaques épaisses. Le comportement en flexion de la poutre pré - fissurée et renforcée par des composites a été étudié par Sharif *et al.* (1994). Ces derniers ont étudié l'effet de l'épaisseur de la plaque de composites, qui a varié entre 1 et 3 mm, sur le comportement de la poutre endommagée. Ils ont montré que le comportement structurel n'est pas très modifié par le degré d'endommagement, mais ils ont observé le mode de rupture par délaminage lorsque l'épaisseur du composite augmentait.

1.4 Rupture par délaminage

Bien que la technique de collage des plaques comporte beaucoup d'avantages pratiques, la rupture finale des poutres de béton armé (RC) renforcées peut se

manifester en raison du délaminage soudain du renfort externe collé (le composite ou l'acier) . Un tel mode de rupture diminue non seulement la capacité ultime de la structure, mais est aussi inacceptable du point de vue de la sécurité structurelle. La rupture prématurée par délaminage du composite a été identifiée dans de nombreux essais en laboratoire (Johnson et Tait, 1981; Jones *et al.*, 1982; Hamoush et Ahmad, 1990; Sharif *et al.*, 1994; Fanning et Kelly, 2001). Différents mécanismes de délaminage ont été identifiés (Karbhari, 1997). En général, on peut classer le mécanisme de délaminage dans deux catégories distinctes : (1) la rupture qui survient dans la zone de haut moment de flexion et de faible effort tranchant et (2) la rupture qui provient à ou près de l'extrémité coupée de la plaque dans la région de grand effort tranchant et de haut moment de flexion.

Beaucoup d'auteurs ont essayé de prévoir la force causant la rupture par délaminage pour les plaques d'acier. Zibraba *et al.*, 1994; Roberts et Haji-Kazemi, 1989; Oehlers, 1988 et Malek *et al.*, 1996, présentent une méthode analytique pouvant servir à prévoir la distribution des contraintes normales et de cisaillement à l'interface de la plaque de composites et de la couche adhésive. Ces méthodes ont été mises au point en s'appuyant sur l'équilibre des forces et la compatibilité de déformation dans la couche adhésive. En utilisant ces méthodes analytiques, on peut évaluer la force causant le délaminage à la zone de raccourcissement de la plaque.

À l'extrémité du composite, le transfert de contrainte longitudinale de la poutre de béton au renfort collé engendre une grande contrainte de cisaillement à l'interface. À la terminaison du renfort externe, un changement de la rigidité et la discontinuité créent une concentration de contraintes dans le béton, déclenchant souvent des fissures susceptibles de causer le délaminage (Oehlers et Moran, 1990). Aussi, la différence de déformation entre la poutre et le composite entraîne une contrainte de traction normale élevée dans cette région. À la terminaison du composite, ces contraintes normales sont des contraintes de traction qui facilitent le délaminage. Ces contraintes font en sorte que le composite se détache de la surface de béton. Ce mode de rupture par délaminage débute à l'extrémité terminale du composite et se propage dans le béton, vers les points de chargement.

Dans d'autres études expérimentales, on a observé que le délaminage commence à d'autres endroits que les extrémités du renfort par des composites (Buyukozturk et Hearing, 1998). Sato et Ueda (2000) ont observé le délaminage du composite en raison du développement de fissures de flexion ou de fissures diagonales de traction au niveau de l'interface béton-composite. Le lien entre la plaque de composite et le béton peut se fracturer de manière soudaine à cause de la propagation catastrophique d'une fissure le long de l'interface béton-composite. Cette sorte de délaminage commence quelque part dans la poutre et se propage vers les appuis.

Tout mode de rupture autre que la rupture en flexion est caractérisé par une capacité d'absorption d'énergie très basse à la charge limite et devrait être évité (Sharif *et al.*, 1994). Les recherches scientifiques pour expliquer le mécanisme de rupture prématurée des plaques par délaminage se répartissent en deux grandes catégories : (1) une approche empirique qui tente d'établir un rapport entre le délaminage et divers paramètres géométriques et de chargement et (2) une approche analytique où l'on prévoit les concentrations de contraintes qui entraînent le délaminage des plaques.

L'approche empirique amène la présentation de diverses techniques destinées à prévenir le délaminage des composites, dont le contrôle de la géométrie de renfort des composites en réduisant graduellement les contraintes internes des plaques lorsque les plaques sont épaisses ou l'ancrage par une technique de boulonnage ou de collage d'un renfort additionnel aux parois de la poutre, dans la travée de cisaillement où le délaminage s'observe le plus souvent (Swamy *et al.*, 1987; Hussain *et al.*, 1995). Différentes techniques d'ancrage comme le boulonnage de l'acier et le gainage de plastique renforcé de fibre de verre ont été mises au point pour limiter ces modes de rupture fragile (Grace *et al.*, 1999; Teng *et al.*, 2000). Les études révèlent que la séparation des composites est toujours probable même si les plaques épaisses de composites sont effilées. Hussain *et al.*(1995) ont signalé que la mise en place d'un ancrage terminal à un renfort de composites épais au moyen des boulons d'ancrage ne pouvait pas empêcher la rupture prématurée, mais que la technique d'ancrage au moyen de colle est la plus efficace. Le résultat montre que même si ces techniques

d'ancrage peuvent augmenter la force portante ultime de la structure hybride, elles ne sont pas capables de modifier le mode de rupture de la structure par délaminage.

En présence de lamellés minces, de nombreux essais ont aussi montré que le choix judicieux d'un système d'ancrage en forme de canaux en U collés ou de blindage aux extrémités des plaques peut empêcher le délaminage et entraîner une déformation ductile. On a montré qu'en utilisant une technique d'ancrage appropriée, on peut maintenir l'action des composites jusqu'à 70 % de la capacité ultime conçue de sorte qu'on augmente la ductilité structurelle de la poutre renforcée (Spadea , 1999). Dans certains cas, cependant, le boulonnage ou le gainage ne peut pas être effectué en raison du manque d'espace autour de la poutre. Les valeurs de cisaillement maximal et de contrainte normale dérivées indirectement des charges de rupture obtenues lors d'un essai expérimental ne peuvent pas être généralisées puisqu'on n'a pas justifié l'existence d'un état de contrainte réel au point de rupture. D'autre part, l'état de la charge de rupture et des contraintes locales dépendant de la proportion de béton et de composite varie d'une combinaison à l'autre.

Les études théoriques exhaustives sur les poutres renforcées suggèrent que le délaminage se produise à l'extrémité du renfort externe et peut être empêché en limitant les contraintes maximales à l'interface (Roberts *et al.*, 1988; Roberts et Haji-Kazemi, 1989; Malek *et al.*, 1998; Taljsten, 1997). Une formule simplifiée a été mise au point pour prévoir les concentrations de contraintes normales et de cisaillement à

l'extrémité de la plaque (Roberts *et al.*, 1989; Sharif *et al.*, 1994). L'effet d'un renforcement de la proportion d'acier et de l'épaisseur du béton a été examiné et on a proposé une formule analytique pour prévoir la charge de rupture correspondant à ce mode de rupture (Nguyen *et al.*, 2001). Oehlers (1988) a suggéré des méthodes pour prévenir le délaminage en flexion (délaminage dans la région de moment maximal) et le délaminage par cisaillement dans la travée de cisaillement. Ces modèles analytiques ont constitué la base d'une analyse numérique pour prévoir le mode de rupture prématurée par délaminage (Arduini et Di Leo, 1996; Taljsten, 1997). Une analyse des éléments finis a été effectuée pour prévoir les contraintes à l'intérieur du plan de collage à l'interface béton-composite (Hutchinson et Rahimi, 1992). Dans ces études, on a examiné l'effet de différents paramètres comme l'épaisseur du composite sur la distribution des contraintes à l'interface. On a montré que les contraintes normales et de cisaillement augmentaient à l'extrémité du composite lorsqu'on augmentait l'épaisseur de la plaque.

La généralisation de ces approches est difficile en raison de l'effet de divers facteurs qui ne sont pas indépendants. Dans la pratique, il est inévitable de couper le composite près des appuis, tandis qu'il est dangereux sur le plan structurel de couper la plaque dans la zone de moment maximal, ce qu'on ne peut donc pas recommander (Oehlers, 1992). Le mode de rupture par délaminage est modifié par le rapport entre la longueur du composite collé à l'intérieur de la travée de cisaillement de la poutre et la travée de

cisaillement de la poutre (Fanning et Kelly, 2001). On a montré que l'efficacité du renforcement par des composites diminue à mesure que raccourcit la longueur.

Des études analytiques confirment que l'existence d'une combinaison de concentrations de contraintes normales et de cisaillement près de l'extrémité de composite où commence la rupture par délaminage. Ces études ont essayé d'établir un modèle prévisionnel pour les concentrations de contraintes normales et de cisaillement à l'extrémité de composite (Saadatmanesh et Malek, 1998; Mukhopadhyaya et Swamy, 2001; Nguyen *et al.*, 2001). Un certain nombre de recherches analytiques basées sur les propriétés élastiques linéaires des matériaux et l'état des contraintes dans la zone terminale de composite sont validées par quelques données expérimentales. Tous les résultats expérimentaux et analytiques confirment que la rigidité du composite influe sur la valeur de la contrainte de cisaillement à l'interface qui entraîne le délaminage.

Bien que le délaminage le long de la poutre ailleurs qu'aux extrémités du composite soit couramment observé dans les essais expérimentaux, peu d'analyses sont disponibles sur ce sujet. Les modèles théoriques suggérés pour prévoir le délaminage révèlent que, dans le cas des plaques d'acier, le délaminage prend naissance à partir du moment de flexion maximal et s'étend ensuite plus loin vers l'appui (Zhang *et al.*, 1995). Ce modèle théorique n'est probablement pas applicable aux matériaux composites en raison du manque de sensibilité à la rigidité de la plaque, ce qui a un

effet direct sur le nombre de fissures et leur espacement dans le béton du côté en traction. Rahimi et Hutchinson (2001) ont tenté de prévoir le mode de rupture par délaminage de la poutre en utilisant un deuxième modèle d'éléments finis non linéaires. Ils concluent que le mécanisme de rupture par délaminage est régi par une valeur de contrainte limitante à l'interface béton - composite. En général, les modèles théoriques disponibles sont trop complexes pour les procédés de conception technique et n'ont pas été validés par suffisamment de données expérimentales. Dans la recherche effectuée par Leung *et al.* (2001), la contrainte de cisaillement maximale à l'interface est reliée à l'ouverture de fissures; au moyen d'une formule théorique, l'effet de la rigidité du composite a été examiné. Les résultats montrent que le délaminage est favorisé par une grande rigidité du composite. Les efforts destinés à empêcher la rupture par délaminage reposaient sur une conception intuitive sans compréhension claire des mécanismes fondamentaux de délaminage en cause. Avant de pouvoir formuler une directive à l'intention d'un ingénieur de structure pour que ses conceptions soient simples et rationnelles, il importe d'établir un critère valable pour prévoir le délaminage et identifier les paramètres en cause dans le processus de délaminage.

1.5 Mécanisme de transfert de charge à travers l'interface

D'après un grand nombre de données expérimentales, la rupture par délaminage survient à l'interface béton-composite. On peut conclure qu'il existe une valeur limite

de résistance à l'interface entre le composite et le béton qui devient cruciale là où se forment les fissures ou de discontinuité à l'interface.

Quelques chercheurs ont effectué des essais mécaniques sur les interfaces composite-béton (Chajes *et al.*, 1996; Lee *et al.*, 1999). Les objectifs de ces essais étaient d'étudier la distribution des contraintes de cisaillement dans les joints collés, d'évaluer quantitativement les longueurs d'ancrage et d'examiner l'influence de la résistance du béton et de l'épaisseur de la ligne de colle sur la résistance de l'interface. On a montré que le résultat expérimental était fonction des propriétés et de la géométrie des spécimens et qu'il dépendait aussi de la préparation de la surface. Pour comprendre le mécanisme de transfert de force et déterminer la longueur de transfert du joint béton-composite, un essai expérimental et analytique a été réalisé au moyen d'un essai «*single lap shear test*» (cisaillement par simple enroulement) (Bizindavyi et Neale, 1999). Dans ces essais, les paramètres comme le type et l'épaisseur du composite sont étudiés. On a montré que la longueur du lien suffisante pour développer le plein pouvoir de flexion du composite dépend du type, de la largeur et de l'épaisseur du composite.

D'autre part, la rupture à l'interface béton-composite peut commencer loin de l'extrémité de la plaque de composite et peut provenir de fissures de flexion existant dans le béton à l'interface béton-composite. Les résultats expérimentaux sur les poutres de béton armé renforcées de composite montrent que les caractéristiques du

lien à l'interface béton-composite sont des facteurs significatifs qui influent sur le comportement structurel à la fois pendant la formation de fissures de flexion et dans la phase subséquente de mode de la rupture.

Pour augmenter la fiabilité du renforcement des structures en béton armé au moyen de composites et mieux comprendre le mode de rupture par délaminage, il est crucial de comprendre le comportement de l'interface béton-composite. Un mécanisme de transfert de contraintes au niveau de l'interface et la longueur efficace du composite ont été étudiés par quelques chercheurs, en utilisant un certain nombre de configurations de spécimens. La distribution des contraintes de cisaillement à l'interface béton-composite a été examinée au moyen des essais «*single lap shear*» (Rostasy, 1993; Neubauer et Rostasy, 1997; Bisby *et al.*, 2000), «*double lap shear*» (Nakaba *et al.*, 2001), «*modified contoured double cantilever beam*» (CDCB) [Boyajian *et al.*, 2000] et «*push part*» pour béton (Kamel *et al.*, 2000). Les études expérimentales sur la comparaison des paramètres montrent que la résistance de l'interface et la distribution des contraintes dépendent de la qualité de préparation de la surface, des propriétés mécaniques du composite et de la résistance du béton en compression. Il existe cependant une longueur de lien au-delà de laquelle aucune nouvelle augmentation de la charge de rupture ne peut être réalisée et la rupture du composite en traction ou du béton en compression survient. Dans ces recherches, la rupture de l'interface par cisaillement a été définie comme la rupture du béton sous l'interface. L'approche développée dans les études précédentes a révélé une certaine

information très utile pour la compréhension du comportement global du lien qui se trouve modifié par les propriétés mécaniques de l'interface et pour l'évaluation de la longueur efficace du composite. Les résultats obtenus de ces études expérimentales sont cependant limités aux études comparatives. Les joints «*double lap*» et «*double strap*» ne sont en outre pas libres en soi de toutes les contraintes de délaminage déclenchées aux extrémités du chevauchement. Il faut mettre au point des méthodes pour déterminer les caractéristiques de l'interface béton-composite. Idéalement, une telle méthode ferait intervenir des concepts de mécanique de rupture.

Au moyen d'un test d'adhésion «*peel test*» modifié, Kharbhari et ses collaborateurs ont mesuré l'énergie de rupture G à partir du travail élastique fait par un test d'adhésion (Karbhari et Engineer, 1995; Kharbhari et Engineer, 1996; Karbhari *et al.*, 1997). Ils ont utilisé le test d'adhésion modifié pour obtenir les énergies de fracture interfaciale associées à l'interface béton-composite et étudier l'effet des propriétés des matériaux composites ainsi que les effets environnementaux sur l'interface. Weimer et Haupert (1999) ont étudié l'interface béton-composite sous le mode III d'ouverture de fissures en présentant un essai de flexion à 3 points. La propagation des fissures à l'interface pour les divers types d'interface entre le béton et les plastiques renforcés de fibre de carbone a été étudiée et la résistance au cisaillement à l'interface béton-composite a été calculée au moyen d'une formule simple.

On a utilisé de petits spécimens pour étudier l'effet de raidissement en traction «*tension stiffening*» (Tripi *et al.*, 2000). On a montré que l'augmentation de la rigidité de la plaque de composite augmentait considérablement la rigidité globale en traction.

En raison de la distribution différente des contraintes à l'interface béton-composite, à cause de la géométrie différente des spécimens utilisés pour les tests, la distribution des contraintes d'adhérence obtenue à partir de ces essais diffère d'une expérience à l'autre et les résultats doivent être comparés avec soin.

Bien que la réparation et le renforcement des éléments structuraux en béton à l'aide d'un matériau composite extérieurement collé soient bien établis, il reste encore à étudier de façon exhaustive des aspects cruciaux liés à l'initiation et à la propagation des fissures, à la ductilité des structures et à la durabilité des joints, ainsi qu'aux dispositions sur la sécurité. Il faut rappeler que contrairement à l'acier, les composites renforcés de fibres sont des matériaux anisotropes et leur réponse aussi bien individuelle que comme partie inhérente d'un système structurel dépend du choix et de la combinaison des constituants et de la méthode de fabrication et de collage dans le chantier. Il faut donc accorder de plus en plus d'importance au choix des matériaux et aux aspects liés aux processus afin d'assurer la sécurité et l'utilisation efficace du composite dans cette méthode réparation. Nous sommes confrontés à des défis significatifs concernant la conception et la philosophie du dessin de détail et

l'optimisation du type et de la forme de composite utilisé dans les applications pratiques.

CHAPITRE 2

SYNTHÈSE

Cette étude du comportement de l'interface béton-composite est faite dans le but ultime de mieux prédire le mode de rupture de poutres en béton armé renforcées de composite laminé in-situ afin d'éviter les ruptures catastrophiques. Les objectifs secondaires de cette étude sont: l'étude expérimentale de l'interface béton-composite sur des poutres et sur des échantillons et plus particulièrement l'étude à l'influence des propriétés mécaniques du composite sur le mode de rupture de cette interface.

Pour réaliser cette étude, nous utiliserons une approche expérimentale sur des poutres et des échantillons et nous tenterons de développer un modèle de comportement. Dans un premier temps pour l'étude expérimentale sur les poutres, nous utiliserons deux composites totalement différents, soit un époxy à fibres de carbone et un époxy à fibre de verre afin de renforcer par laminage in-situ des poutres préalablement chargées et endommagées et ainsi analyser l'influence de la fissuration du béton sur le comportement de l'interface béton-composite. Dans un deuxième temps, nous étudierons le mode de rupture de l'interface béton-composite sur des petits échantillons par une approche expérimentale typique de la mécanique de rupture.

Chacun des chapitres 3, 4, 5 et 6 de cette thèse est constitué de l'un des quatre articles écrits dans le cadre de la présente étude. Ces chapitres sont respectivement intitulés:

«Structural strength and failure mode of reinforced concrete beams, strengthened by carbon and glass fibre laminas» (Résistance structurelle et mode de rupture de poutre en béton armé renforcées par un laminé de carbone ou verre), «The effect of external composite reinforcement on the behavior of structurally damaged RC beams» (Effet du renforcement de matériau composite sur le comportement en flexion de poutres en béton armé endommagées), «A proposed approach to evaluate the composite-concrete interfacial fracture resistance using sandwich specimen»(Une approche pour évaluation de la résistance de l'interface béton-composite en utilisant des échantillons sandwich) et «Effect of composite material properties on the composite-concrete interfacial resistance» (Effet des propriétés du matériau composite sur la résistance de l'interface composite-béton).

Le chapitre 3 contient les résultats d'une étude expérimentale effectuée sur des poutres de béton armé renforcées par des matériaux composites. Le but de ces essais était de bien identifier le comportement structurel des poutres et d'étudier l'effet de la rigidité structurelle des composites (EI_{com}) sur le comportement des poutres. Le changement de la rigidité structurelle du composite est effectué soit par changement de type de renfort, carbone ou verre, ou par changement d'épaisseur. Il a été observé que la charge à laquelle l'écoulement d'acier se produit augmente avec ce paramètre, tandis que ces conclusions ne peuvent être transposées à la charge à laquelle la rupture de la poutre se produit. En effet, des ruptures prématurées peuvent se produire quand la rigidité du composite augmente. Ce mode de rupture est observé dans les poutres

renforcées par du carbone/epoxy, soit dans la région du moment constant ou du moment variable.

Une poutre de béton armé est normalement conçue pour une rupture après le point d'écoulement de l'acier. Ce mode de rupture est accompagné par de grandes fissurations et déformations. Pour une poutre de béton armé, la capacité limite est calculée par l'analyse d'équilibre simple. Le mode de rupture peut être contrôlé par la quantité d'acier. La capacité limite d'une poutre renforcée avec composite ne peut pas être calculée de la même manière. À cause du comportement rigide du composite et du béton, la rupture de cette poutre est toujours fragile. Les résultats expérimentaux démontrent une diminution de ductilité, dans le sens d'une diminution de la flèche maximale, quand la rigidité augmente. Il se peut qu'il existe une flèche limite au-dessus de laquelle une rupture de l'interface béton-composite peut se produire avant que la poutre n'ait atteint son potentiel de résistance en flexion.

L'objectif premier du chapitre 4 est de tester l'efficacité d'une technique de réparation. Nous avons pour cela décidé d'endommager les poutres en béton armé avant d'appliquer le renforcement en composite. Ainsi, nous avons amené à la rupture une poutre témoin, laquelle nous a permis de choisir deux degrés d'endommagement pour les autres poutres. L'étude du comportement de ces premières poutres a permis d'observer le motif de fissuration du béton, les déformations, le seuil de plastification de l'acier et la charge limite. Durant les essais de pré-fissuration, l'ouverture des

fissures a été suivie et reliée à la charge. La fissuration est apparue plus diffuse et répartie en présence du composite, comparée à la poutre témoin. Encore une fois, l'effet de la rigidité du composite a été étudié en choisissant deux types de composites de base: fibre de carbone et fibre de verre. Les deux types de fibres sont préimprégnées avec la même résine époxy et laminés directement sur la surface de béton non endommagée ou endommagée. Les résultats montrent que l'effet de la réparation est fonction à la fois du degré de pré-fissuration et de la rigidité du composite. La réparation avec un composite peut conduire à des poutres réparées présentant des caractéristique mécaniques supérieures à celles d'origine. Le degré d'endommagement ne change pas le mode de rupture, mais les poutres endommagées et renforcées avec un composite montrent un comportement plus ductile que les poutres non dommagées et renforcées avec un composite.

La propriété principale qui influence le plus le comportement à court terme des poutres renforcées est la valeur de la rigidité en flexion EI. Le moment d'inertie de la poutre, sous l'influence du pourcentage d'acier et du niveau de fissuration, n'est pas constant le long de la poutre même pour une section de poutre constante. La diffusion et la longueur des fissures en flexion dépendent du moment appliqué et des propriétés des matériaux composites. Le béton entre les fissures supporte un peu de traction et contribue légèrement à la rigidité efficace de la poutre. Ainsi, même dans la partie de poutre avec les fissures, la rigidité efficace sera plus grande que celle prédite dans les calculs qui supposent une section en traction entièrement fissurée. L'effet du matériau

composite sur le changement du moment d'inertie de la section est faible. Cependant, le moment d'inertie est en pratique augmenté à cause de la participation du béton traction entre les fissures.

L'initiation et la propagation des fissures à l'interface béton-composite jouent un rôle significatif dans la rupture par délaminage. Les propagations des fissures dans le béton dépendent à la fois des propriétés mécaniques de béton et du composite et de l'état des contraintes au fond de la fissure. La rupture finale arrive par la formation de fissures continues dans le béton joignant les fissures de flexion. La contrainte est transférée au composite par l'interface et l'état de contrainte au niveau de l'interface béton-composite est complexe.

Quand une fissure de flexion se développe dans le béton, une concentration de contrainte est créée dans l'interface. Au bout de la fissure, à l'interface, il y a deux sources de contrainte de cisaillement local : la contrainte de cisaillement due au chargement et la contrainte induite par le changement rapide de moment au bout de la fissure. La rupture d'interface commence probablement au bout d'une fissure de flexion, parce que c'est là où les contraintes localisées de cisaillement sont superposées. Donc, le mécanisme de rupture de l'interface peut être expliqué par une initiation de fissure à l'interface au bout d'une fissure de flexion qui casse le lien adjacent à la fissure. Cette partie séparée de lien augmente la concentration de contraintes. La fissure s'étend finalement et le processus se répète très rapidement.

Dans les essais en flexion, les fissures d'interface apparaissent d'habitude à l'interface comme résultant d'une fissure de flexion et des fissures de traction diagonales dans le béton. Parce que le composite n'est pas capable de redistribuer la contrainte au bout de la fissure de flexion, le délaminage est fragile. Dans les études expérimentales sur les poutres renforcées avec composite, il a été observé qu'une fissure d'interface peut être déviée et se propager dans la direction d'une fissure de cisaillement déjà existante ou arrêtée à la position d'un granulat à l'interface et se propager ensuite dans le béton. Les résultats expérimentaux démontrent que le délaminage commence à l'interface béton-composite. On peut conclure qu'il existe là une valeur limite de résistance d'interface entre le composite et le béton qui devient critique à l'emplacement d'une ouverture de fissure de flexion où la discontinuité est présente à l'interface.

Il n'y a pas une procédure standard pour évaluer les propriétés de l'interface béton-composite. Les procédures d'essai habituelles pour évaluer un joint collé, bien qu'elles puissent être utilisées pour comparer les propriétés pour des adhésifs différents, sont d'habitude incapables de donner une valeur appropriée de résistance de l'interface.

Dans le chapitre 5, nous essayons d'évaluer les propriétés de l'interface béton-composite en utilisant l'approche de la mécanique de la rupture. Ce concept est utilisé pour présenter à la fin d'une nouvelle méthodologie expérimentale pour obtenir la ténacité de l'interface en utilisant des spécimens sandwich. Un spécimen sandwich est défini comme une couche très mince de matériel (2) serré entre deux pièces de

matériel (1), avec une fissure pré-insérée à une interface. Dans cette étude, le composite représente le matériel (2) et le béton est le matériel (1). En raison de la petite épaisseur de composite comparé aux autres dimensions, ces spécimens sont considérés appropriés pour l'évaluation des propriétés composite-béton. Deux sortes de spécimens sandwich ont été utilisées à cette fin : le spécimen de disque de sandwich Brésilien et le spécimen de sandwich poutre. L'avantage du spécimen de disque Brésilien est que la rupture peut être réalisée sous plusieurs modes de chargement. Le spécimen de poutre a été utilisé pour obtenir l'ouverture de fissures en mode I, qui est difficile à obtenir avec le disque Brésilien.

Finalement, au chapitre 6, on applique la méthode suggérée dans le chapitre précédant pour évaluer l'effet des propriétés mécaniques du composite sur la résistance de l'interface.

Le carbone/époxy et le verre/époxy ont été utilisés comme matériaux composites. La courbe de ténacité est obtenue en testant le spécimen Brésilien sous différents angles de chargement. Les résultats d'essais montrent que la ténacité de l'interface est une fonction de l'angle de phase de chargement et augmente généralement avec ce paramètre. Alors que la propriété de l'interface dépend des propriétés du composite. Une rupture d'interface semblable à celle des poutres renforcées par des composites a été observée.

CHAPITRE 3

STRUCTURAL STRENGTH AND FAILURE MODE OF REINFORCED CONCRETE BEAMS, STRENGTHENED BY CARBON AND GLASS FIBRE LAMINAS

Katayoun Soulati, École Polytechnique de Montréal, Canada

Raymond Gauvin, École Polytechnique de Montréal, Canada

3.1 Abstract

This research examines the strength and failure mode of reinforced concrete (RC) beams strengthened in flexure with glass fibre epoxy (GFRP) and carbon fibre epoxy(CFRP), single layers, laminated directly on the beam surface. The beams are loaded under four point flexure. The loading position and composite thickness are varied for CFRP strengthened beam. GFRP strengthened beam failed by compression failure of concrete while CFRP strengthened beams failed by debonding. Debonding is due to the composite-concrete interface failure which can be traced to a stress concentration at a interface crack tip. The position at which debonding occurs depends on the amount of composite used and on the stress state at the interface.

3.2 Introduction

Fibre reinforced composite materials are more often used for strengthening and rehabiliation of reinforced concrete members. Reinforced concrete (RC) members need repair and strengthening when the internal steel reinforcement is not sufficient or severely damaged by corrosion. Composite materials in the form of sheets or plates can be bonded to the tension face of flexural members to strengthen and stiffen them, in much the same manner as for steel. This method of repair increases the capacity of the structure, while only minimally altering its weight and dimensions. Structural members like bridges and buildings are strengthened by this method in Europe, Japan and North America (Sika Canada, 1998; Meier, 2000).

Experimental results on the composite strengthened reinforced concrete beams (hybrid beam) show considerable increase in load carrying capacity and stiffness (Ritchie et al. 1991; Saadatmanesh and Ehsani, 1991). Different failure modes have been observed in strengthened RC beam which depend on various parameters. If both, steel and FRP reinforcement ratio are small, steel yielding may be followed by rupture of the composite reinforcement. If FRP reinforcement ratio is large the failure is due to concrete crushing on the compression side while the steel may yield or not. These modes of failure are known as flexural failure and depend on the amount of tensile reinforcement and mechanical properties of materials (Hutchinson and Rahimi, 1996; Chajes et al., 1994; Picard et al. 1995). The strength of the structure showing flexural failure can be predicted by theory. This theory is based on the strain compatibility

method assuming the uniformity of the section and the perfect bond between concrete and composite (Triantafillou and Plevris, 1992; ISIS Canada, 2000; Ross et al. 1999).

To obtain local flexural behaviour and to predict the entire load deflection response of the reinforced concrete beam up to the ultimate failure, the behaviour of the hybrid beam was simulated numerically using finite element method (Nitereka and Neale, 1999). In these studies the non-linearity of the material properties was considered and the effect of different parameters on the overall behaviour of the beam was investigated. These models can predict general behaviour and flexural mode of failure of strengthened beam and showed good agreements with the experimental results.

Due to limited strain capacity of concrete and linear elastic behaviour of composite, reinforced concrete beam strengthened by composite makes a hybrid beam which exhibits a brittle failure mode. The ductility for the hybrid beam can be defined as the ability of the member to undergo large deflections to failure, so that high deformation before failure would give the necessary warning of upcoming collapse (Razagpur and Ali, 1996). To develop a ductile failure mode, in the design of hybrid beam, it is recommended that steel yielding occurs before composite rupture in tension or concrete rupture in compression. (Meier and Kaiser, 1991).

Other types of failures of hybrid beam observed in experimental works reported in the literature are shear failure and debonding mode of failure. These failure modes cannot

be predicted by theory and they also depend on the parameters like existing shear reinforcement and composite geometry. When tensile reinforcement ratio of RC beams is increased by adding composite to its tension face, shear failure of the structure may occur before reaching the flexural strength of the beam. Experimental investigation show that when RC beams does not have enough reinforcement in shear, shear failure can occur at relatively low loads, by development of shear diagonal cracks in shear span of the beam. To avoid this mode of failure, shear capacity of RC beam should be evaluated before strengthening and shear reinforcement should be added if necessary.

Debonding mode of failure has been observed by many authors (Bonacci, 1996; Deblois et al., 1992; Malek et al. 1996). In this mode of failure, composite delaminates from concrete surface in a sudden and unpredictable manner. When composite delaminates from concrete surface the structure is no longer able to support load and collapses in a sudden and catastrophic manner. Debonding mode of failure is brittle. Different mechanism has been reported to cause delamination; debonding may occur by (i) sudden propagation of cracks at the interface, (ii) shear failure of concrete layer between the FRP and steel longitudinal reinforcement. In many cases, the second mechanism of debonding occurred at the composite plate curtailment zone. Since the transition zone at the end of the plate creates a region of high bond stress, composite sheet peels off due to high stress concentration at the plate end which can proceeds away from the support and leads to development of shear critical crack and premature

failure. This mode of failure is likely to happen when composite is thick. To prevent this mode of failure, different anchorage techniques were suggested (Arduini et al. 1996; Varastehpour and Hamelin, 1996; Spadea et al., 1998). Although the experimental results reported show that by carefully positioning external anchorage the ductility of the hybrid beam can be increased, the failure mode of debonding cannot be eliminated, and composite separates from concrete surface between the anchored areas. Debonding mode of failure cannot be predicted by theory and prevents the hybrid structure to attain its maximum capacity. Unpredictable delamination mode of failure limits the application of this method of reinforcement so that the safe maximum capacity of the structure is limited.

The main objective of this study is to investigate the premature mode of failure of debonding and to emphasise on the choice of composite material to achieve a ductile mode of failure of the hybrid beam. Test results of beams strengthened with carbon fibre reinforced plastic (CFRP) and glass fibre reinforced plastic (GFRP) laminas are presented and to study composite-concrete interface failure, the loading points and amount of composite reinforcement were varied.

3.3 Experimental program

A total of six reinforced concrete beams were tested in this study. The experimental program is summarised in Table. 3.1. The experimental program reported in this paper

is part of a larger program in which concrete beams were molded in four batches. Here the flexural testing of beams from batch 1 and 4 is reported. Test results on other beams are reported somewhere else. All the beams had the same overall dimensions and they also had the same internal longitudinal steel reinforcement and stirrup arrangements, which are shown in figure 3.1. All the beams were tested under four point flexural loading. Beam B11 was the control beam without composite reinforcement. Beam B12 was reinforced with one layer of glass-epoxy composite. To study the behaviour of composite concrete interface the loading points and composite reinforcement ratio were varied for beams B13, B41, B42 and B43 which were strengthened with one layer and two layers of carbon epoxy composite. Beams B41, B42 and B43 were slightly over reinforced in shear, to prevent shear failure of the structure.

3.3.1 Beam design and fabrication

As shown in figure 3.1., the beams were 150x200 mm in cross section and 2000 mm long. The beams were reinforced with two M10 steel bars at the tension side. The basic reinforced concrete beam (RC beam) was designed according to ACI Code 318-92 to fail in flexure. To represent a beam designed with insufficient flexural steel, the steel reinforcement ratio was chosen low ($A_{steel/bd}$=0.007). Before applying composite to the concrete surface, the surface of the concrete was sandblasted to remove laitance and to expose aggregates. The surface was then primed by Sikadur Hex 300 epoxy.

SikaWrap Hex 103C, unidirectional carbon and SikaWrap Hex 100G unidirectional glass fabrics were impragnated with Sikadur Hex 306 epoxy resin in laboratory using hand lay-up technique and right after, laminated directly on the primed concrete surface. The composite was left to cure on the beam surface in the laboratory conditions for two weeks before final testing. The CFRP and GFRP single layers had the same dimensions of 1 mm thick, 190 mm width and a length of 1760 mm.

3.3.2 Materials

3.3.2.1 Concrete and steel

One concrete mix with an average 28 days compressive strength of 35 MPa was used to mold the reinforced concrete beams in three batches. Type 10 Portland cement with no admixture was used and the maximum aggregate size was 20 mm. The ratio of cement/ sand / water/ aggregate in the mortar mix was 1/2/0.5/3 by weight. Cast RC beams were moist cured for one week and let to cure in the laboratory conditions. For each batch, four 152x305 mm(6 x 12 in) concrete cylinders were cast and tested according to ASTM C39-94 and ASTM C469-94 procedures to determine the compressive strength, modulus of elasticity and Poisson's ratio of concrete. Also, for each batch, samples were molded to determine the modulus of rupture and the splitting tensile strength of the concrete, according to standard procedures ASTM C496-96 and ASTM C78-94 respectively. These properties are summarised in table. 3.2. The concrete has an average cylinder compressive strength of 43.53 MPa and average

modulus of elasticity of 27.96 GPa. The steel rebars were tested in the laboratory. They have a yielding strength of 456 MPa and an ultimate strength of 734 MPa. The beam testing as well as the standard characteristic tests were conducted at the same time, one year after concrete casting.

3.3.2.1 Composite

To measure the composite properties, one layer of carbon fabric and one layer of glass fabric were respectively impregnated with epoxy using hand lay-up technique and let to cure in laboratory conditions for two weeks. The thickness of the cured laminas were measured at 1mm for both types of composite. These CFRP and GFRP lamina were tested for tensile properties according to ASTM D3039 testing procedure. The measured mechanical properties are summarised in table. 3.3.

3.3.2.2 Beam testing

All the beams were tested under four point bending over an effective span of 1800 mm, with the load applied symmetrically at either side of midspan, as shown in figure 3.1. The loading position was varied as can be seen in table 3.1. The load was applied gradually until failure occurred in one cycle. The mid span deflection was measured using LVDT. Electrical strain gages were used to measure the strains at mid span of the rebars, of the composite lamina and of the concrete on the extreme compression

side of the beam. Computer controlled instrumentation were used to record the loads at regular intervals.

3.3.3 Test results

Figure 3.2. shows the load deflection behaviour of control beam compared to strengthened beams. As we can see the ultimate load carrying capacity and stiffness of composite strengthened RC beams are higher than un strengthened control beam. The flexural cracks are formed initially at the constant moment region of the beam, when the tensile strength of the reinforced concrete is reached. Before concrete cracks in tension (point 1) the composite has almost no effect on the flexural rigidity of the beam, that is because the second moment of inertia of the section is hardly changed by composite. After concrete cracking in tension, the post cracking stiffness which can be defined by the straight line between point1 (first crack load) and point 2 (steel yielding point) is highly increased compared to RC control beam. This is because the composite provides a mechanism by which the concrete between the cracks can contribute to the support of tensile stresses. The degree of increase depends on the composite material properties. The post-cracking stiffness of the CFRP strengthened beam is higher than that of the GFRP strengthened beam. This increase becomes more significant after the steel yielding point. After steel yielding, the composite continues to support load. Flexural rigidity of the strengthened beam is much higher than the non strengthened control beam.

Although the general behaviour of the CFRP and GFRP strengthened beam was the same, they showed different final modes of failure. The GFRP strengthened beam failed by concrete failure on the compression side after internal steel yielding, as is shown in figure 3.3a. The compression failure of the concrete happens shortly before complete structural failure by gradual crack development in compression side and leading to high deformation at failure. So the failure mechanism is relatively ductile and did not have a catastrophic collapse. The CFRP reinforced beam failed by debonding of the composite in the constant moment region, showing highly reduced deflection at failure compared to the GFRP strengthened beam and control beam. Experimental result shows that debonding in the constant moment region occurs at the position of widest crack, as shown in figure 3.3b.The widest crack at the constant moment region, causes interface failure when opening. The crack at this location progressed in the concrete and caused the isolation of a layer of concrete which diminishes further to a thin layer. The failure characterised by debonding is followed by the rupture of the composite reinforcement in a sudden and catastrophic manner.

Figure 3.4. shows the composite strain for the GFRP and CFRP reinforced beams. As can be seen the composite does not attain its maximum capacity and ultimate strain at failure. Before concrete cracking in the tension zone, the rate of strain developed in the composite is low indicating that the concrete is supporting a large proportion of the tensile bending moment. The strain rate developed in composite increases after the concrete cracking in tension. The different post-cracking slope of the load

displacement curves and before yielding of steel indicates that the nature of stress transfer between the composite and concrete depends on the composite material properties and cracking pattern which is obviously different for the two beams.

Figure 3.5. shows load deflection curve for beams B41 having one reinforcement layer and B43 having two reinforcement plies, reinforced with two different number of layers. The ultimate deflection of the hybrid beams is the same, despite the fact that the ultimate load and the steel yielding point of the beam with thicker reinforcement is higher than the ultimate load of the single plied reinforced beam. The post cracked stiffness is also the same for both beams.

Figure 3.6 and figure 3.7. show the concrete strain and composite strain at mid span for the same two beams. It can be seen that these beams reached their ultimate capacity before reaching the CFRP ultimate strain and concrete compression strength. These figures show that beam B43 shows lower composite strain and higher concrete compression strain at failure compared to beam B41, that is because the additional tensile component of the internal tensile moment supported by the higher composite reinforcement ratio of B43 is resisted by an equal force on the compression side. Failure of both beams occurs after internal steel yielding and because of composite debonding from concrete. Debonding occurs in the shear span, close to the loading point, at the position of relatively high and rapidly changing bending moment as it can be seen in figure 3.8a. and figure 3.8b. Shear cracks developed at this point propagate

in concrete towards the constant moment region. Debonding occurs in a sudden unpredictable manner. Concrete crushed in compression side and composite failed in tension side shortly after debonding took place and the beam collapsed.

Beam B42 and B43 had the same design parameters but they had different length of shear span. The measured load-deflection and moment-deflection for these beams, are shown in figures 3.9 and 3.10. As can be seen, the failure of B42 (shear span to depth ratio of 3,75) occurs at higher loads and the same moment compared to B42 (shear span to depth ratio of 5). Both beams show approximately the same deflection at failure. The failure of these beams is caused by debonding of the composite. Debonding occurs in a sudden and brittle manner, and concrete crushes shortly after debonding on the compression side. The beams could not carry extra load after debonding and both beams failed in a catastrophic unpredictable manner. Delamination of composite from concrete surface occurred at shear span. For B42, interface crack originated at a crack tip close to the support and extended towards the support, figure 3.8c. On the other side it entered into the concrete, oriented in the direction of shear crack, moves towards higher moment region along the internal steel reinforcement. The position of debonding for B43 is closer to the loading position, it enters into the concrete and moves towards constant moment region as it is shown in figure 3.8b.

Figure 3.11 shows the load versus strain in CFRP for these beams. The strain in the composite increases almost linearly. The measured strain at failure for B43 is smaller than the one for B42. Load versus strain in the extreme compression fibre of concrete for both beams is shown in figure 3.12. Again we can see that the concrete strain on the compression side at failure is slightly higher for beam B42.

The measured strain distribution through the depth at the mid-section of the beam and the position of the neutral axis at different loads for the beam B41 is shown in figure 3.13. The vertical axis represents the beam depth while the horizontal axis represents strain. The intersection of the straight line joining the strains in concrete in the compression side and composite and steel in the tension side, with the vertical line at zero gives the location of the neutral axis which moves up slightly during the various phase of loading and fracture. After the concrete reaches the tensile cracking (load, 12kN), the neutral axis rises quickly. Around the steel yielding point (load,78 kN) the position of the neutral axis is almost fixed. Beyond the steel yielding point, the neutral axis moves up again. As the load is increased, tensile strains in composite and concrete continue to increase till final rupture occurs.

Figure 3.14 shows strain distribution across the depth corresponding to the steel yielding point for GFRP and CFRP reinforced beam compared to the control beam. It can be seen that the position of the neutral axis is lower for the composite reinforced beams at the steel yielding point showing the fact that a portion of the tensile moment

is supported by the composite. Since the beams are under-reinforced, the rupture is accompanied by extensive cracking in the tension side. Tensile strain towards the base of the section which represents the strain in the concrete and accumulation of crack widths, is higher for GFRP reinforced beam compared to CFRP reinforced beam. Figure 3.15 shows strain distribution through the depth at failure for the four CFRP strengthened beams. The location of the neutral axis varies based on the amount of composite in the cross section. We can see that neutral axis is lower for hybrid beams reinforced with two layers of CFRP. Extra tensile reinforcement increases the capacity of the beam and keeps the neutral axis down.

3.4 Theory

Flexural strength of the hybrid beam is calculated using strain compatibility method (ISIS Canada). The theory is based on the assumptions that plane section before bending remains plane after bending, tensile resistance of the concrete may be neglected and perfect bond exists between the concrete and composite. Considering uniformity of the section and applying geometrical conditions as it is illustrated in figure 3.16 we may write:

$$\frac{\varepsilon_{cu}}{c} = \frac{\varepsilon_s}{d-c} = \frac{\varepsilon_{frp}}{h-c} \qquad (3.1)$$

where ε_c, ε_s, ε_{frp} are the concrete, steel and composite strains respectively, c is the distance from extreme compression face to the neutral axis in millimetre, d is the distance from extreme compression face to the centeriod of tension steel reinforcement and h is the overall depth of the beam in millimetre. Equilibrium of forces on the section gives:

$$C_c = \alpha_1 f_c' \beta_1 c b \tag{3.2}$$

C_c is the internal force due to compression in concrete in Newton, f_c' is the compressive strength of concrete in MPa, b is the width of the beam in millimetre, α_1 and β_1 are the coefficients defined in design codes for RC structures by the following equations:

$$\alpha_1 = 0.85 - 0.0015 f_c' \geq 0.67 \tag{3.3}$$

$$\beta_1 = 0.97 - 0.0025 f_c' \geq 0.67 \tag{3.4}$$

$$T_s = A_s f_y \tag{3.5}$$

$$T_{frp} = A_{frp} E_{frp} \varepsilon_{frp} \tag{3.6}$$

$$f_{frp} = E_{frp}\varepsilon_{frp} \tag{3.7}$$

T_s and T_{frp} are the internal forces due to tension in steel reinforcement and composite reinforcement respectively, A_s and A_{frp} represent area of steel and composite material respectively. E_{frp} is the modulus of elasticity of composite, f_{frp} is the composite tensile stress , f_y is steel yielding point and f_s in figure 3.16 represents steel tensile stress correspondingly. Combining geometry conditions and equilibrium equations the position of the neutral axis can be computed by the following equation:

$$\alpha_1 f'_c \beta_1 bc = f_y A_s + E_{frp} A_{frp} \varepsilon_{frp} \tag{3.8}$$

finally the nominal resistance in flexure can be determined by the following equation:

$$M_n = f_y A_s (d - \frac{a}{2}) + E_{frp} A_{frp} \varepsilon_{frp} (h - \frac{a}{2}) \tag{3.9}$$

where:

$$a = \beta_1 c \tag{3.10}$$

In equation (9) a is the depth of equivalent of concrete stress block in figure 3.16 and M_n is the nominal moment capacity of the beam. The above equations demonstrate the state of the hybrid beam at failure. Assuming a flexural failure mode (composite tensile failure or concrete compression failure after steel yielding) the position of the neutral axis at failure is obtained with equation 3.8. The assumption must be checked with geometrical conditions.

Table 3.4. summerizes the ultimate moment capacity, neutral axis position and composite strain at failure, calculated by the strain compatibility method as explained above and the values obtained experimentally. Theoretical values were calculated assuming concrete failure in compression after steel yielding. For GFRP reinforced beam the predicted failure mode was like the one observed experimentally. However, all CFRP strengthened beams failed by delamination at moments lower than the theoretically predicted values. Strain compatibility method evaluates a higher position for neutral axis at failure which overestimates the strain developed in CFRP at failure. This is because in theory we assume no concrete in tension while in reality CFRP bridges the cracks and concrete supports some tensile load between cracks and the moment of inertia of the section is greater than the theoretical value. For GFRP strengthened beams it is not the same, which is because of lower modulus of elasticity of GFRP. The GFRP strain obtained theoretically is very close to ultimate GFRP tensile strain GFRP (2%) indicating that , by theory, the compressive failure of concrete and tensile failure of GFRP occur almost simultaneously.

3.5 Discussion

When reinforced concrete beams strengthened with composite material is loaded under flexure, at relatively low loads, flexural cracks are produced in the concrete on the tension side of the hybrid beam. Then the tension is transferred from concrete to composite through interface. The tensile stresses supported by the composite are not uniform across the length. They are higher at the locations of a flexural crack, where the tension in the concrete is zero as illustrated in figure 3.17. At a crack, a short length of the interface is subjected to higher stresses than its surroundings and stress in the composite at a crack location rises to a peak. A stress concentration is induced at the interface when crack opens in the concrete which causes a short length of composite be debonded from the concrete. The strain in the composite across the crack is very large. Thus at each side of the crack, for a certain distance, a transfer length is required to build up the tensile stress in the concrete surrounding the composite. The composite can not yield to distribute the strain along its length and a bond failure crack will propagate along the interface. Also on each side of the crack, a transfer length is required to build up the tensile stress in the concrete surrounding the composite, this tensile stress may rise to a peak high enough to cause interface crack propagation in the concrete.

The reason for bond failure is not only the bond characteristics of the FRP and concrete surfaces, in fact if concrete and composite surfaces are extremely rough so

that the bond strength is theoretically infinite, the interface will fail by snapping at the crack location. Debonding occurs when composite-concrete interface resistance is exceeded. The interface fails by crack propagation at crack location. Crack propagation at the interface cause premature failure of the structure.

Failure of composite-concrete interface of a strengthened RC member occurs under combined stresses resulting from an applied shear force and bending moment. As the load increased, the new cracks develop and composite-concrete surface should transfer and support more shear stress. In shear span, flexural load creates a non uniform stress distribution along the length. As the concrete cracks, the average interface transferring the bending stress to the composite reduces meanwhile the tensile stress supported by the composite increases because of ineffective concrete in supporting extra tensile moment. Progressive cracking in the tension zone, prevents a uniform distribution of shear stress at the composite-concrete interface. Interface failure originated from a crack tip in the shear span can propagate in the concrete, causing a thick piece of concrete be separated from the beam.

So an interfacial crack initiates at the location of a principal crack, which is apparently random, and propagates whenever the stress state at the interface exceeds interface resistance. The mechanical properties of concrete and composite affect the formation of stress concentration at the location of a crack.

3.6 Conclusion

In this research the performance of reinforced concrete beams strengthened in flexure by composite laminate was investigated. Experimental results show that the stiffness and strength of the RC beam are increased by using composite as the external reinforcement. The strength and mode of failure of hybrid beam depend on composite material type and its reinforcement ratio. Higher strength can be obtained while attaining acceptable ductility in the sense of ultimate deflection. The strength of hybrid beam is less sensitive to the increase in composite material rigidity, due to debonding mode of failure. Debonding mode of failure cannot be predicted using strain compatibility method. Structures that are designed for flexural failure of concrete compression failure in compression side or composite failure in tension side after internal steel yielding, may experience structural failure by composite-concrete interface failure. This mode of failure can be traced to stress concentrations on generated localised damage. The rigidity and thickness of the plate have an important influence on the strength of the hybrid beam failed by delamination.

Due to the difference in the properties of the individual materials and to practical conditions of loading, cracking of the interface involves mixed mode of fracture effects. It is necessary to study the crack, once initiated at the interface, to propagate along the interface versus to penetrate into the second material. This study is essential to obtain the interface resistance and to optimise the structural behaviour of the

composite strengthened beam. To retain structural safety the brittle mode of failure should be prevented and the rupture should be predictable.

3.7 Acknowledgement

The authors wish to thank Sika Canada for providing free composite materials including carbon and glass fibres and epoxy resin. Also the authors gratefully acknowledge the technical support of Mr Mario Desroches, Sika Canada technical sales representative. The experimental program of this research were carried out at the structure laboratory, of École Polytechnique de Montréal. The authors wish to express their appreciation to Mr Gérard Degrange, structure laboratory director and laboratory technicians for their valuable assistance.

3.8 References

ARDUINI, M., DI TOMMASO, A., MANFRONI, O. NANNI, A. (1996). Failure mechanisms of concrete beams reinforced with FRP flexible sheets. Advanced composite materials in bridges and structures , M. El Badry, The Canadian Society for Civil Engineering, 253-60.

BONACCI, J.F., (1996). Strength, failure mode and deformability of concrete beams strengthened externally with advanced composites, Advanced composite materials in bridges and structures, M. El Badry, The Canadian Society for Civil Engineering, 419-26.

CHAJES, M.J., THOMSON JR. TA., JANUSZKA. TF., FINCH. JR. WW. (1994). Flexural strengthening of concrete beams using externally bonded composite materials. Construction and Building Materials, 8, 191- 201.

DEBLOIS, M., PICARD, A., BEAULIEU, D., (1992). Renforcement de poutres en béton armé a l'aide de matériaux composites: études théorique et expérimental. Advanced composite materials in bridges and structures, M. El Badry, The Canadian Society for Civil Engineering, 265-75.

HUTCHINSON, AR., RAHIMI, H. (1996). Flexural strengthening of concrete beams with externally bonded FRP reinforcement. Advance composite materials in bridges and structures, M. El Badry, The Canadian Society for Civil Engineering, 519-26.

ISIS CANADA, Strenghtening reinforced concrete structures with externally-bonded fiber reinforced polymers, spring 2000.

MALEK, AM., SAADATMANESH, H., EHSANI, MR., (1996). Shear and normal stress concentrations in RC beams strengthened with FRP plates. Advanced composite materials in bridges and structures. 629- 37.

MEIER, U., (2000). Composite materials in bridges repair. Applied Composite Materials, 7, 75-94.

MEIER, U., KAISER, H., (1991). Strengthening of structures with CFRP laminates. Proceedings of the specialty conference on advanced composites materials in civil engineering structures, 224-232.

NITEREKA, C., NEALE, K.W., (1999). Analysis of reinforced concrete beams strengthened in flexure with composite laminates, Can J Civ Engng 26 , 646-54.

PICARD, A., MASSICOTTE, B., BOUCHER, E., (1995). Strengthening of reinforced concrete beams with composite materials: theoretical study, Composite Structures, 33, 63-75.

RAZAGPUR, AG., ALI, MM., (1996), Ductility and strength of concrete beams externally reinforced with CFRP sheets. Advanced composite materials in bridges and structures, 505-512.

RITCHIE, PA., THOMAS, DA., LU, LW., CONNELLY, GM., (1991), External reinforcement of concrete beams using fiber reinforced plastics, ACI Struct J, 88(4) , 490-500.

ROSS, CA., JEROME, DM., TEDESCO, JW., HUGHES ML., (1999), Strengthening of reinforced concrete beams with externally bonded composite laminates. ACI Struct J. 96(2), 212-220.

SAADATMANESH, H., EHSANI, MR., (1991), RC Beams strengthened with GFRP plates. I- experimental study, J of Struct Engng, 117(11), 3417-3433.

SIKA CANADA INC., (1998), Sika Carbodur, Engineering guidelines for the use of CarboDur (CFRP) laminates for structural strengthening, first edition.

SPADEA, G., BENCARDINO, F., SWAMY, RN., (1998), Structural behavior of composite RC beams with externally bonded CFRP. J Composites Construction, 2(3), 132-37.

TRIANTAFILLOU, TC., PLEVRIS, N. (1992). Strengthening of RC beams with epoxy-bonded fibre-composite materials. Materials and Structures; 25 , 201-211.

VARASTEHPOUR, H., HAMELIN, P., (1996). Experimental study of RC beams strengthened with CFRP plate. Advanced composite materials in bridges and structures, 555-563.

Table 3.1 Experimental program

Beam	Composite type	Number of composite layers	Loading
B11 (control beam)	-	-	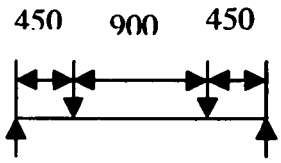
B12	GFRP	1	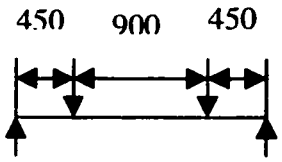
B13	CFRP	1	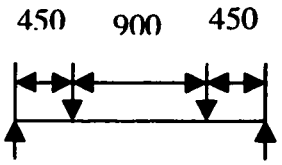
B41	CFRP	1	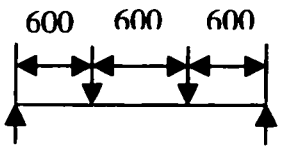
B42	CFRP	2	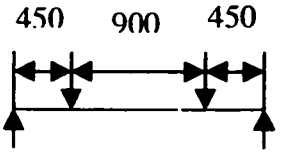
B43	CFRP	2	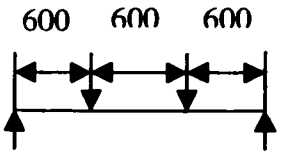

Table 3.2 Concrete Mechanical Properties

Batch No.	Compressive strength MPa	splitting Tensile strength MPa	Modulus of rupture MPa	Modulus of elasticity GPa	Poisson's ratio
1	44.75	3.9	6.41	28.1	0.17
4	42.31	3.76	6.08	27.82	0.2
Average	43.53	3.83	6.26	27.96	0.19

Table 3.3 Mechanical properties of composites

Composite	Fibre volume fraction	Longitudinal tensile strength, Mpa	Longitudinal modulus of elasticity, GPa	Strain at failure
GFRP	50%	400	20	2%
CFRP	50%	640	64	1%

Table 3.4 Structural response of the beam

Beam	Ultimate moment, N-m, Theo.	Ultimate moment, N-m, Exp.	N.A.* Position, mm, Theo.	N.A.* Position, mm, Exp.	Composite strain, Theo.με	Composite strain, Exp. με
B12	19977	19962	26	20	0,019	0,014
B13	25298	20826	39	41	0,0098	0,006
B41	25298	23400	39	40	0,0098	0,006
B42	35796	30888	47	50	0,0076	0,006
B43	35796	31000	47	55	0,0076	0,005

* Neutral axis position, 'c' in Fig. 16.

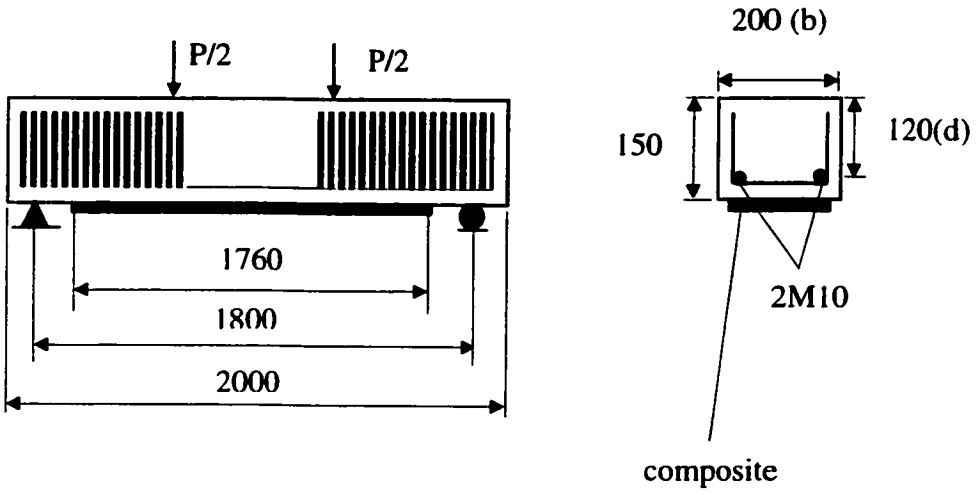

Dimensions in mm

Figure 3.1 Beam design and geometry

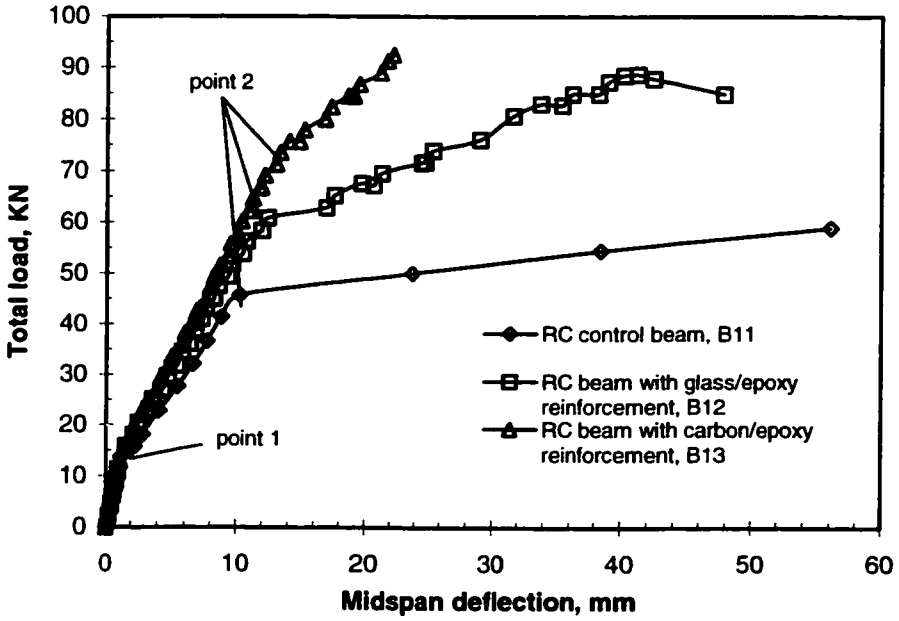

Figure 3.2 Total load versus mid span deflection of RC control beam, GFRP and CFRP strengthened beams (point 1: first crack load, point 2: steel yielding point)

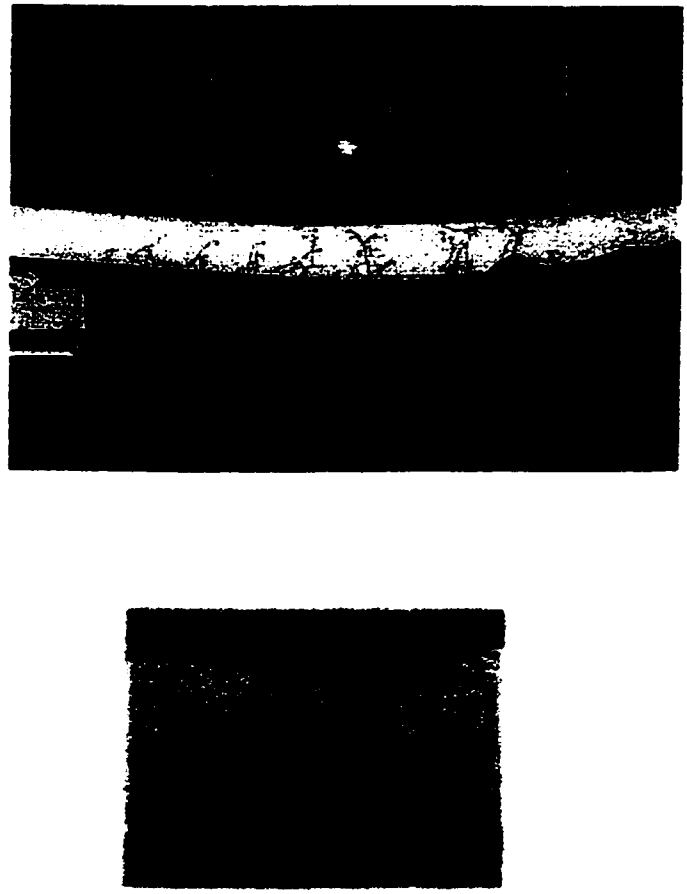

(A)

Figure 3.3 Failure pattern, (A) compression failure of concrete in GFRP strengthened beam

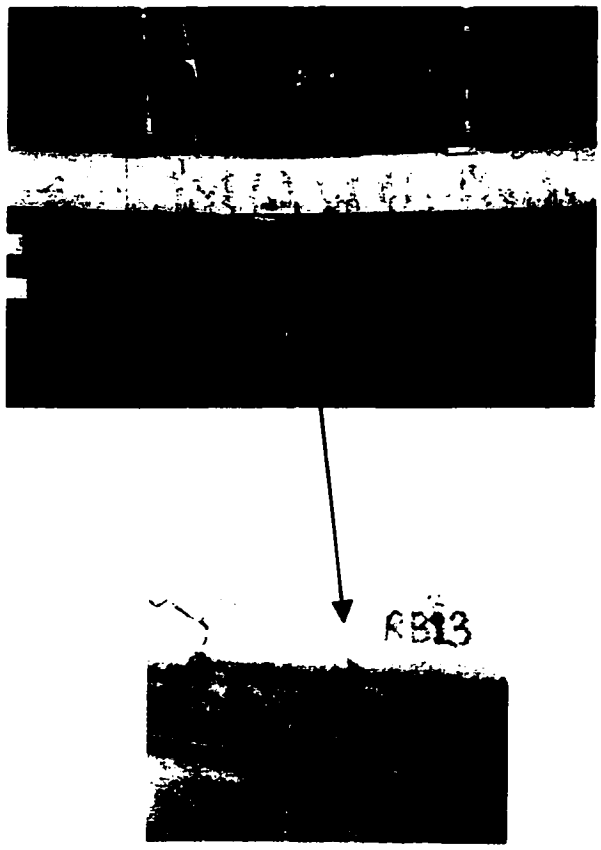

Figure 3.3 Failure pattern, (B) debonding failure mode of CFRP strengthened beam

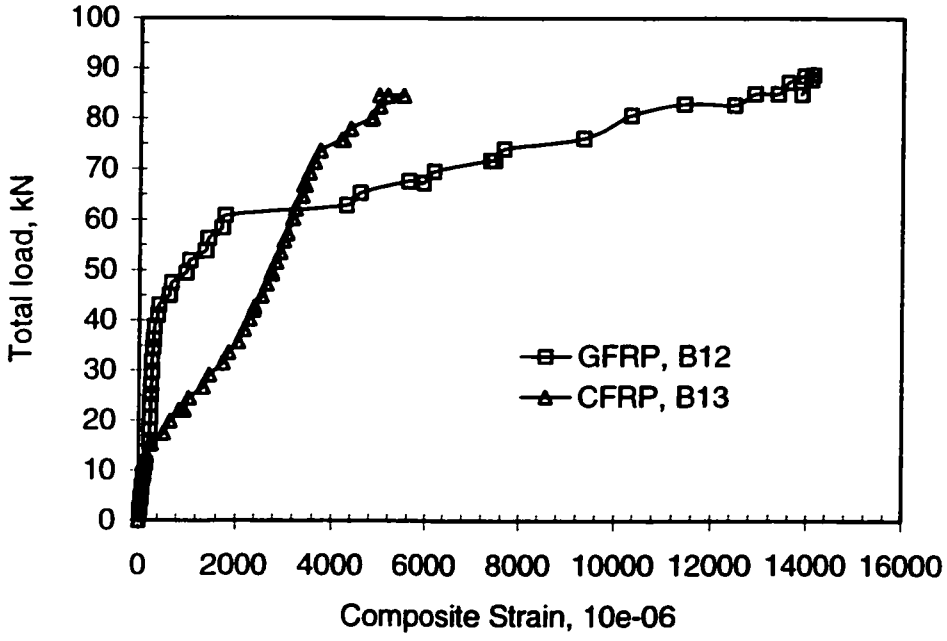

Figure 3.4 Composite tensile strain at various applied load levels measured at mid span

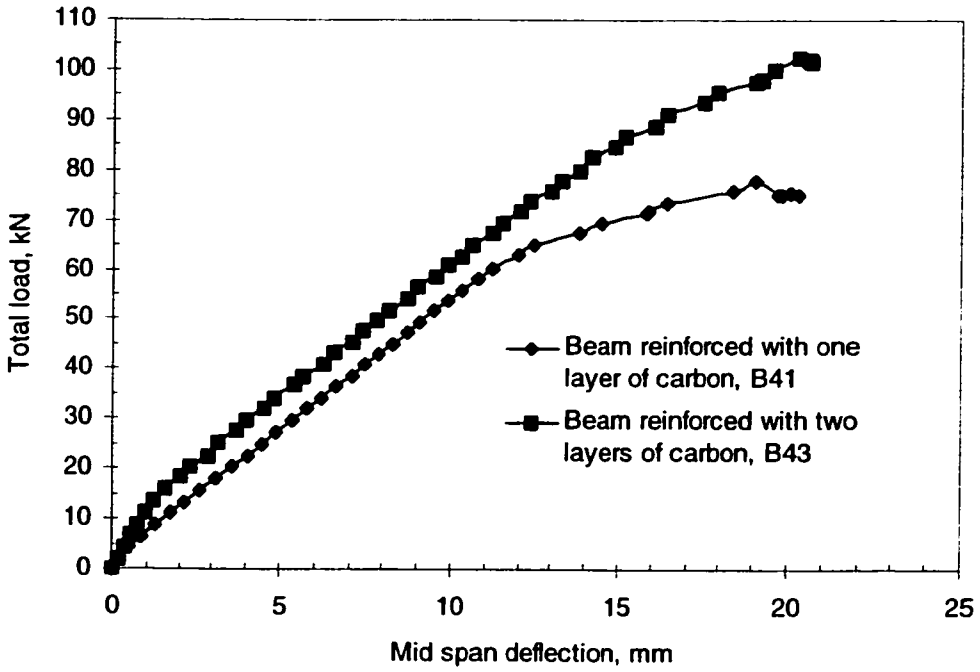

Figure 3.5 Deflection responses to applied load of beams with one layer and two layers of carbon reinforcement

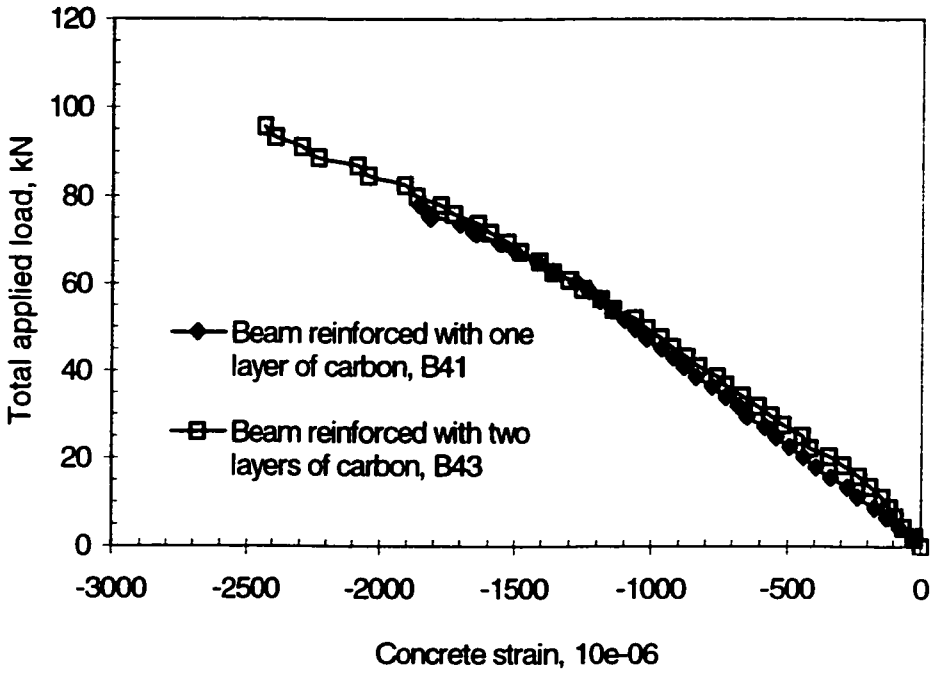

Figure 3.6 Concrete strain measured at mid span on extreme compression surface for beams reinforced with one layer and two layers of CFRP

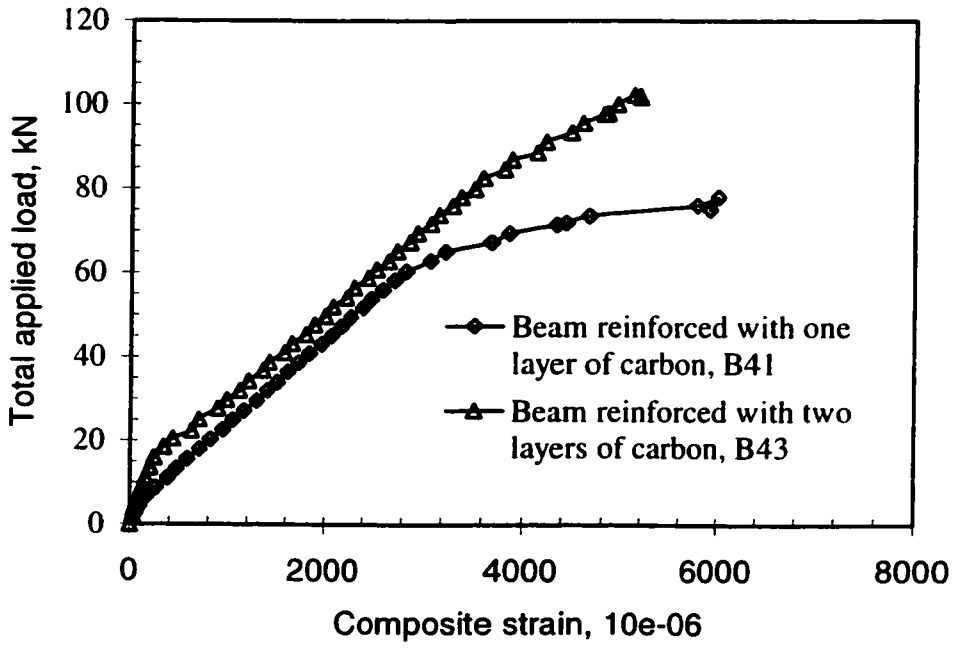

Figure 3.7 CFRP strain measured at mid span on extreme tension fibres

(a)

(b)

(c)

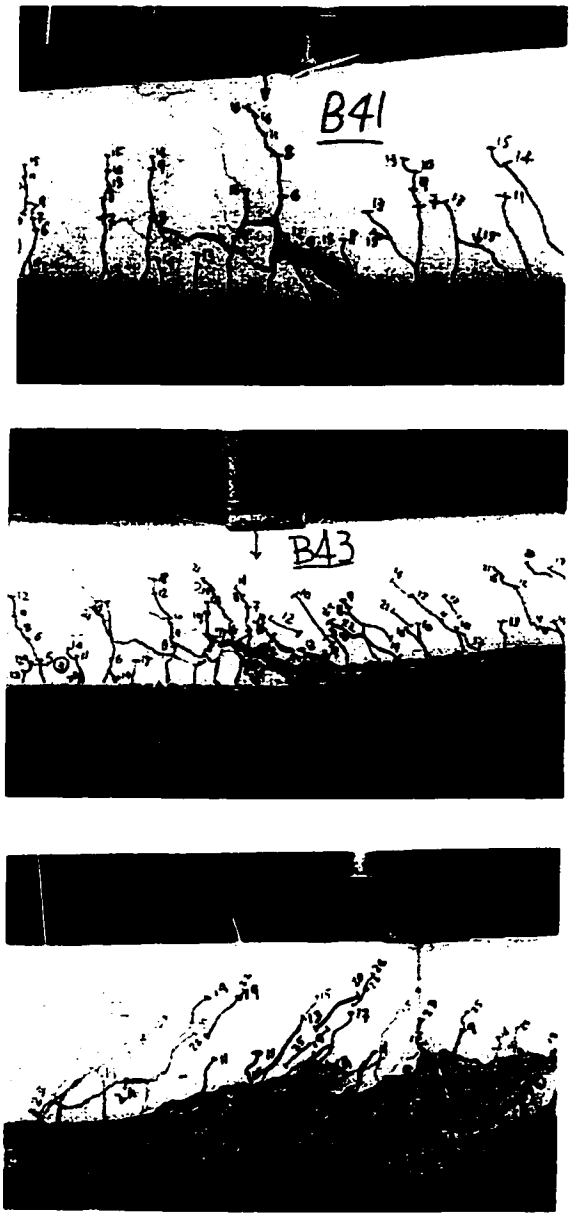

Figure 3.8 Failure pattern of beams reinforced with CFRP, (a) beam B41, (b) bam B43 (c) beam B42

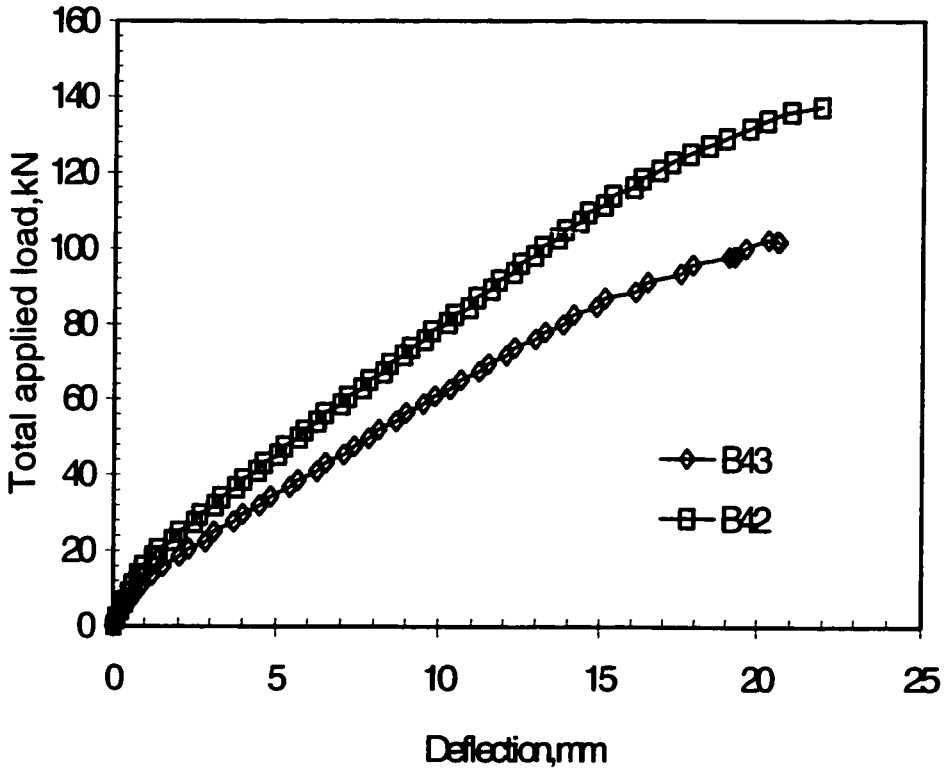

Figure 3.9 Total Load versus mid span deflection of beams strengthened with two layers of CFRP

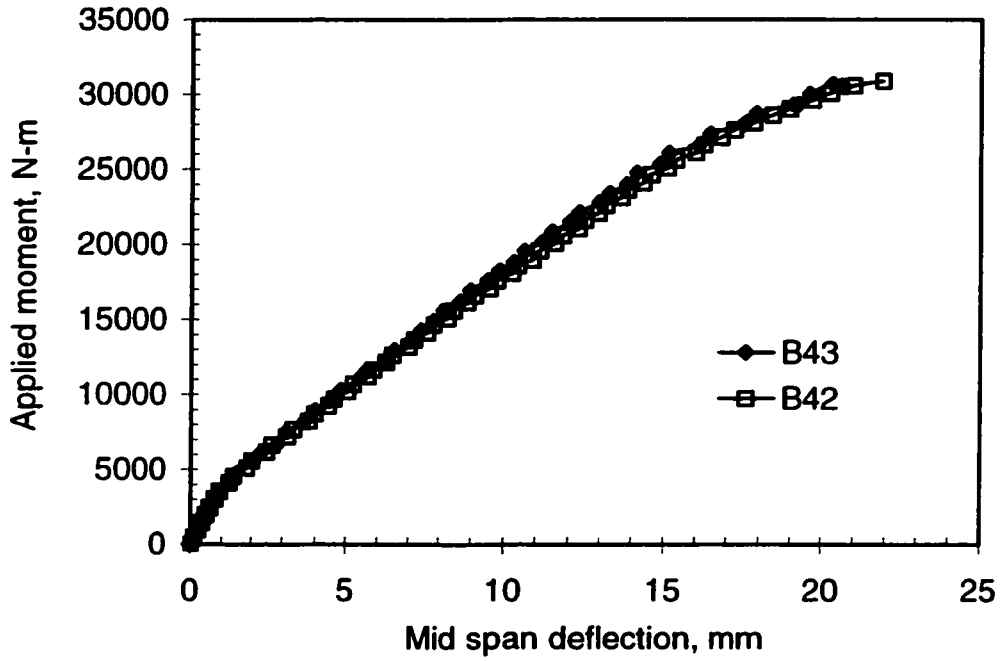

Figure 3.10 Moment versus mid span deflection of beams strengthened with two layers of CFRP

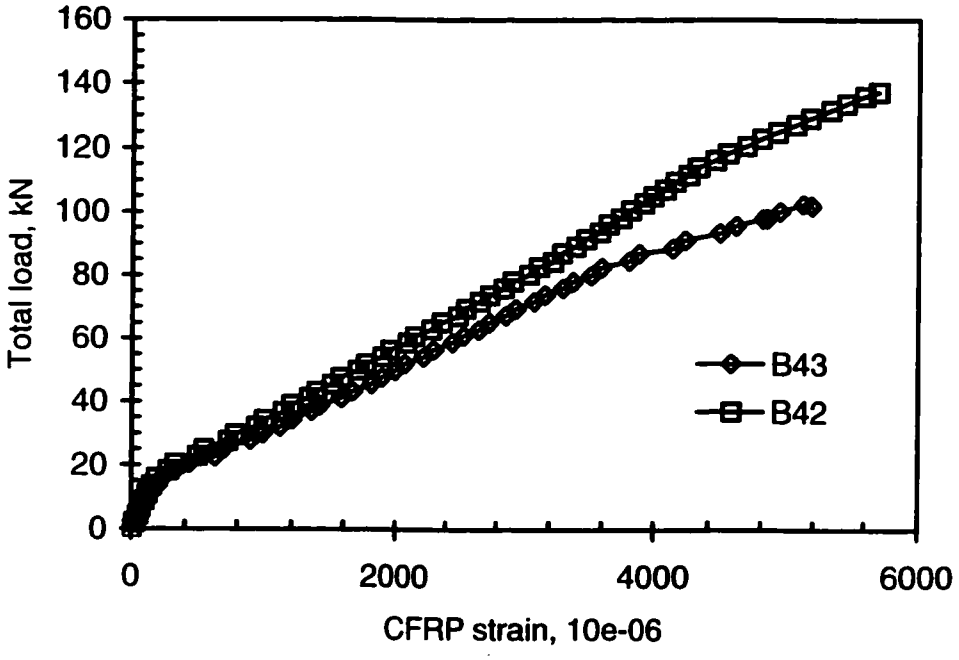

Figure 3.11 CFRP strain measured at mid span on extreme tension fibres

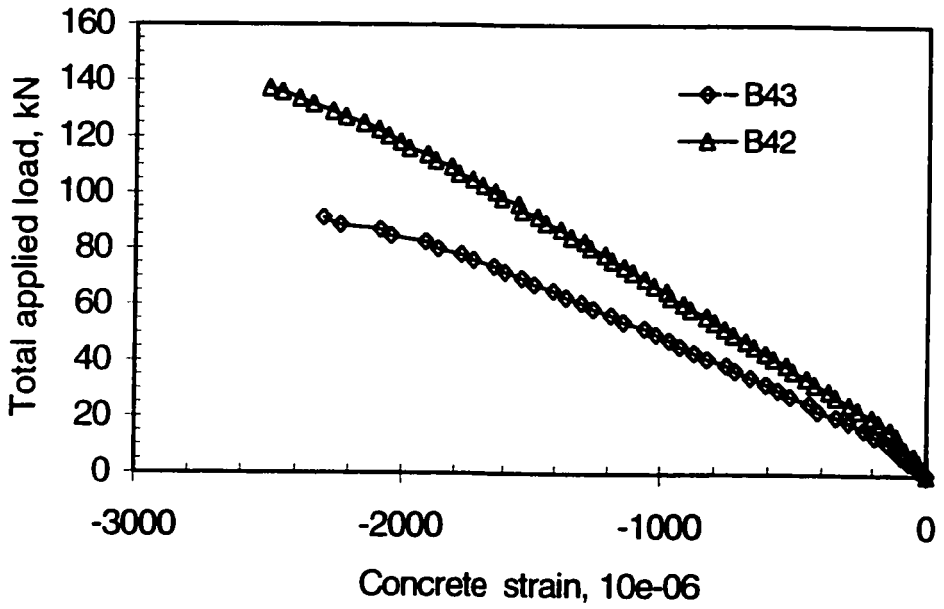

Figure 3.12 Concrete strain at mid span on extreme compression surface for beams reinforced with two layers of carbon

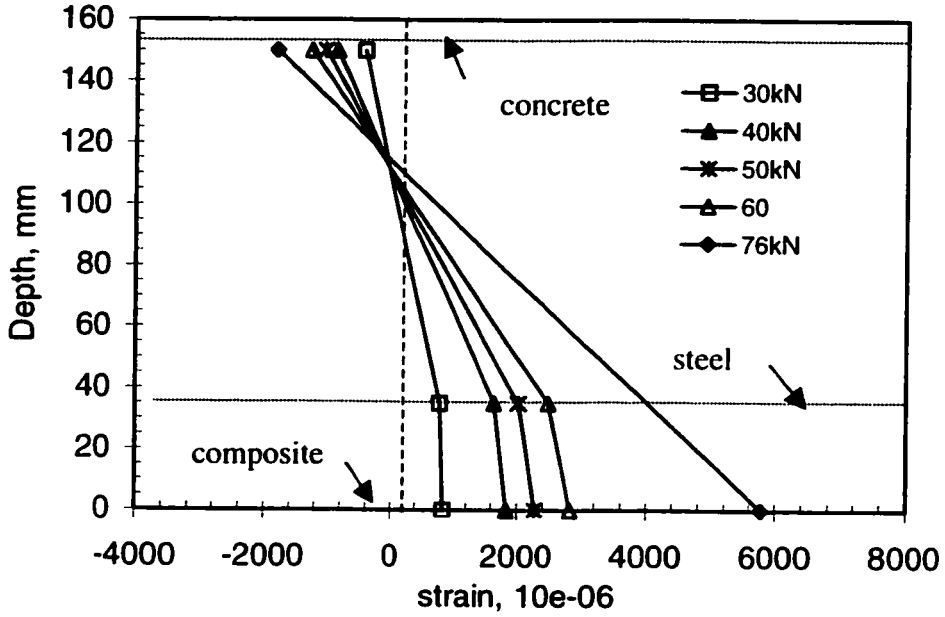

Figure 3.13 Neutral axis position at different stages of loading for beam B41

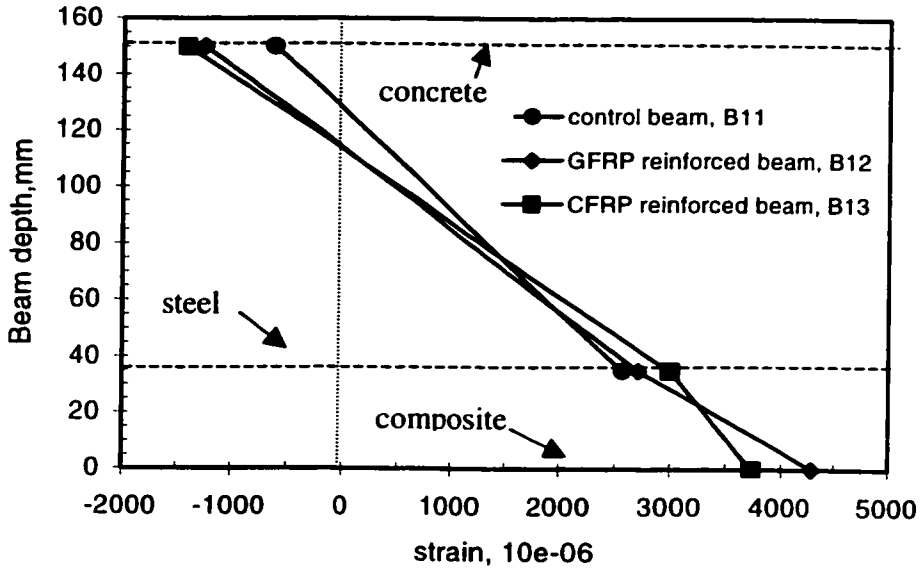

Figure 3.14 Neutral axis position at different stages of loading for control beam, GFRP reinforced and CFRP reinforced beam

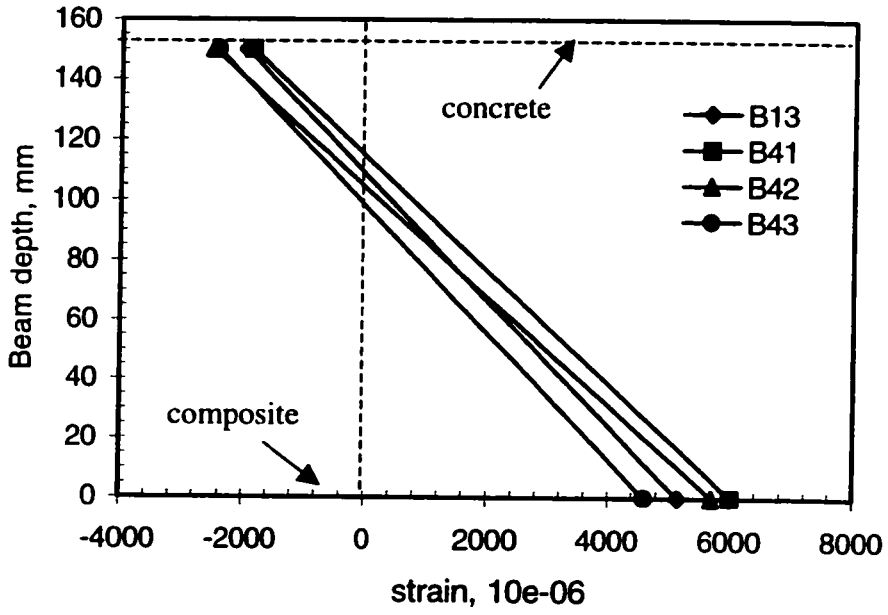

Figure 3.15 Neutral axis position at failue for CFRP strengthened beams

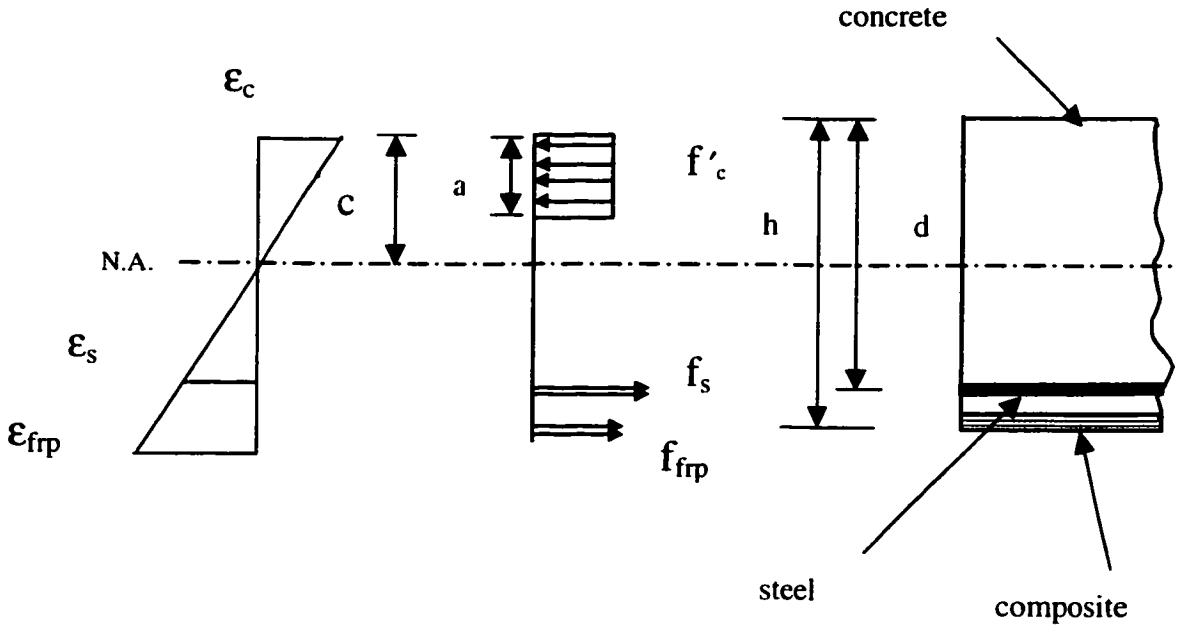

Figure 3.16 Stress distribution in beam cross section

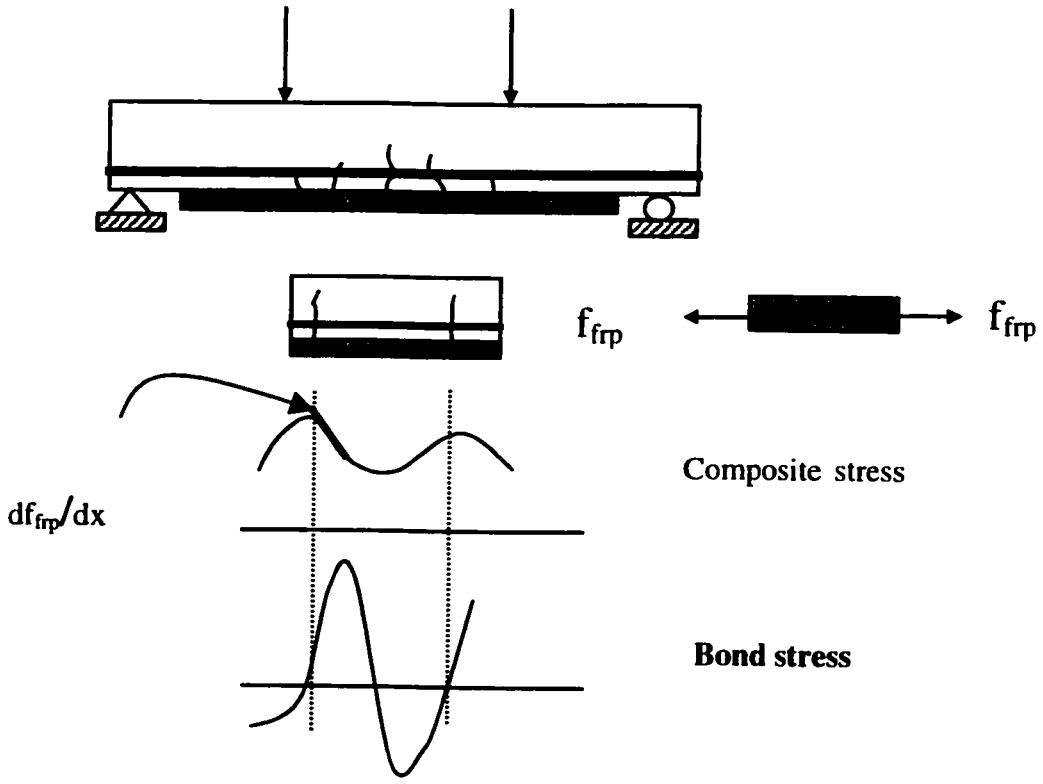

Figure 3.17 Interface stress distribution at the location of a tensile crack

CHAPITRE 4

THE EFFECT OF EXTERNAL COMPOSITE REINFORCEMENT ON THE BEHAVIOUR OF STRUCTURALLY DAMAGED RC BEAMS

Katayoun Soulati, École Polytechnique de Montréal, Canada

Raymond Gauvin, École Polytechnique de Montréal, Canada

4.1 Abstract

This paper investigates the flexural behaviour of damaged reinforced concrete beam (RC beam), strengthened externally with composite material laminated directly on the tensile side of the beam. In the experimental program, tests were carried out on nine RC beams. Some of the beams were pre-loaded to 30% and 60% of their ultimate strength before the application of carbon-epoxy and glass-epoxy composites. The behaviour of the beams are reported and compared in terms of deflection, strains, cracking and flexural stiffness. The results show that the composite layer substantially controls deflection and cracking. In spite of extensive pre-cracking before strengthening, the repaired beam preserved its structural integrity, confirming the effectiveness of this repair technique.

4.2 Introduction

The repair of structurally deteriorated reinforced concrete structures becomes necessary when the structural element cannot provide satisfactory strength and serviceability. Functional deficiency of existing RC structures could be an excessive deflection and cracking or an inadequate ultimate strength. One of the methods used to repair damaged RC structures is plate bonding technique. External reinforcement in the form of steel or composite plate or sheet is epoxy bonded to the concrete surface to upgrade its structural performance. This method of repair increases the load carrying capacity of the structure, while only minimally altering its weight and dimensions and can be applied when the structure is in use.

Research and field application of steel plates bonded to concrete have been the subject of many studies and shown to be effective (Swamy et al.1987, Jones et al., 1982), but it has the disadvantage of steel corrosion in outdoor applications which reduces the bond strength. An alternative to steel is to use of fibre reinforced polymers as strengthening material which gained interest in recent years. Composite materials have superior properties compared to steel in corrosion resistance, high strength to weight ratio and tailorability. This method has already been applied to strengthen buildings and bridges in Europe, North America and Japan (Karbhari, 2000; Meier, 2000). Bonding of composite plates on the tension face of undamaged reinforced concrete beams, has been studied by many researchers (McKenna and Erki, 1994). These

studies have shown that using composite as external reinforcement results in the reduction of deflection and increase load carrying capacity of the member. However, the composite action between concrete and composite cannot be maintained at all stages of loading. One of the major concerns in design is the reduction in ductility because of the brittle failure mode of debonding. This catastrophic mode of failure prevents the hybrid structure to attain its maximum capacity (Fanning and Kelly, 2001; Ritchie et al., 1991) and is theoretically unpredictable (Bonacci and Maalej, 2001). To prevent this mode of failure, different kinds of anchorage technique were suggested (Spadea et al., 1998).

There is only limited data published on the performance of plating technique when used to repair structurally damaged RC beams. The applicability of steel plate bonding technique to strengthen structurally damaged reinforced concrete beams was studied by Swamy et al. (1989). They reinforced pre-damaged beams while they were unloaded and also when they were still under loading. Their experimental results show that the strengthening of pre-damaged RC beams by bonding steel plates is efficient and plated beams showed stiffness and strength values superior to those of original unplated beam. Hussain et al. (1995) studied the effect of steel plate thickness, with thickness varying from 1 to 3 mm, on the behaviour and mode of failure of pre-damaged strengthened beams. They observed premature failure by debonding at plate curtailment zone when the thickness of the plate increased. They also reported that even the provision of end anchorage by means of anchor bolts could not prevent

premature failure of thick plates. Flexural behaviour of pre-cracked composite strengthened RC beams was studied by Sharif et al. (1994). The effect of composite plate thickness, varied between 1-3 mm, on the behaviour of pre-damaged beam is investigated in their study. The premature failure mode of debonding initiated at the plate end was prevented by the use of different types of anchorage. The effectiveness of anchorage technique in increasing the ductility of the structure is discussed. Research was conducted by Grace et al. (1999) on the effectiveness of anchorage in preventing debonding mode of failure in composite strengthened pre-damaged beam. They concluded that by proper choice of anchorage technique the ultimate load carrying capacity of the structure can be upgraded. However debonding mode of failure cannot be totally prevented.

A plain concrete beam subjected to bending load will form cracks when the bending tensile strain exceeds the concrete fracture tensile strain. This is the same when an external reinforcement like steel or composite is used to strengthen the beam. When the cracks are formed in the tension side of the beam and opens at the level of the interface, the stress in the external reinforcement will be higher at the crack location since the tensile stress at that point in the concrete is zero. While steel plates can yield at the locations of high stress concentrations, composites can not yield to build up the tensile stress in the concrete close to the crack tip. At the crack a short length of the composite will be debonded from the concrete, a failure of the bond could propagate along the interface, causing a premature mode of failure by debonding. Thus, failure

of composite-concrete interface can initiate away from the composite ends, due to stress concentration at a concrete crack tip. The key factor in the efficiency of this method of repair is the preservation of the bond between the composite reinforcement and the concrete surface. In this paper, we have tried to evaluate the effect of the level of pre-cracking in the concrete beam on the structural response of a composite strengthened beam. We have also looked at the structural integrity under load of a concrete beam strengthened with composites. The experimental program presented in this paper was designed to address two issues; the structural response of the pre-damaged RC beams repaired by laminating composite material on the tension face, and the effect of the composite material rigidity on the overall behaviour of the hybrid beam, while emphasising on the choice of composite material to illustrate the basic concept to obtain a ductile mode of failure.

In this investigation, RC beams previously loaded to a significant portion of their ultimate strength, then consequently cracked, were strengthened with GFRP and CFRP layers. The experimental results showed that applying the composite to severely damaged RC beam, significantly increased the stiffness and strength of the beam. Pre-damaged beams showed higher ductility at failure compared to undamaged RC strengthened beam and in spite of extensive cracking the integrity of the structure is maintained up to the failure point.

4.3 Experimental program

A total of nine instrumented reinforced concrete beams were tested in this study. The experimental program is summarized in table 4.1. All the beams had the same overall dimensions and they also had the same internal longitudinal steel reinforcement and stirrup arrangements, which are shown in figure 4.1. All the beams were tested under four-point flexural loading. Beams A11, A21 and A31 were the control beams. Beam A11 was loaded to failure, like any other reinforced conventional beam. Based on the results obtained from this test, two pre-loading conditions were defined. The first pre-loading level was chosen close to the service load of the control beam, which was 30% of its ultimate loading capacity. The second pre-loading was chosen close to the steel yielding point of control beam which was 60% of its ultimate loading capacity. To pursue the experimental program two other control beams were needed. Thus, A21 was loaded to 30% of ultimate capacity of beam A11, unloaded and reloaded to failure. Beam A31 was loaded to 60% of ultimate capacity, unloaded and then reloaded to failure. Beams G11 and C11 are reinforced concrete beams strengthened respectively with one layer of glass-epoxy (GFRP) and carbon-epoxy (CFRP) composite. Their behaviour could be compared to beam A11. Beam G21 and C21, are RC beams pre-loaded to 30% of ultimate, unloaded, and then strengthened in the unloaded state with glass-epoxy and carbon-epoxy composites respectively. They were then reloaded to failure and their behaviour could be compared to the control beam A21. Finally, beams G31 and C31 are RC beams, loaded to 60% of ultimate ,

unloaded, strengthened with one layer of GFRP and CFRP respectively, then reloaded to failure. Their behaviour could be compared to control beam A31.

4.3.1 Beam design and fabrication

As shown in figure 4.1, the beams were 150x200 mm in cross section and 2000 mm long. The beams were reinforced with two M10 steel bars at the tension side. The basic reinforced concrete beam (RC beam) was designed according to ACI code 318-92 to fail in flexure. It is important to notice that to prevent over strengthening after composite bonding, the reinforcement ratio of the RC beam was chosen low (A_{steel}/bd =0.007). Also the low reinforcement ratio of the beam was intended to represent either a beam with insufficient flexural steel, or one in which corrosion has caused a significant reduction in the steel rebars section, for which composite strengthening is often used. Before applying the composite to the concrete surface, the surface of the concrete was sand-blasted to remove laitance and to expose aggregates. The surface was then primed by Sikadur Hex300 epoxy. SikaWrap 103C, unidirectional carbon and SikaWrap100G unidirectional glass fabrics were impregnated with Sikadur Hex306 epoxy resin in the laboratory using hand lay-up technique and right after, laminated directly on the primed concrete surface. The composite was left to cure on the beam surface in the laboratory conditions for two weeks before final testing. The CFRP and GFRP single layer had the same cured dimensions of 1mm thick, 190 mm width and a length of 1760 mm.

4.3.2 Materials

4.3.2.1 Concrete and steel

One concrete mix with an average 28 days compressive strength of 35 MPa was used to mold the reinforced concrete beams in three batches. Type 10 Portland cement with no admixture was used and the maximum aggregate size was 20 mm. The ratio of cement /sand /water/aggregate in the mortar mix was 1/2 /0.5 /3 by weight. Cast RC beams were moist cured for one week and let to cure in the laboratory conditions. For each batch, four 152x305 mm (6x12in) concrete cylinders were cast and tested according to ASTM C39-94 and ASTM C469-94 procedures to determine the compressive strength, modulus of elasticity and Poisson's ratio of concrete. Also, for each batch, samples were molded to determine the modulus of rupture and the splitting tensile strength of the concrete, according to standard procedures ASTM C496-96 and ASTM C78-94. These properties are summarised in table 4.2 The concrete has an average cylinder compression strength of 42.9 MPa and an average modulus of elasticity of 27.8 GPa. The steel rebars were tested in laboratory. They have a yielding strength of 456 MPa and an ultimate strength of 734 MPa. The beam testing as well as the standard characteristic tests were conducted at the same time, one year after concrete casting.

4.3.2.2 Composite

To measure the composite properties one layer of carbon fabric and one layer of glass fabric were respectively impregnated with epoxy using hand lay-up technique and let to cure in laboratory conditions for two weeks. The thickness of the cured lamina was measured at 1 mm for both types of composite. These CFRP and GFRP laminas were tested for tensile properties according to ASTM D3039 testing procedure. The measured mechanical properties are summarised in table 4.3.

4.3.3 Beam testing

All the beams were tested under four point bending over an effective span of 1800 mm with the load applied at 450 mm on either side of the midspan, as shown in figure 3.1. The load was applied gradually until failure occurred in one cycle. The midspan deflection was measured using LVDT. Electrical strain gages were used to measure the strains at midspan of the internal rebars, of the composite lamina and of the concrete on the extreme compression side of the beam. Computer controlled instrumentation was used to record the loads at regular intervals. Cracking of the beams on the tension side was recorded during loading by tracing the cracks on the beam surface at equal load intervals. For all beams, the width of the three largest cracks in the constant moment region were measured and recorded at these loading intervals using a pocket-telescope.

4.4 Experimental results

4.4.1 Pre-loading

The pre-loading cycle for control beams A21 and A31 is shown in figure 4.2. After unloading, these beams had residual deflection of 1.1 and 2.5 mm respectively, which of course translates into different level of damage. At the first level of pre-loading, 30% of ultimate for beam A21, flexural cracks propagated to 90 mm from the bottom side of the beam at midspan, with a maximum crack opening of 0.2 mm which reduced to 0.05 mm after unloading. At the second level of pre-loading, 60% of ultimate, cracks propagated to 120 mm from the bottom side of the beam at midspan, with a maximum crack width of 0.4 mm, which reduced to 0.15 mm after unloading.

4.4.2 Load - deflection behavior

To illustrate the composite strengthening effect as well as the influence of composite stiffness, figure 4.3 and figure 4.4 show the load versus midspan deflection curves for undamaged beams and beams pre-loaded to 60% of ultimate capacity before strengthening. As can be seen in these figures the general behavior to failure of all the composite-reinforced beams were similar, although the flexural stiffness and final mode of failure varied with the type of composite used. Figure 4.4 shows that the

control beam, A31 behaved like a typical under reinforced RC beam, while the external composite reinforcement had a distinctive stiffening effect on the beam G31 and C31. As expected, because of higher modulus elasticity of carbon the resulting beam stiffness, defined as the slope of load- deflection curve, was higher for CFRP strengthened beam compared to GFRP strengthened beam. This difference becomes more evident as we approach the steel yielding point which occurred at midspan deflection around 10 mm. After this point, the carbon fibre reinforced beam showed a significant higher stiffness and lower deflection at failure compared to the glass fibre reinforced beam. Both composite strengthened beam, also showed different modes of failure. The failure is said to occur when the load starts to decrease sharply. The beam G31 with glass reinforcement failed by failure of the concrete on the compression side while the beam C31 with carbon, failed by debonding of the composite in the constant moment region. The cracks then propagated in the concrete, leaving a thin layer of concrete bonded to the composite. It should be noted here that all the GFRP failed similarly by concrete failure in the compression side and all the CFRP reinforced beams showed a failure mode of debonding, as explained above. The non strengthened control beams failed by compressive failure of concrete on the compression side after steel yielding.

The effect of pre-cracking of the beams prior to strengthening with composite is shown in load-deflection curves, figure 4.5 and figure 4.6, for both composites. As can be seen in these figures, there are practically no loss in stiffness for pre-damaged

strengthened beams. Both pre-damaged strengthened beams showed a higher deflection at failure compared to the undamaged strengthened beam. There is a limiting deflection beyond which no significant increase in loading can be achieved. For GFRP reinforced beams, this limiting value is controlled by concrete ultimate strain in compression and for CFRP reinforced beams, the ultimate deflection is governed by the interface strength, since debonding is the controlling mode of failure.

4.4.3 Strains

In spite of extensive cracking before composite strengthening, under reloading, large strains developed in the composite and in the concrete which indicates the composite action in the composite strengthened RC beam (hybrid beam). To illustrate, figure 4.7 shows the concrete compressive strain for the three beams reinforced with CFRP. It can be seen that for CFRP strengthened beams the concrete did not attain its ultimate capacity, which is 0.0035. It also shows that beams C21 and C31 had slightly lower concrete strain at failure than beam C11. However the load at failure was slightly higher for the pre-loaded strengthened beams. Figure 4.8 and figure 4.9 show the strain at midspan for the three GFRP strengthened beams and the CFRP strengthened beams respectively. The yielding of the steel rebars causes a change in the slope of the curves which leads to an increase in the rate of strain as the stiffness of the hybrid beam is reduced. The load at which the steel yields is similar for all beams. However

for different level of damage, the composite strain is different at the steel yielding point.

Unlike concrete strain, the maximum recorded strain in the composite increases with a larger structural damage prior to strengthening. This increase is not proportional to the level of pre-loading. Beams pre-loaded to 60% of ultimate showed lower composite strains at failure compared to beams pre-loaded to 30% of ultimate. The different slopes of load-strain curves before steel yielding indicate that the nature of stress transfer between the composite and concrete depends on the cracking pattern and on the composite material mechanical properties. This is illustrated in figure 4.8 and figure 4.9 where the slope of the curve is different for different levels of pre-loading and the change of slop is different for glass and carbon reinforced beams.

4.4.3 Cracking

4.4.3.1 Cracking moment, M_{cr}

In a traditional RC beam, when the concrete cracks in the tension zone the neutral axis position shifts upward and the variation of bending stiffness changes the slope of the load-deflection curve. The same behaviour was observed for composite strengthened RC beams as shown in figure 4.3. This change of slope in the load-deflection curve was absent for pre-loaded strengthened beam as noticed in figure 4.4. The moment at which concrete cracks is called 'cracking moment, M_{cr}'. The cracking moment of the RC beams is estimated based on the concept of a transformed section:

$$M_{cr} = \frac{f_r I_g}{y_t} \tag{4.1}$$

where f_r is the modulus of rupture of concrete, I_g is the moment of inertia of gross concrete section and y_t is the distance from centroid of transformed section to the outer most fibres. The same trend should be expected for composite reinforced beam since the small cross section of the composite hardly change the moment of inertia of the section. So I_g for a composite strengthened RC beam can be obtained theoretically using the theory of elasticity of transformed section for reinforced concrete beam without composite reinforcement. This method was used to evaluate theoretical value of M_{cr}, for composite strengthened RC beam. In the calculation of I_g the internal steel reinforcement was considered. The experimental cracking moment is obtained from cracking load, defined as the first bending knee in load-deflection curve, point 1 in figure 4.3. Table. 4.4 Summarises the experimental and theoretical value of M_{cr} and average crack spacing at two levels of loading for control beam A11, and undamged strengthened beams, G11 and C11. As can be seen, for FRP strengthened beam crack initiation started at a moment, M_{cr}, slightly higher than the one predicted by the theory. Crack spacing was measured as the distance between adjacent cracks at the level of composite-concrete interface. As can be seen composite highly reduced the number of cracks. The average crack spacing was also reduced by the application of composite and it is affected by the type of composite used. GFRP strengthened beam showed smaller crack spacing at failure compared to CFRP reinforced beam.

4.4.3.2 Cracking pattern

The crack pattern, in concrete, its propagation and length of cracks in the composite reinforced beam were different from those in RC control beams. For all beams, flexural cracks initiated in the constant moment region, when the principal stress exceeds the concrete tensile strength, and they are oriented perpendicular to the direction of principal stresses. Cracks in the shear span started as flexural cracks but changed direction, as inclined shear cracks, as loading increased. Shear cracks were longer and higher in number for composite reinforced beams due to their higher ultimate capacities. The cracks propagated upwards as loading progressed, but remained very narrow through out the loading history. Figure 4.10 illustrates the on scale reproduction of crack distribution and length at steel yielding point for the three carbon reinforced RC beams. As can be seen the cracks are evenly distributed and they are fewer in number when the beam is reinforced in an undamaged state. The maximum measured crack opening versus applied load for the three CFRP beams are presented in figure 4.11. This figure shows that for the same level of loading, the beam pre-loaded to 60% of ultimate strength before applying the composite reinforcement showed a wider crack compared to the 30% pre-loaded and unloaded strengthened beam. The reason is that after applying the composite to the pre-damaged beam by increasing the load, new cracks appeared in between the existing cracks, leading to denser crack pattern compared to the undamaged RC strengthened beams. As a

consequence, a larger number of cracks, as well as wider cracks openings are recorded for the pre-damaged beams. In order to understand the effect of the composite material properties on the cracking behaviour of the RC beams, maximum measured crack opening in the constant moment region as loading proceeds for RC control beam and composite strengthened beam is compared in figure 4.12. As can be seen, the largest crack was smaller in width for the composite strengthened beam, compared to RC control beam. The application of a composite, highly reduced maximum crack width even after steel yielding. This reflects the restraining effect that the composite has on the crack openings when the composite provides a mechanism by which tensile stress can be redistributed in the concrete between cracks and thus limits crack openings. Also as can be seen in figure 4.12, the maximum crack width is smaller for CFRP reinforced beam than for GFRP reinforced beam, for similar loading, in accordance with the respective rigidity of both composites.

4.4.4 Flexural rigidity, EI

As the load increases, the principal property that influences the deflection is the value of effective bending rigidity E_cI_e. The effective bending rigidity is the product of two quantities, E_c, which is the modulus of elasticity of concrete and I_e which is the effective moment of inertia of the RC beam section. Up to cracking moment, M_{cr}, the effective moment of inertia is equivalent to I_g which represents the gross uncracked section. After cracking the bending rigidity E_cI_e decreases considerably and when we

approach the ultimate moment M_u, it approaches E_cI_{cr}. I_{cr} represents the moment of inertia of completely cracked section and is calculated using the theory of the transformed section while ignoring the concrete in tension side. According to CSA A23.3-94 code, for a reinforced concrete beam and for practical purposes, after cracking, the effective moment of inertia I_e, can be calculated using Branson's equation:

$$I_e = I_{cr} + (I_g - I_{cr})(\frac{M_{cr}}{M_{max}})^3 \leq I_g \qquad (4.2)$$

where M_{max} is the maximum moment at the load stage at which deflection is being computed.

The flexural rigidity 'EI', is defined as the slope of moment-curvature curve. The curvature of elastic curve in constant moment region can be obtained from the following equations illustrated in figure 4.13:

$$\varphi = \frac{M}{E_c I_e} \qquad (4.3)$$

where φ is the curvature, M is the applied moment and E_cI_e is the effective flextural rigidity. In the method of analysis of the composite strengthened beam section, if we consider the plane section principal and assume that the deformation of fibres

(elongation and contraction) is proportional to the distance from the neutral surface, in the region of constant bending moment, the curvature can be defined as:

$$\varphi = \frac{\varepsilon_{com} + \varepsilon_{con}}{h} \tag{4.4}$$

where ε_{com} is composite strain, ε_{con} concrete strain and h is the beam depth. The progressive cracking of the beams, can be illustrated by plotting the bending rigidity EI versus the moment. Using the measured values of composite and concrete strains at mid-span and calculating moment from experimental loading, this curve was plotted for RC control, GFRP and CFRP strengthened beams in figure 4.14. The theoretical values of I_g and I_{cr} are shown in figure 4.14 as two straight lines defining the upper and lower limits of flexural rigidity. In this figure, Branson's equation is also plotted for comparison. As can be seen below the cracking moment, the experimental curve is roughly horizontal. When the ultimate moment approached, the curve became asymptotic to the horizontal level of the calculated E_cI_{cr}. It can be seen that for FRP strengthened beam, there was a sudden change in slope at the steel yielding point. When the moment exceeds the cracking moment the concrete in tension develops flexural cracks at random spacing. However, the concrete close to the neutral axis and in between cracks contributes to the effective stiffness of the beam which is called tension stiffening effect. That is why even in the portion of the beam with flexural cracking the effective stiffness is greater than that corresponding to a fully cracked

transformed section. Figure 4.14 shows that as the bending moment increases, the change of rigidity in the beam which is a function of flexural cracking is not the same for GFRP and CFRP strengthened beam. This is an indication of the different extend of flexural cracking and stress transfer between composite and concrete at the level of interface, as loading increase. This figure shows that the effective rigidity of the CFRP strengthened beam can be approximated using Branson's equation to evaluate I_e. This is not the same for GFRP reinforced beam.

To illustrate the effect of pre-damaging the beam, the result for CFRP reinforced beams are shown in figure 4.15. It shows that even for 60% pre-loaded beams, the initial effective rigidity of the beam was highly preserved due to the crack restraining effect of the composite reinforcement.

4.5 Conclusion

The external bonding of composite layers offers an effective means of strengthening damaged RC beams in flexure. The pre-loaded RC beams when strengthened by composites showed higher strain and higher strain absorption capacity compared to undamaged strengthened RC beams. Composite materials had little effect on the initiation of flexural cracks but they did provide a resistance to both propagation and opening of the cracks. Examination of the crack distribution indicates that the size and the density of the cracks are less in the strengthened beams than in control beams for

the same loading. The nature of crack pattern, propagation and height depends on the composite type. By adding composite to the tension face of the reinforced concrete beam, we can benefit from added flexural rigidity provided by the concrete in tensile region due to crack restraining effect. The theory used to estimate the effective moment of inertia of RC beams under estimates the equivalent flexural rigidity of the hybrid beams. It is evident from the experimental results that the bond between the composite and the concrete is the most important factor affecting the beam response. In spite of extensive pre-cracking before strengthening, the repaired beam preserved its structural integrity, confirming the effectiveness of this repair technique.

4.5 Acknowledgement

The authors wish to thank Sika Canada for providing free composite materials including carbon and glass fibres and epoxy resin. Also the authors gratefully acknowledge the technical support of Mr. Mario Desroches, Sika Canada technical sales representative. The experimental program of this research was carried out at the structure laboratory, of École Polytechnique de Montréal. The authors wish to express their appreciation to Mr. Gérard Degrange, structure laboratory director and laboratory technicians for their valuable assistance.

4.6 References

Bonacci, JF. , Maalej, M., (2001). Behavioral trends of RC beams strengthened with externally bonded FRP. J Composites Construction;5(2), 102-13.

Fanning PJ., Kelly O., (2001). Ultimate response of RC beams strengthened with CFRP plates. J composites Construction, 5(2), 122-27.

Grace, NF., Sayed, GA., Soliman, AK., Saleh, KR., (1999), Strengthening reinforced concrete beams using fiber reinforced polymer (FRP) laminates, ACI Struct J, Sept.-Oct., 96(5), 865-75.

Hussain, M., Sharif, A., Basunbul, IA., Baluch, MH., Al-Sulaimani, GJ., (1995), Flexural behavior of precracked reinforced concrete beams strengthened externally by steel plates, ACI Struct J, Jan- Feb, 92(1), 14-22.

Jones, R., Swamy, RN., Ang, TH., (1982), Under and over-reinforced concrete beams with glued steel plates, The Int J of cement composites and light weight concrete, 4(1), 19-32.

Karbhari, VM., Seible, F., (2000), Fiber reinforced composites-Advanced material for renewal of civil infrastructure, Applied Composite Materials, 7, 95-124.

McKenna, JK., Erki, MA., (1994),Strengthening of reinforced concrete flexural members using externally applied steel plates and fibre composite sheets- a survey. Can J Civ Eng, 21, 16-24.

Meier, U., (2000), Composite Materials in Bridges Repair, Applied composite materials, 7, 75-94.

Ritchie, PA., Thomas, DA., Lu, LW., Connelly, GM., (1991), External reinforcement of concrete beams using fiber reinforced plastics, ACI Struct J, Jul.-Aug.; 88(4), 490-500.

Sharif, A., Al-Sulaimani, GJ., Basunbul, IA., Baluch, MH., Ghaleb, BN., (1994), Strengthening of initially loaded reinforced concrete beams using FRP plates, ACI Struct J, Mar- Apr; 91(2), 160-8.

Spadea, G., Bencardino, F., Swamy, RN., (1998), Structural behavior of composite RC beams with externally bonded CFRP, J Composites Construction,Aug., 2(3), 132-37.

Swamy, RN., Jones, R., Bloxham, JW., (1987), Structural behavior of reinforced concrete beams strengthened by epoxy-bonded steel plates, The Struct Engineer, 65(2), 59-68.

Swamy, RN., Jones, R., Charif, A., (1989), The effect of external plate reinforcement on the strengthening of structurally damaged RC beams, The Struct Engineer, 67(3), 45-56.

Table 4.1 Experimental program

Beam	Test specimen	Description	Number of specimens
A11	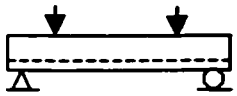	Control beam without external reinforcement	1
A21	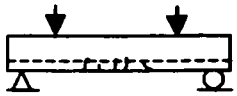	RC beam pre-loaded to 30% of its ultimate capacity, unloaded then loaded to failure	1
A31	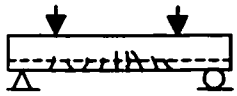	RC beam pre-loaded to 60% of its ultimate capacity,	1
G11	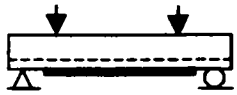	Undamaged RC beam reinforced with GFRP	1
C11	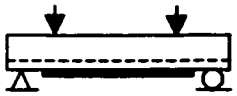	Undamaged RC beam reinforced with CFRP	1
G21	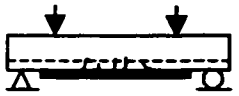	RC beam pre-loaded to 30% of its ultimate capacity reinforced with GFRP sheet	1
C21		RC beam pre-loaded to 30% of its ultimate capacity reinforced with CFRP sheet	1
G31	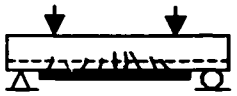	RC beam pre-loaded to 60% of its ultimate capacity reinforced with GFRP sheet	1
C31	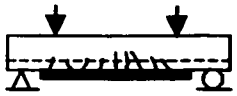	RC beam pre-loaded to 60% of its ultimate capacity reinforced with CFRP sheet	1

Table 4.2 Mechanical properties of concrete

Batch No.	Compressive strength, MPa	splitting Tensile strength, MPa	Modulus of rupture, MPa	Modulus of elasticity, GPa	Poisson's ratio
1	44.75	3.9	6.41	28.1	0.17
2	40.9	3.32	6.49	25.4	0.2
3	43.12	3.44	6.49	28.56	0.20
Average	42.92	3.55	6.46	27.35	0.19

Table 4.3 Mechanical properties of composites

Composite	Fibre volume fraction	Longitudinal tensile strength	Longitudinal modulus of elasticity	Strain at failure
GFRP	50%	400 MPa	20 GPa	2%
CFRP	50%	640 MPa	64 GPa	1%

Table 4.4 Cracking moment and crack spacing

Beam	M_{cr} experimental kN-m	M_{cr}, Theoretical kN-m	Total load, 30kN		Ultimate load	
			Crack spacing, mm	Number of cracks	Crack spacing, mm	Number of cracks
A11	3,08	3,87	29,42	12	58,75	24
G11	3,57	3,87	100	8	39,71	28
C11	3,93	3,87	93	3	54,43	24

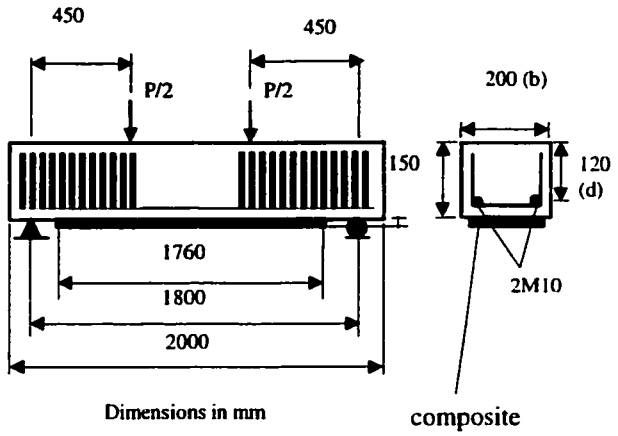

Figure 4.1 Reinforced concrete beam geometry

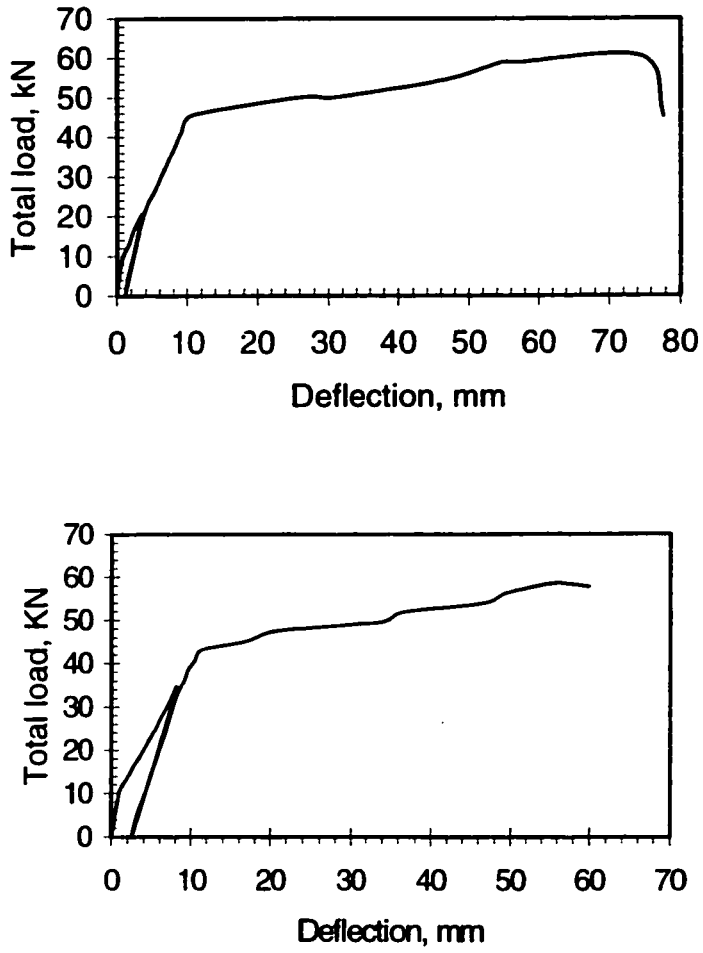

Figure 4.2 Load-unload cycle for pre-loaded beams; a : Beam A21, pre-loaded to 30% of ultimate capacity; b : Beam A31, pre-loaded to 60% of ultimate capacity;

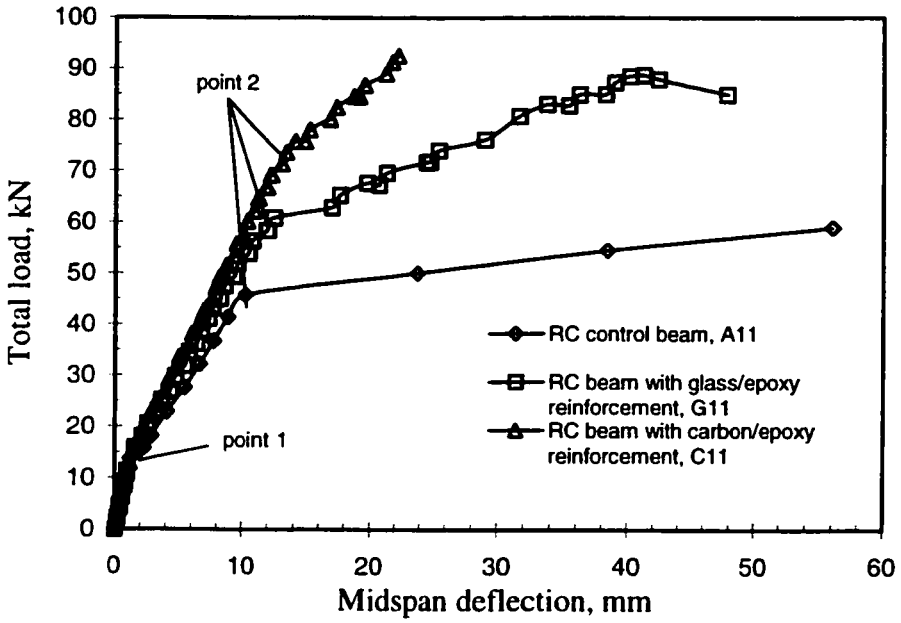

Figure 4.3 Total Load versus mid span deflection of RC control beam, GFRP and CFRP strengthened beams. (point 1: first crack load, point 2: steel yielding point)

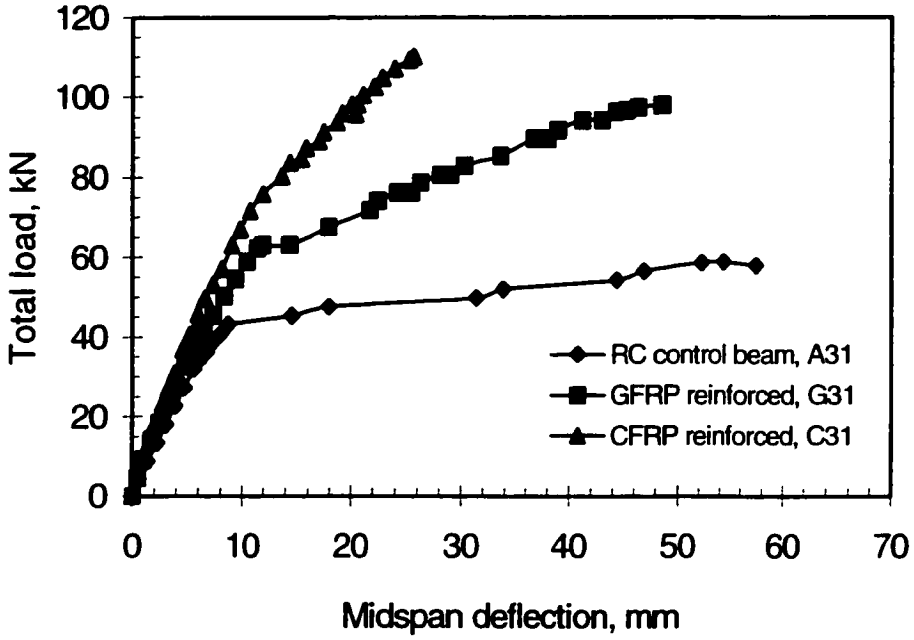

Figure 4.4 Load- deflection curves for control RC beam and FRP reinforced beams pre-loaded to 60% of ultimate before strengthening

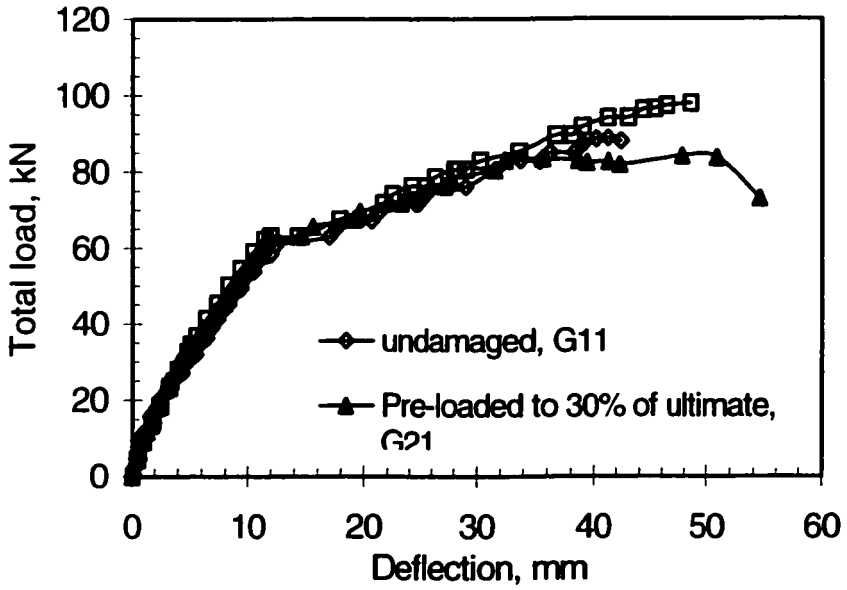

Figure 4.5 Load-deflection curve for GFRP reinforced RC beams

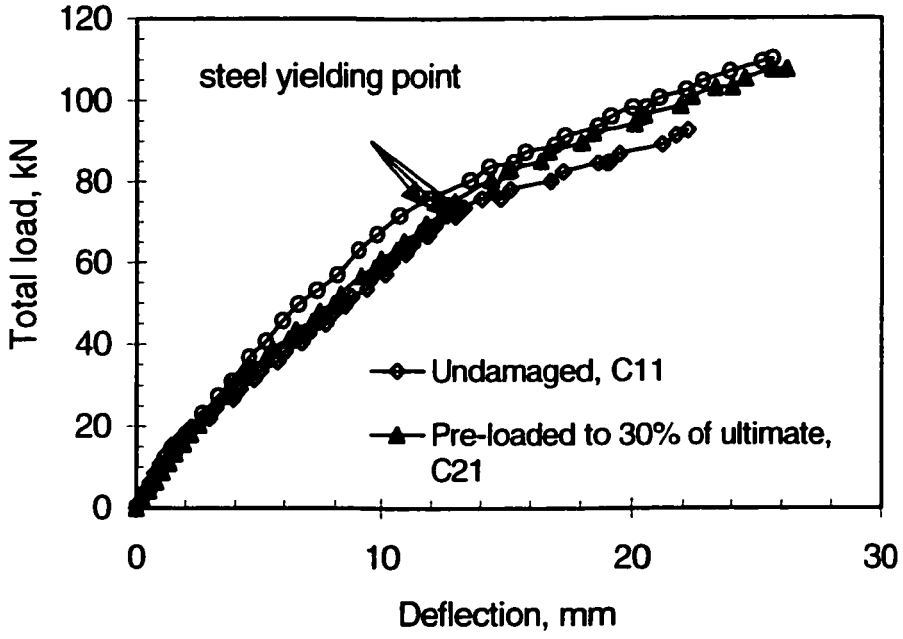

Figure 4.6 Load-deflection curve for CFRP reinforced RC beams

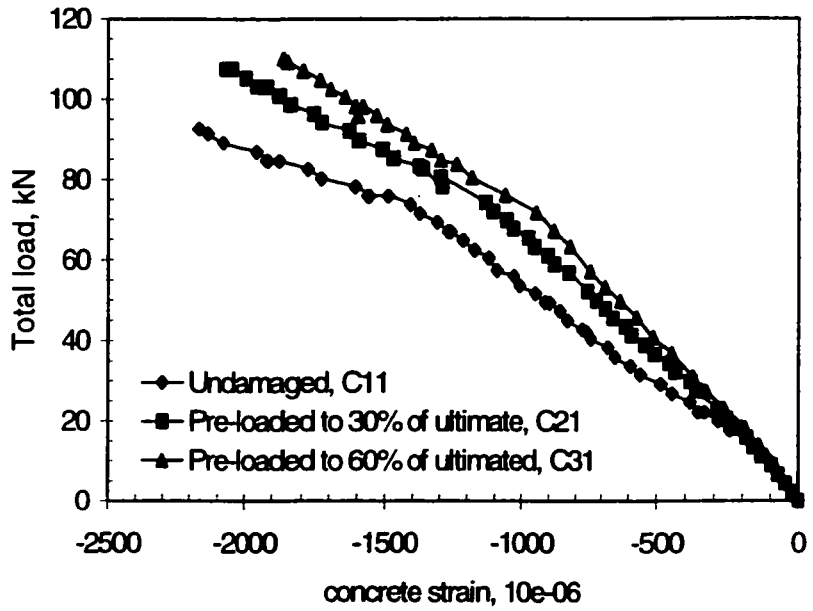

Figure 4.7 Concrete strain for CFRP reinforced beam

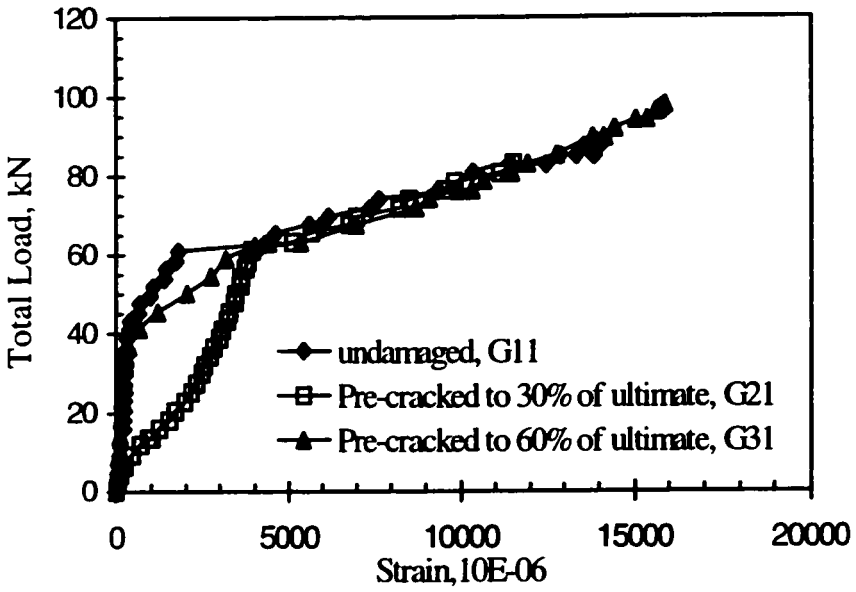

Figure 4.8 GFRP strain at mid-span for beams with different levels of pre-loading

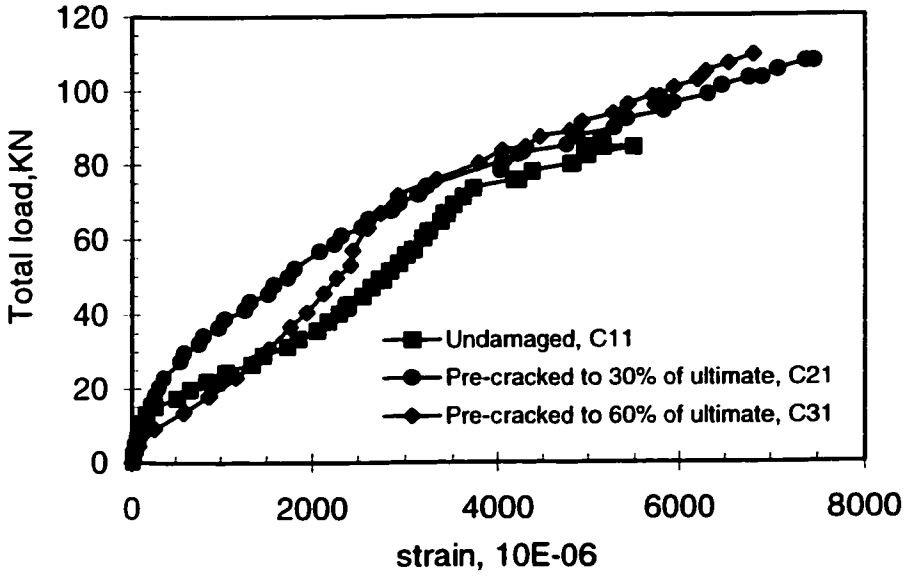

Figure 4.9 CFRP strain at mid-span for beams with different level of pre-loading

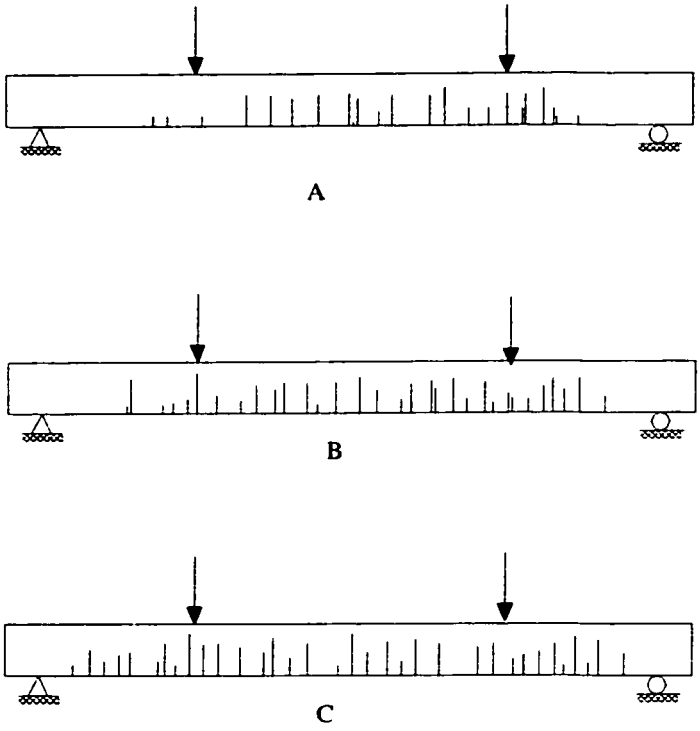

Figure 4.10 On scale reproduction of crack distribution and length at steel yielding point for; A: Beam C11, RC beam reinforced with CFRP, B: Beam C21, RC beam pre-loaded to 30% of ultimate reinforced with CFRP, C: Beam C31, RC beam pre-loaded to 60% of ultimate reinforced with CFRP

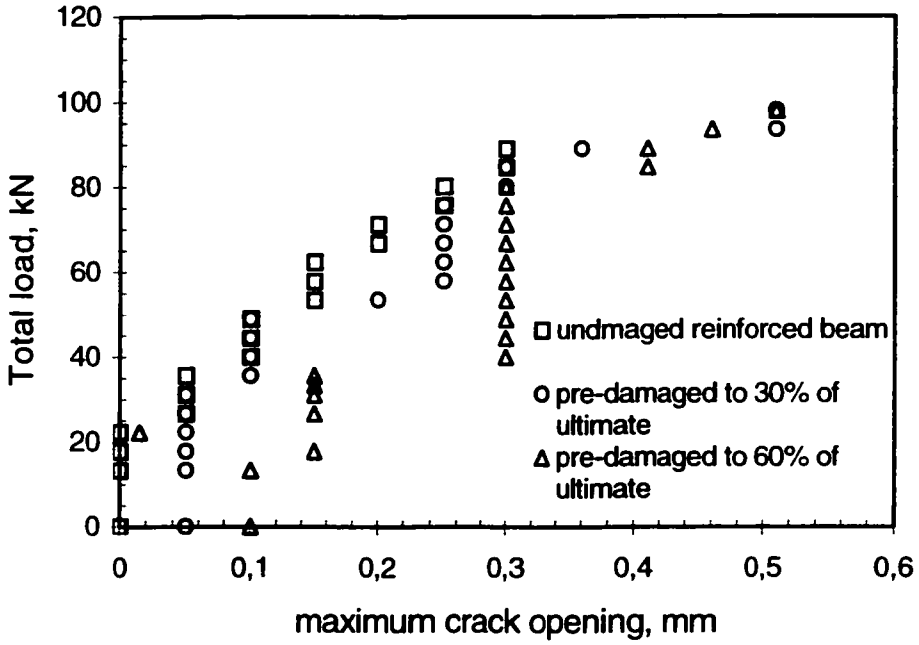

Figure 4.11 Maximum crack opening in constant moment region for CFRP reinforced beams

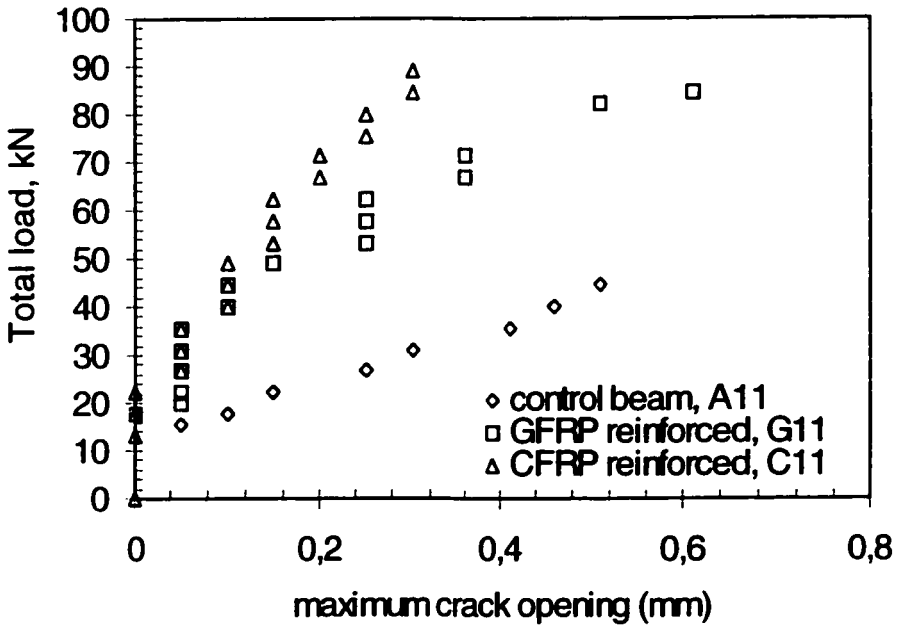

Figure 4.12 Maximum crack opening at constant moment region

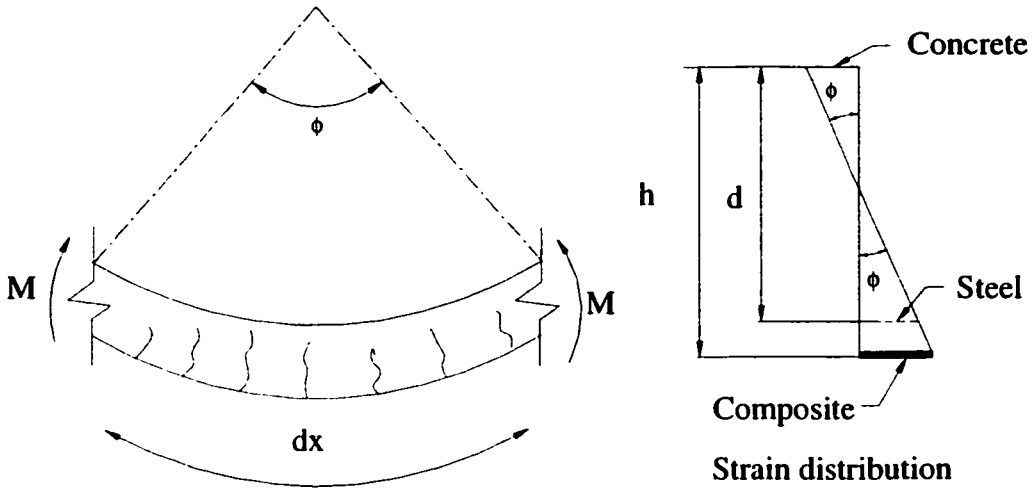

Figure 4.13 Curvature in constant moment region

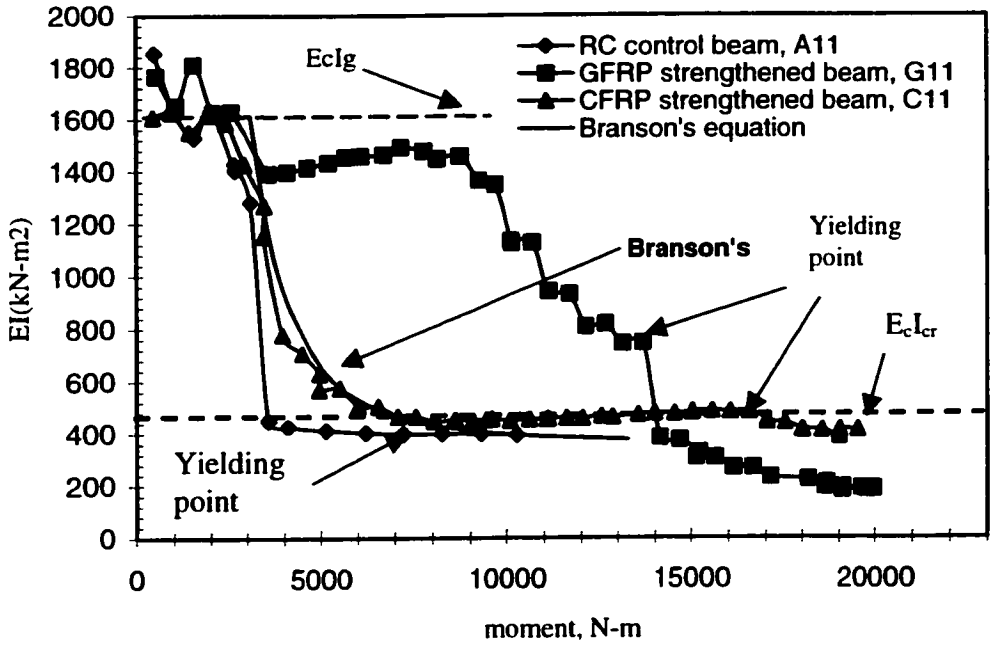

Figure 4.14 Bending rigidity versus moment for control beam, GFRP and CFRP strengthened beams

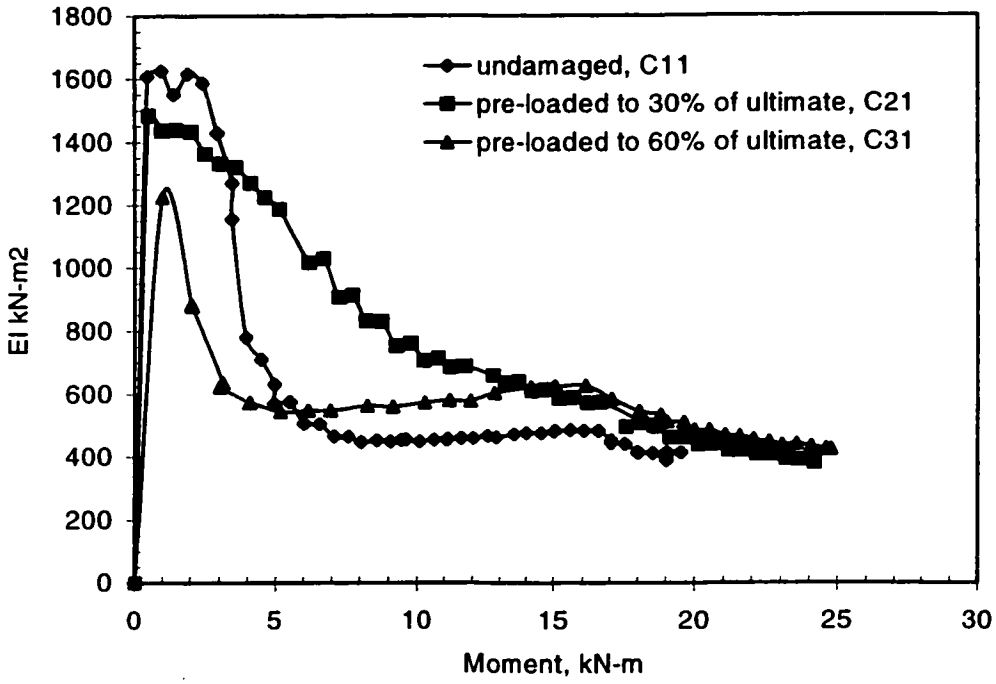

Figure 4.15 Bending rigidity versus moment for CFRP reinforced beams

CHAPITRE 5

A PROPOSED APPROACH TO EVALUATE THE COMPOSITE-CONCRETE INTERFACIAL FRACTURE RESISTANCE USING SANDWICH SPECIMEN

Katayoun Soulati **École Polytechnique de Montreal**

Raymond Gauvin **École Polytechnique de Montreal**

5.1 Abstract

Composite materials in the form of sheet or plate are bonded to reinforced concrete structures to strengthen and stiffen them. Premature mode of failure of debonding by the composite laminate from concrete surface prevents the structure to attain its maximum designed capacity. To understand the mechanism of debonding, the behaviour of the composite-concrete interface under a full range of mixed mode loading should be known. The combined analytical-experimental methodology described herein represents an application of the interface fracture mechanics concept to obtain composite-concrete fracture toughness. This methodology, introduces bimaterial interface fracture mechanics using experimental results from sandwich specimens. In the tested specimens, a thin layer of composite is sandwiched between two pieces of bulk concrete. This approach permits to obtain the fracture toughness as a function of the composite modulus of elasticity.

5.1 Introduction

Composite materials have been used successfully for strengthening reinforced concrete structures. Bonding composites laminates to the tension face of flexural reinforced concrete (RC) members, can upgrade their structural performance. Flexural failure modes such as concrete crushing in compression or composite failure in tension can be predicted theoretically, assuming compatibility of strain and perfect bonding between composite and concrete (ISIS Canada, 2000). However brittle failure mode of debonding of the composite which is commonly observed is so far unpredictable. To prevent this mode of failure, different anchorage techniques such as steel bolting or composite jacketing have been suggested (Grace et al., 1999; Spadea et al., 1998). However, this method of anchorage is not always efficient because of insufficient space around the structure beam, upgrading the local reinforcement ratio at the position of application of the anchor and crack development at the level of concrete-anchore interface which may cause subsequent failure. A better understanding of the failure mechanisms should lead to the development of reliable formulations to limit these brittle failures.

The bond which must be achieved between composite and concrete element is crucial to efficient composite action. Previous experimental investigation reveals that the debonding mode of failure can initiate from a location of the pre-existing, tensile crack in concrete. Continuous cracking of concrete in tension at the level of

composite-concrete interface creates a complex stress state which affects the force transfer between composite and concrete through the interfacial region and consequently the bond strength. It is believed that the evaluation of interfacial fracture resistance of composite-concrete interface to be the key to maintain the integrity of the structure through proper design.

The objective of this paper is to characterise the composite-concrete interface fracture properties using a theoretical and experimental models. The concept of fracture mechanics of bi-material interfaces is used to design two specimens, a Brazilian sandwich disk and a pure bending sandwich beam specimen, to characterise composite-concrete interface. These experimental models allow continuous measurements of interfacial toughness to establish the fracture toughness curve. To illustrate the method, experimental results carbon/fiber- epoxy composite bonded to concrete are presented.

5.2 Debonding mode of failure

Layers of composite material are laminated directly on the tension face of RC beams to upgrade their performance, figure 5.1(a). Because of fully elastic behaviour of the composite and low material ductility, the combination of steel, concrete and composite makes a hybrid structure which shows brittle failure modes. When the hybrid beam is designed for flexure, it is expected to fail by composite rupture in tensile or concrete

crushing in compression after internal steel reinforcement yielding. When delamination is the dominant mode of failure of hybrid beam, the designed strength cannot be fully utilised. From the experimental results in the literature three mechanism of debonding can be distinguished:

1- Figure 5.1a illustrates delamination at the level of the glue line which occurs because of insufficient concrete surface preparation or non-uniformity of the composite-concrete surface. Local unevenness due to inadequate preparation of the concrete will cause deflection of the laminate. This results in high tensile stresses perpendicular to the laminate which eventually cause the laminate shear off along its length from concrete surface. This type of failure can be prevented, by maintaining the uniformity of the concrete surface through proper surface preparation.

2- Shear peeling may occurs at the composite ends in the region of high shear and low moment, as shown in figure 5.1 b. At the termination of the composite laminate, a change in the stiffness and discontinuity of the beam curvature creates a stress concentration in the concrete, often initiating cracks that can lead to debonding (Oehlers and Moran (1990), Jones et al. (1982), Jones et al. (1988), Johnson and Tait, (1981), Mukhopadhyaya and Swamy (2001)). First, diagonal shear cracks form in the concrete at the end of the plate, then followed by horizontal peeling crack at the level of the bottom steel reinforcement. This

sequence of crack formation continues along the length of the composite, causing the composite and the concrete element below the internal reinforcement to fall away. This mode of failure is usually observed with thick composite laminate (more than 1 mm) and can be prevented by changing the end geometry like tapering the composite end or extending the composite towards the support.

3- As illustrated in figure 5.1c flexural delamination of the composite due to tensile cracks developed in concrete during loading occurs when the flexural cracks caused by flexural moment in the concrete induce horizontal interface crack at the interface at the level of the of composite reinforcement, composite. This mode of failure can occur beyond the end of composite reinforcement, anywhere along the beam span.

Flexural delamination, for which the exact mechanism of failure is still unknown, cannot always be prevented by using anchorage techniques The anchorage can fail through composite-concrete bond failure in addition to concrete failure (Spadea et al. 2000). Further information on composite-concrete bond mechanism is necessary to design the structure against this mode of failure.

5.3 Composite-concrete interface

When the composite is laminated on the concrete surface directly, the bonded joint represents a system containing composite, concrete and the interface region that encompass the zone between composite and concrete. The stress transfer mechanism between the concrete and the composite through the interface plays a fundamental role in the collapse mechanisms of the beams reinforced with composite.

The transfer of axial force from reinforcing composite to the surrounding concrete results in the development of shear stress components along the interface. The composite concrete bond is achieved through mechanical interlock between the composite and sandblasted concrete surface. The bond stress showed in figure 5.2 is associated with shear or variation of bending moment in the flexural bond. Actual bond stress in the composite is not uniform along its length. In the constant moment region the shear force V is zero. However the composite force T varies between flexural cracks, figure 5.3b. At the position of a crack the tension is carried by the composite alone, meanwhile in between the cracks concrete carries some tension, partially relieving the composite force.

A stress concentration can be induced in the interface when a crack develops in the concrete. At the crack tip there are two sources of shear stress at the interface. The first is the local shear stress because of loading. The second is due to rapid changing bending moment as illustrated in figure 5.3c. The existence of an open crack at the interface rises stresses to the failure level , even though away from the crack tip, stress

may be low. Bond failure most probably starts at the location of a flexural crack, because crack tip at the interface is the place where the described localized bond stress is superimposed on the local shear stress. Therefore the mechanism of bond failure may involve an interface crack initiated at the flexural crack tip which breaks the bond adjacent to the crack. All missing bond giving rise to stress concentration, crack eventually spreads and the process repeats itself.

In flexural members, interface cracks usually appears at the interface, starting from flexural and diagonal tension cracks in the concrete. Because composite is not able to redistribute the bond stress along its length at the position of distress, the delamination is brittle and occurs in a catastrophic manner. In the experimental studies on the composite strengthened RC beams it was observed that an interface crack can be deviated in the direction of already existing shear crack figure 5.4a or arrested at the position of an aggregate at the interface and then propagate into the concrete, following the aggregate paste interface and separate a thin layer of concrete in delaminating the composite from the beam. In the latter, final failure occurs through the formation of continuous cracks in concrete bridging the bond cracks.

From experimental observations failure by debonding occurs at the composite-concrete interface. It can be concluded that there exist a limiting value of interface resistance between composite and concrete which becomes critical at the location of crack opening or discontinuity presented at the interface. In this study we try to

evaluate composite-concrete interface flexural resistance using fracture mechanics approach.

5.4 Basic bi-material interface fracture mechanics

Composite and concrete are not homogeneous materials. To study the effects of different parameters on the overall mechanical behaviour of composite-concrete interface, idealisation must be made so that relatively simple models could be constructed. While various methods and standards exist for the measurements of fracture toughness of the constituent materials such as composite or concrete, at the present no established method exist for the characterisation of the concrete-composite interface. The present approach is based on linear elastic interface fracture mechanic concepts and was assumed appropriate due to the observed linear elastic behaviour and brittle failure of the composite-concrete interface in the reinforced structure. The purpose of interfacial fracture mechanic approach is to define a measurable material property, toughness, to parameterise fracture mechanics resistance of the interface.

In the basic fracture mechanic approach, a bi-material interface is defined as a combination of two homogeneous material with continuity of traction and displacement maintained at the interface. In a bi-material system, even when geometry and loading are symmetric with respect to the crack, differences between elastic properties across an interface will abrupt the symmetry. A complete characterisation

of an interface requires toughness data over the full range of mode loading combination. This is usually achieved by using a wide range of different sample geometry, each of them having its own mode I and mode II proportions (Cao and Evans, 1989).

Lets consider an infinite free crack lying along the interface between two half plane with material 1 above and material 2 below, with the interface on the x_1 axis, figure 5.5. Let E_1, G_1 and ν_1 be young modulus, shear modulus and Poisson's ratio of material 1 and similar quantities E_2, G_2 and ν_2 for material 2. For bi-material plane problems of elasticity depends on two non-dimensional combination of elastic module. For plane strain problems these parameters of mismatch are (Suo and Hutchinson, 1989);

$$\alpha = \frac{\bar{E}_1 - \bar{E}_2}{\bar{E}_1 + \bar{E}_2} \tag{5.1}$$

$$\beta = \frac{1}{2}\frac{G_1(1-2\nu_2) - G_2(1-2\nu_1)}{G_1(1-\nu_2) + G_2(1-\nu_1)} \tag{5.2}$$

where:

$$\overline{E} = \frac{E}{1-\nu^2} = \frac{2G}{1-\nu} \tag{5.3}$$

Both α and β vanishes when dissimilarity between the elastic properties of the materials is absent and they change sign when materials are switched.

For the plane problems, normal and shear stresses at distance r ahead of crack tip can be written in the form:

$$\sigma_{22} + i\sigma_{12} = \frac{K}{\sqrt{2\pi r}} r^{i\varepsilon} \tag{5.4}$$

$$K = K_1 + iK_2 \tag{5.5}$$

$$\varepsilon = \frac{1}{2\pi} \ln\left(\frac{1-\beta}{1+\beta}\right) \tag{5.6}$$

where K is the real stress intensity factor at the interface and $i = (-1)^{1/2}$. For the case when $\beta \neq 0$, one can define

$$K\hat{L}^{i\varepsilon} = |K| e^{i\hat{\psi}} \tag{5.7}$$

with $\left|\hat{L}^{i\varepsilon}\right| = 1$, $\left|K\hat{L}^{i\varepsilon}\right| = |K|$ and $\hat{\psi}$ being the real angle of complex quantity $K\hat{L}^{i\varepsilon}$. When $\beta = 0$ the phase angle $\hat{\psi}$ is defined as:

$$\hat{\psi} = \tan^{-1}\left(\frac{K_2}{K_1}\right) \tag{5.8}$$

when $\beta = 0$ the phase angle $\hat{\psi}$ is a measure of the ratio of relative shear component to opening experienced by an interface, it represents the components of mode I and mode II interfacial energies. The case in which $\hat{\psi} = 0°$ corresponds to pure mode I and $\hat{\psi} = 90°$ corresponds to pure mode II conditions. The energy release rate per unit length of extension crack at an interface can be defined by:

$$\frac{1}{E^*} = \frac{1}{2}\cdot\left(\frac{1}{\overline{\overline{E_1}}} + \frac{1}{\overline{\overline{E_2}}}\right) \tag{5.9}$$

$$G = \frac{|K|^2}{E^* \cosh^2 \pi\varepsilon} \tag{5.10}$$

where:

$$|K|^2 = K^2{}_1 + K^2{}_2 \tag{5.11}$$

$$\cosh^2 \pi\varepsilon = \frac{1}{1-\beta^2} \tag{5.12}$$

So mechanical properties of the interface can be characterized by the interfacial fracture energy G and phase angle of $\hat{\psi}$. If both G and $\hat{\psi}$ are known one can establish a G_c versus $\hat{\psi}$ curve for the interface. This curve is the fracture toughness curve and it is dependent of specimen geometry and loading system but it is dependent on materials properties and the nature of the interface such as surface preparation and environmental conditions.

5.5 Sandwich specimen

The theory of fracture mechanics for bi-material interfaces was used to introduce sandwich specimens (Suo and Hutchinson, 1989). The common feature of these specimens is that each of them is homogeneous except for a very thin layer of a second material which is sandwiched between two halves of the bulk. A pre-existing crack lies along one of the interfaces for these specimens. The stress intensity factors for homogeneous specimen in the absence of the thin layer is used to characterize the interface crack in the presence of the layer. When the thickness of the middle layer is small compared with other length scales of the structure, a universal relationship is found between the actual interface stress intensity factors at the crack tip and the

apparent mode I and mode II stress intensity factors associated with the corresponding problem for the crack in the bulk material. A interface crack model for a sandwich specimen is shown in figure 5.6. In our case, material 1 refers to concrete and material 2 refers to unidirectional composite with a crack lying in the direction of fibres on one interface. K_I and K_{II} represent mode I and mode II stress intensity factors for the bulk material 1 in the absence of the thin layer, and K^{∞} is the stress intensity factor.

$$K^{\infty} = K_I + iK_{II} \tag{5.13}$$

$$\left|K^{\infty}\right|^2 = K^2{}_I + K_{II}{}^2 \tag{5.14}$$

The energy release rate in the far field is defined as:

$$G = \frac{1}{\bar{E}_1}\left|K^{\infty}\right|^2 \tag{5.15}$$

G is the energy release rate for the bulk material and $\bar{E}_1$ is defined by equation 5.3 for material (1), concrete in our case. At the interfacial zone, when crack lies on one interface of a thin layer, thickness h bounded to thick bodies, the strain energy release rate can be estimated by ignoring the layer if the thickness h, is small compared with other specimen dimensions and crack length. The relationships between the interface

intensity factors and applied stress intensities is obtained by equating equation 5.9 and 5.15 (Suo and Hutchinson, 1989).

$$Kh^{i\varepsilon} = \sqrt{\frac{1-\alpha}{1-\beta^2}} k^{\infty} e^{i\omega(\alpha,\beta)} \tag{5.16}$$

$$\left|h^{i\varepsilon}\right| = 1 \tag{5.17}$$

where $\omega(\alpha,\beta)$ is a real function defining the shift in phase of the interface intensity factors relative to apparent stress intensity. However the phase angle near the crack tip is modified from that of asymptotic field by the following relationship:

$$\hat{\psi} = \phi - \varepsilon \ln h + \omega(\alpha,\beta) \tag{5.18}$$

where:

$$\phi = \tan^{-1}\left(\frac{K_{II}}{K_I}\right) \tag{5.19}$$

and

$$K^{\infty} = \left|K^{\infty}\right| e^{i\phi} \tag{5.20}$$

the function $\omega(\alpha, \beta)$ is extracted from numerical solution (Suo and Hutchinso, 1989) and is summerized in table 5.1.

A list of the values α, β and ε for different systems shows that ε is very small when $\beta \neq 0$, and it is likely that other problems and issues such as difficulty in preparing specimen and measurements have more effect on the results than ε (He et al. 1993). It was observed that ω is stronger function of α than β, (Ojdrovic and Petroski, 1987). So the interpretation of the interface intensity factors is much clearer when β is taken zero and a little of the physical consequences is lost by this assumption. The values of α, β, ω and ε were obtained for two composite- concrete interface systems, glass epoxy and carbon epoxy concrete interfaces. The properties of the materials are summarised in table 5.2 and the calculated values based on these properties are shown in table 5.3. It can be seen that for these composite-concrete systems ε is small and ω is practically insensitive to β.

Rotation of ω caused by the presence of a thin layer for $\beta=0$ is shown in figure 5.7. A polynomial is fitted to the function $\omega(\alpha,0)$ to obtain a the values of α for different

composite-concrete systems. Parameter α measures the relative stiffness of two material.

5.6 Composite –concrete interface properties

Due to small thickness of composite reinforcement compare to other RC structural dimensions sandwich interface crack model is recognised to be appropriate to obtain the composite-concrete interface properties. We start with specimens that are used to obtain the fracture toughness of concrete and with a proper technique we sandwich the composite layer into the bulk of specimen. Based on this approach two types of sandwich specimen are designed. Sandwiched Brazilian disk specimen and pure bending sandwich beam specimen.

5.6.1 Sandwich Brazilian disk specimen

Basically, a Brazilian disk specimen is a homogeneous circular disk of radius R, with a centre crack of length 2a. The loading phase angle, ψ, of the homogeneous specimen is controlled by compression angle θ. It is assumed the specimen is in mode I when $\theta=0$. Brazilian disk specimen is sometimes used to measure the fracture toughness of concrete (Ojdrovic and Petroski, 1987).

Brazilian sandwich disk specimens consist of thin layer of material 2 sandwich between two halves disk of bulk material 1, with a centre crack induced on one interface as shown in figure 5.8. This specimen was used to measure the fracture toughness of mortar-aggregate interface (Lee and Buyukozturk, 1992), for mixed-mode fracture testing of polycrystalline ceramics (Singh and Shetty, 1989) and for fracture toughness testing of steel-epoxy interface (Wang and Suo, 1990).

In Brazilian disk specimen, mixed mode stress states ranging from pure mode I to pure mode II can be achieved by selecting the inclination angle, θ of the central through crack with respect to the diametrical line of compression loading. So the loading phase of this specimen is controlled by load angle 'θ' as shown in figure 5.8 At a prescribed loading angle θ, and consequently a real phase angle, $\hat{\psi}$, the maximum loading amplitude that an interface can sustain without debonding is used to evaluate the toughness of the interface at this phase angle, noted as $G_c(\hat{\psi})$. An analytical formulation for stress-intensity factors for the inclined cracks in the Brazilian disk specimen is available (Atkinson et al., 1982). In general, mode I and mode II stress intensity factors in bulk material without internal sandwich layer, are obtained by the following equations;

$$K_I = \frac{P\sqrt{a}}{\sqrt{\pi}Rt} N_I \qquad (5.21)$$

$$K_{II} = \pm \frac{P\sqrt{a}}{\sqrt{\pi} Rt} N_{II} \tag{5.22}$$

where P represents the load, R is the disk radius and t is the specimen thickness and the plus sign is for tip A and minus sign is for tip B as shown in figure 5.8. N_I and N_{II} are non-dimensional calibration factors and are functions of loading angles θ and relative crack size (a/R). N_I and N_{II} are presented as fitting polynomial for (a/R)<0.3, as follow (Shah et al., 1995):

$$N_I = 1 - 4\sin^2\theta + 4\sin^2\theta(1 - 4\cos^2\theta)(a/R)^2 \tag{5.23}$$

$$N_{II} = \left[2 + (-5 + 8\cos^2\theta)(\frac{a}{R})\right]\sin(2\theta) \tag{5.24}$$

By substituting equations (5.21) and (5.22) in equation (5.15) energy release rate can be obtained as follow:

$$G = \frac{P^2 a}{\overline{E}_1 \pi R^2 t^2}(N_I^{\,2} + N_{II}^{\,2}) \tag{5.25}$$

when $\beta \neq 0$ and $\varepsilon \neq 0$, the real phase angle is calculated by:

$$\hat{\psi} = \pm \tan\left(\frac{N_{II}}{N_I}\right) + \omega - \varepsilon \ln(h) \tag{5.26}$$

$$\phi = \pm \tan^{-1}\left(\frac{N_{II}}{N_I}\right) = \tan^{-1}\left(\frac{K_{II}}{K_I}\right) \tag{5.27}$$

To calibrate the Brazilian sandwich disk specimen, equations (5.25) and (5.27) are plotted for various a/R ratio in figure 5.9 and figure 5.10 respectively. These curves can be used to obtain the toughness curves from the measured critical loads and compression angles. It should be noted that the loading angle as defined has no absolute physical significance. The sensitivity of real phase angle to material properties is shown in figure 5.11. It is clear that the real phase angle increases by increasing the relative material modulus of elasticity. Even though, it is theoretically possible, in practice it is difficult to obtain mode I crack opening results for a sandwich Brazilian disk specimen. For that reason, we propose a pure bending sandwich specimen for mode I.

5.6.2 Pure bending sandwich beam specimen

A homogeneous beam specimen with a crack at midspan on tension side, loaded in four point bending can be used to measure mode I crack opening of a homogeneous

material. To create a sandwich pure bending beam specimen a thin layer of composite is inserted at midspan and a crack is initiated along one interface in the tension side as shown in figure 5.12. In the presence of the thin sandwich layer the specimen is not in pure mode I opening. We will show later that for composite-concrete system the shift angle ω is very small so that the assumption of mode I crack opening is an acceptable one.

To apply the universal relation the thickness h should be small compared with the crack length. For pure bending specimen, the apparent intensity factor K_I is calculated by the following equation (Tada et al. 2000):

$$K_I = f_1 \sigma_r \sqrt{\pi a} \tag{5.28}$$

where:

$$\sigma_r = \frac{6M}{bd^2} \tag{5.29}$$

Where a is the crack length, M is the applied moment in the constant moment region, b is the width of the specimen, d is the height and f_1 is a geometrical correction factor which is a function of crack length and beam width. The value of $f_1(a/b)$ can be obtained by an empirical formulas as follows:

$$f_1(a/b) = 1.122 - 1.4(a/b) + 7.33(a/b)^2 - 13.08(a/b)^3 + 14.0(a/b)^4 \qquad (5.30)$$

the energy release rate in the case of small h can be calculated from:

$$G = \frac{1}{\bar{E}_1}\left|k_1\right|^2 \qquad (5.31)$$

5.7 Specimen Design and calibration

Brazilian sandwich disk specimen have the same diameter of the standard Brazilian test samples used to specify the tensile strength of concrete (ASTM C496). Due to insensitivity of these specimen to cylinder length (Ojdrovic and Petroski, 1987) a shorter length was chosen, 75 mm. Shorter specimen are easier to fabricate and handle, requires less material and may be tested in machines of smaller capacity. A crack is introduced in the middle of the specimen along one interface. The dimensions of the four point bending test specimen have been chosen according to the prisms used in *ASTM* test to obtain the modulus of rupture of concrete, except that it is molded in two parts so that the composite sheet can be sandwiched between the two halves.

In the Brazilian sandwich disk specimen fracture data, are sensitive to a/R ratio. It is reported that in concrete with smaller cracks, the crack propagation and failure are simultaneous. The fracture is brittle in nature. When the initial notch crack is increased, less load is needed to initiate microcrack are growth so that not enough

energy is stored to cause cylinder failure. Deviation of the crack from linear path occurs as microcracking around aggregate followed by a crack growth proceed. Figure 5.10 shows that the normalised energy release rate is less sensitive to relative crack length for smaller cracks also demonstrates that the change in normalised energy release rate is small for relative crack lengths between 0.15 and 0.3. In this study, for Brazilian sandwich disk specimen the relative crack length was chosen 0.15. The critical crack length was chosen small enough for the calibration to be valid and large enough not to interfere with any existing small porosity in the concrete.

5.8 Results

Specimen with cabon-epoxy composite sandwiched between two parts of bulk concrete were made. The materials properties of material are shown in table 5.2 and table 5.3. A composite prepreg is fabricated using handlay up technique and directly laminated directly on the sandblasted concrete surface. The crack was introduce by a parafin smeared thin stainless steel strip position on one interface. Diametral compression test on the Brazilian specimen and four point bending tests on the sandwich beam were performed in laboratory conditions using a servohydraulic testing machine with displacement control, under constant relatively slow cross head speed of 0.002 mm/sec. To achieve a mixed mode loading condition the angle of loading for the Brazilian disk specimen was ranging from 0 degrees to 30 degrees corresponding to real phase angle from 2 degrees to 90 degrees. So the 0 degree

corresponds approximately to crack opening mode I and 30 degrees corresponds to crack opening mode II.

The peak load P_c at which failure occurred was converted to fracture toughness G_c by equations (5.25) and (5.31). Following the relationship mentioned earlier, between the phase angle of loading and phase angle $\hat{\psi}$, the interface toughness curve can be traced for carbon epoxy-concrete interface figure 5.13. shows the interfacial fracture energy changes with the angle of loading. The failure of all the specimens were brittle and no crack propagation could be observed before final rupture. An interface mode of failure similar to that of composite strengthened RC beams was observed. A crack initiated at the interface, showed a tendency to enter into the concrete. As shown in figure 5.14 the thickness of the concrete layer separated from the bulk increased by increasing the angle of loading.

5.8 Conclusion

In a composite reinforced concrete structure, concrete and composite work through interfacial bond. Bond stresses develop at the interface because of differences of the stresses in concrete and composite due to different mechanical properties. Since concrete cracks under tensile stresses and some cracks are usually developed at the interface, fracture mechanics approach have been used to characterise the failure of

composite-concrete bond. The interface in the presence of crack should not be regarded as a material with a geometric discontinuity under mode I crack opening.

An interfacial crack is subjected to combine normal and shear loading. The paths of the crack depends on the variation of principal tensile stresses, and it is not always in the direction of joints. The application of linear fracture mechanics to composite-concrete interface should be interpreted with care because first the crack once initiates does not stays in the interface and does not propagate in a straight line but follows a tortuous path, along the interface. Second the fracture toughness obtained is not a fundamental property, because concrete and composite are not homogeneous isotropic materials and the fracture process complicated by debonding or crack arrest by an aggregate particle at the interface. It is believed that in a large specimen, when the crack is small compared to other geometry dimensions, the effects of heterogeneity are greatly reduced and composite-concrete interface may approximate a bimaterial interface to which principles of fracture mechanics can be applied.

The advantage of Brazilian disk specimen is that failure can be achieved under a mixed mode of loading. The results obtained from both specimens are sensitive to the change of phase angle of loading. Although the present experimental sandwich models may look conceptual in nature it seems it captures many salient features of the behaviour of composite-concrete interface. The critical interface release rates obtained

from these experimental procedures can be valuable in this context when used to calculate thresholds below which initial damage will not propagate.

5. 9 Reference

ISIS CANADA, Strengthening reinforced concrete structures with externally-bonded fiber reinforced polymers, spring 2000.

GRACE, N.F., SAYED, G.A., SOLIMAN, A..K., SALEH K.R. (1999). Strengthening reinforced concrete beams using fiber reinforced polymer (FRP) laminates, ACI Struct. J. , 96, 865-875.

SPADEA, G., BENCARDINO, F., SWAMY, R.N. (1998). Structural behavior of composite RC beams with externally bonded CFRP, Journal of Composite for Construction, 2, 132-137.

SINGH, D., SHETTY, D.K. (1989). Fracture toughness of Polycrystalline ceramics in combined mode I and mode II loading. J. Am. Ceram. Soc., 72(1), 78-84.

OEHLERS, D. J., MORAN, J. P. (1990). Premature failure of externally plated reinforced conrete beams. J. Struct. Eng., 116, 978-995.

JONES, R., SWAMY, R. N., ANG, T. H. (1982). Under and over reinforced concrete beams with glued steel plates, Int. J. cement composite and light weight concrete, 1, 19-32.

JONES, R., SWAMY, R. N. CHARIF, A. (1988). Plate separation and anchorage of reinforced concrete beams strengthened by epoxy-bonded steel plates, The Struct. Eng., 66, 47-56.

JOHNSON, R. P., TAIT, C. J. (1981), The strength in combined bending and tension of concrete beams with externally bonded reinforcing plates, Building and Environement, 16, 287-298.

MUKHOPADHYAYA, P., SWAMY, N., (2001) Interface shear stress: A new design criterion for plate debonding. J. composite Const., 5, 35-43.

SPADEA, G., BENCARDINO, F., SWAMY, R. N., MUKHOPADHYAYA, P. (2000), Design against premature debonding and brittle behavior the key to structural integrity with FRP bonded structural strengthening, Advanced composite materials in bridges and structures, J. L. Humar, A. G. Razagpur, 15-18.

CAO, H. C., EVANS, A.G. (1989), Experimental study of the fracture resistance of bimaterial interfaces, Mechanics of Materials, 295-304.

SUO, Z., HUTCHINSON, J. W. (1989), Sandwich test specimen for measuring interface crack toughness, Material Science and Engineering, A107, 135-143.

HE, M. Y., SHIH, C. F., EVANS, A. G. (1993), The geometry effects of stress intensity factor of sandwich specimen for measuring interfacial fracture toughness, Int. J. Frac., 59, 377-385.

OJDROVIC, R. P., PETROSKI, H. J. (1987), Fracture behavior of notched cylinder, J. Engng Mech., 113, 1551-1564.

LEE, K. M., BUYUKOZTURK, O. (1992), Fracture analysis of mortar-aggregate interfaces in concrete, J. Engng Mech., 118, 2031-2046.

WANG, J. S., SUO, Z. (1990), Experimental determination of interfacial toughness curves using Brazil-nut sandwiches, Acta Metall. Mater., 38, 1279-1290.

ATKINSON, C., SMELSER, R. E. (1982), Combined mode fracture via the cracked Brazilian disk test, Int. J. Fract., 18, 279-291.

SHAH, S. P., SWARTZ, S. E., OUYANG, C. (1995), Fracture mechanics of concrete: Applications of fracture mechanics to concrete, rock and other quasi-brittle materials, John Wiley & Sons, Inc.

TADA, H., PARIS, P.C., IRWIN, G.R. (2000), The stress analysis of cracks handbook, The American Society of Mechanical Engineers,

Table 5.1 $\omega(\alpha,\beta)$in degrees (Suo and Hutchinson, 1988)

β \ α	-0,8	-0,6	-0,4	-0,2	0,0	0,2	0,4	0,6	0,8
-0,4	2,2	3,5							
-0,3	3,0	4,0	3,3	1,4					
-0,2	3,6	4,1	3,4	2,0	-0,3	-3,3			
-0,1	4,0	4,1	3,3	2,0	0,1	-2,3	-5,5	-10,8	
0,0	4,4	3,8	2,9	1,6	0,0	-2,1	-4,7	-8,4	-14,3
0,1			2,3	1,1	-0,5	-2,3	-4,5	-7,4	-11,6
0,2					-1,3	-3,0	-4,9	-7,3	-10,5
0,3							-5,8	-7,8	-10,4
0,4									-11,1

Table 5. 2 Mechanical properties of concrete

Batch No.	Compressive strength, MPa	Modulus of elasticity (E), GPa	Poisson's ratio (ν)	Shear* modulus, GPa	$\bar{E} = \frac{E}{1-\nu^2}$, GPa
1	45	35.18	0.23	14.3	37.14
2	49	39.31	0.24	15.9	41.71
3	41	39.26	0.2	16.4	40.9
4	37	33.92	0.21	14	35.48
Average	43	37	0.22	15.15	38.8

*Calculated value, $G = \frac{E}{2(1+\nu)}$

Table 5.3 Mechanical properties of composites

Composite	Fibre volume fraction	Longitudinal tensile strength	E_l^*	ν	G**, GPa	$\bar{E} = \frac{E}{1-\nu^2}$
GFRP	50%	400 MPa	20 GPa	0.2	8.3	21 GPa
CFRP	50%	640 MPa	64 GPa	0.2	26.7	67 GPa

*Longitudinal modulus of elasticity

** Calculated value, $G = \frac{E}{2(1+\nu)}$

Table 5.4 Dundurs' parameters for different bi-material systems

System	α	β	ε	ω(α,β)	ω(α,0)
Glass/epoxy-concrete	0.3	0.1	-0.03	-3.4	-3.76
Carbon/epoxy-concrete	-0.27	-0.1	0.032	2.65	2.56

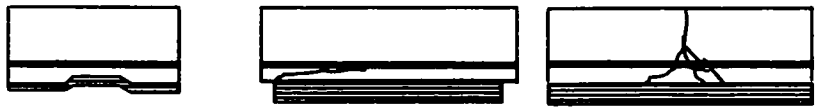

Figure 5.1 Different failure modes in reinforced concrete beam strengthened with FRP plate; (a) peeling-off the FRP sheet because of non-uniformities on the concrete; (b)Shear failure of the concrete layer between the steel reinforcement and FRP sheet; (c) Interface crack propagation because of flexure crack development

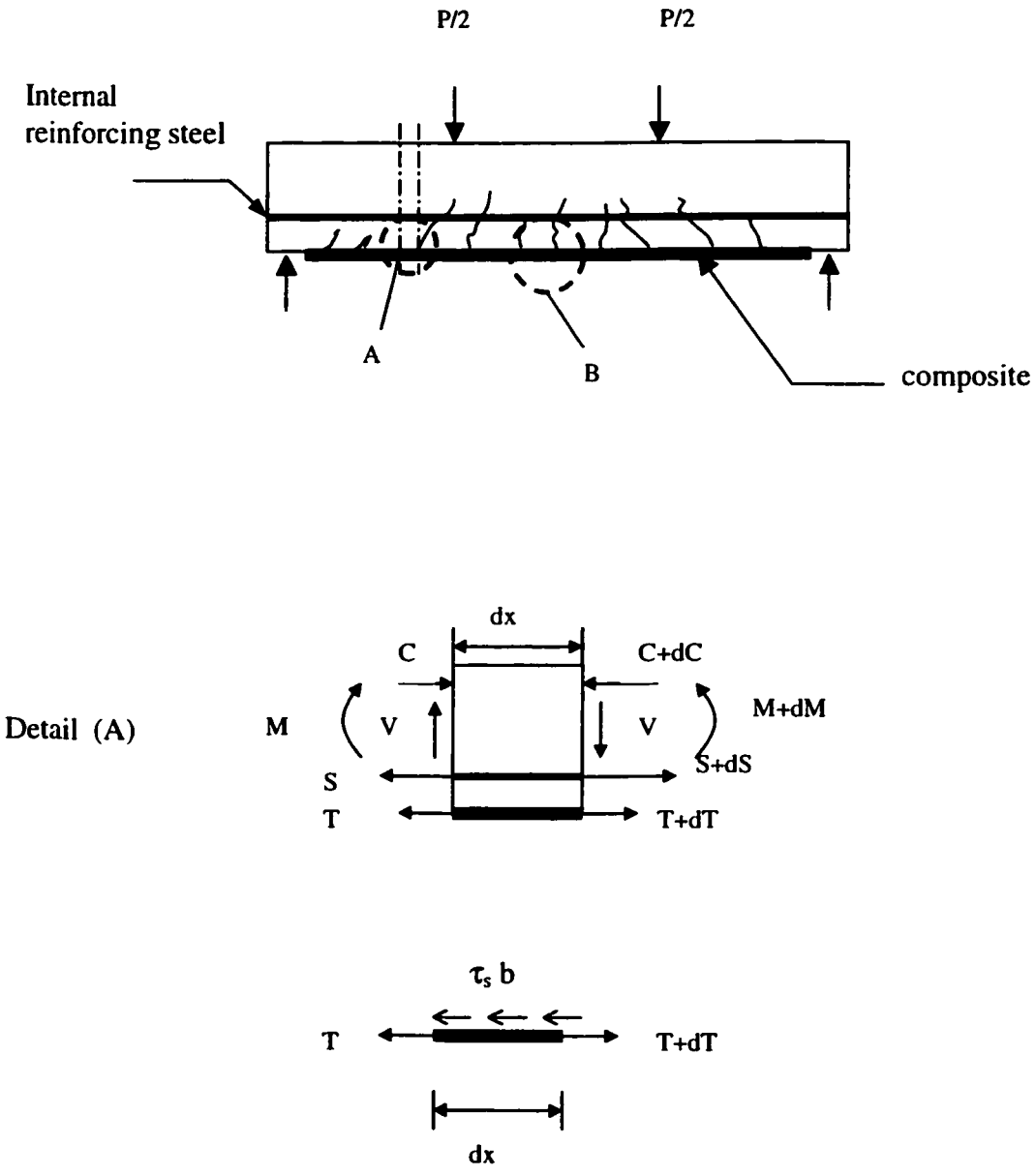

Figure 5.2 Bond stress in the composite strengthened RC beam; (a) reinforced beam, (b) detail A, (c) bond stress in composite

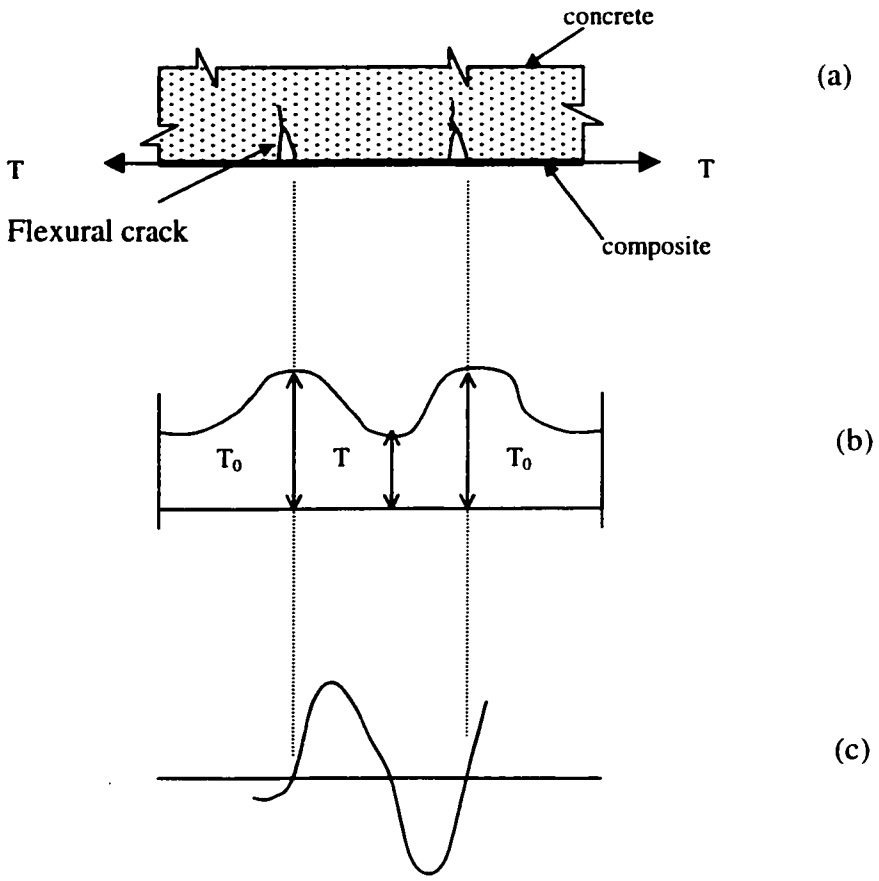

Figure 5.3 Effect of flexural cracks on bond stress in constant moment region, (a) detail B in figure 5.2 constant moment region between flexural cracks, (b) variation of composite tension between cracks, (c) variation of bond stress

(a)

(a)

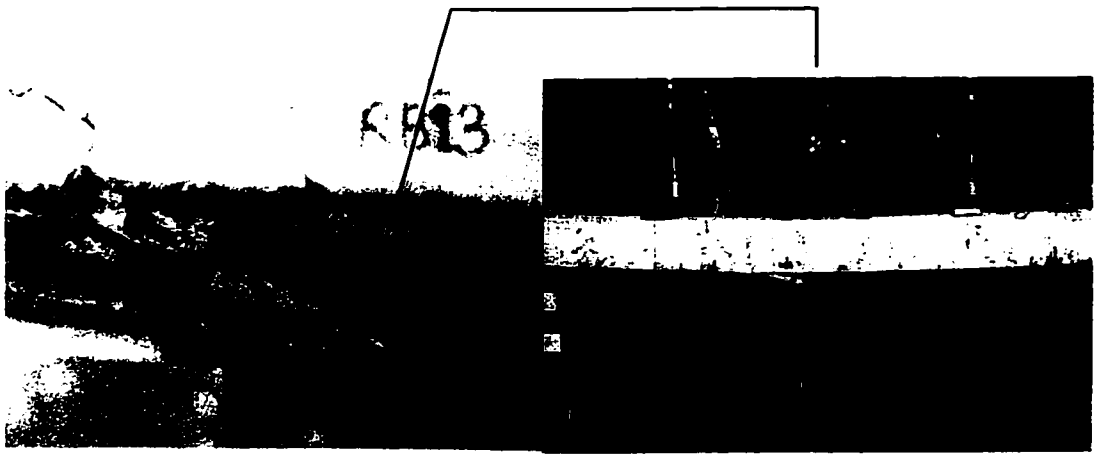

(b)

Figure 5.4 Debonding of composite, (a) interface crack propagation in the direction of already existing flexural shear crack (b) interface crack propagation in constant moment region

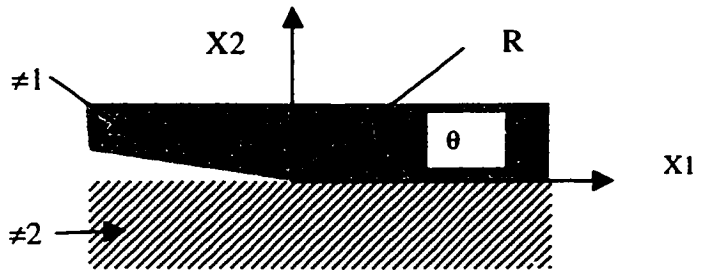

Figure 5.5 Geometry of interfaces Crack

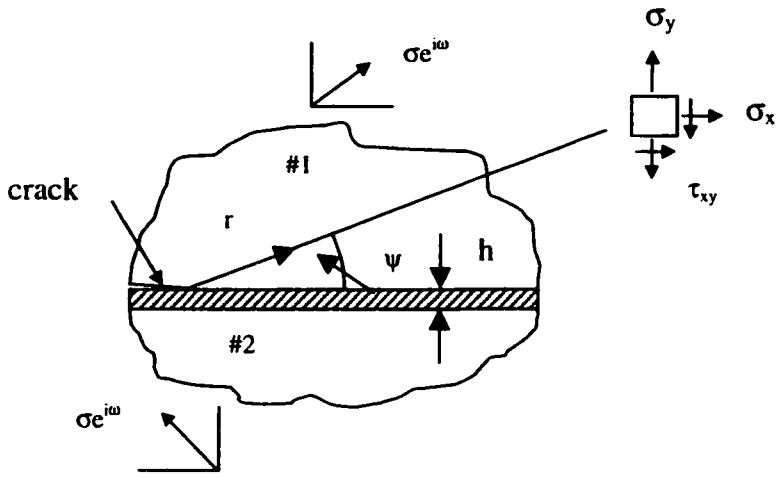

Figure 5.6 Interfacial crack in a sandwich model

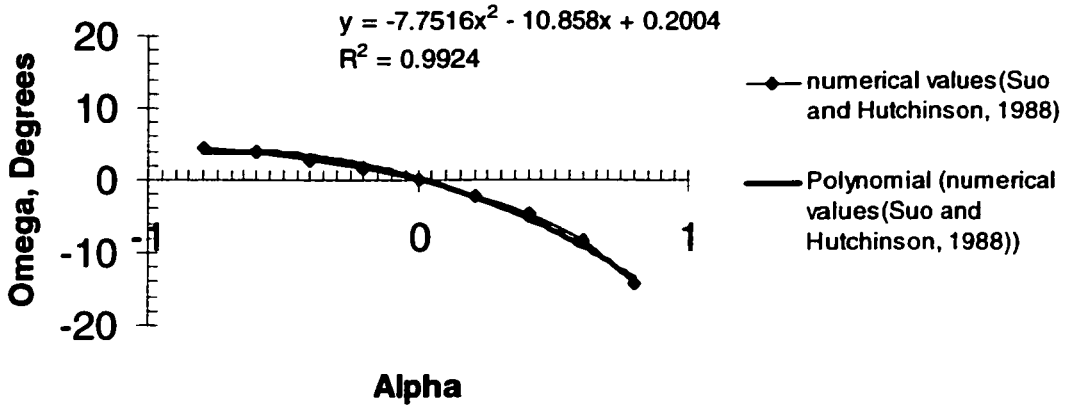

Figure 5.7 α-ω relationships

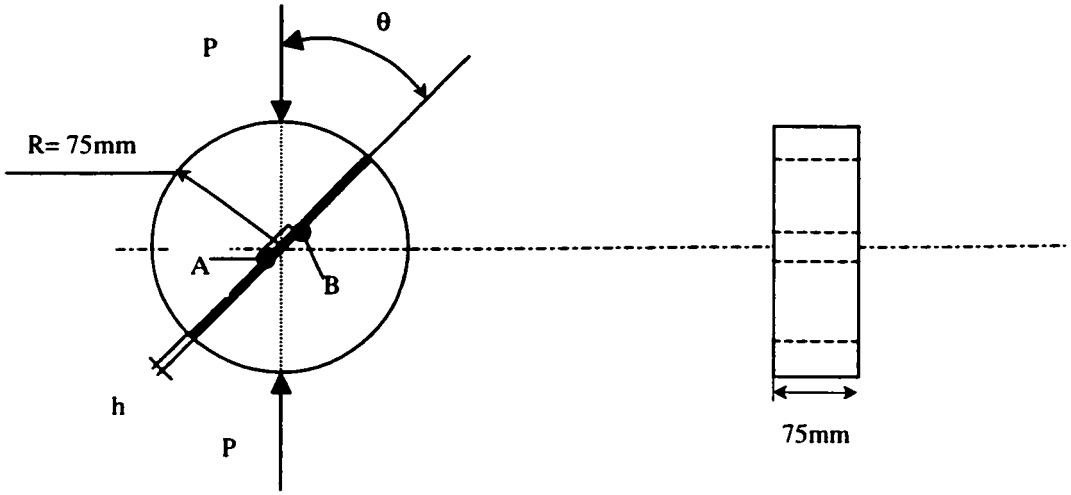

Figure 5.8 Brazilian sandwich disk specimen in diametral compression

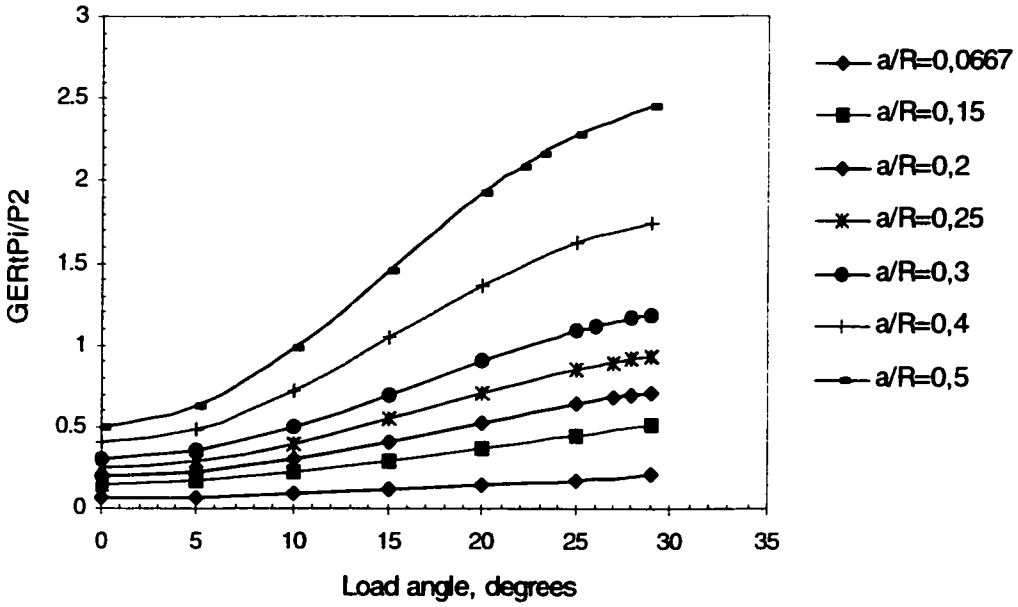

Figure 5.9 Brazilian nutched calibration

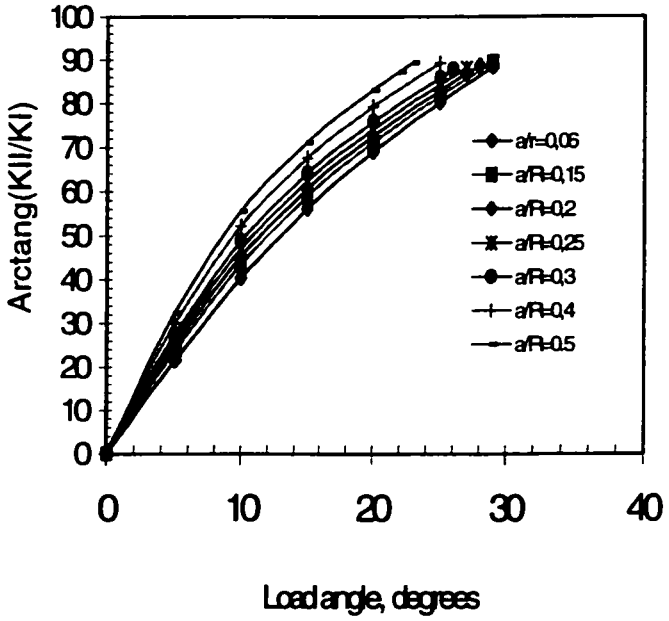

Figure 5.10 Relationships between loading phase and loading angle for different a/R ratios

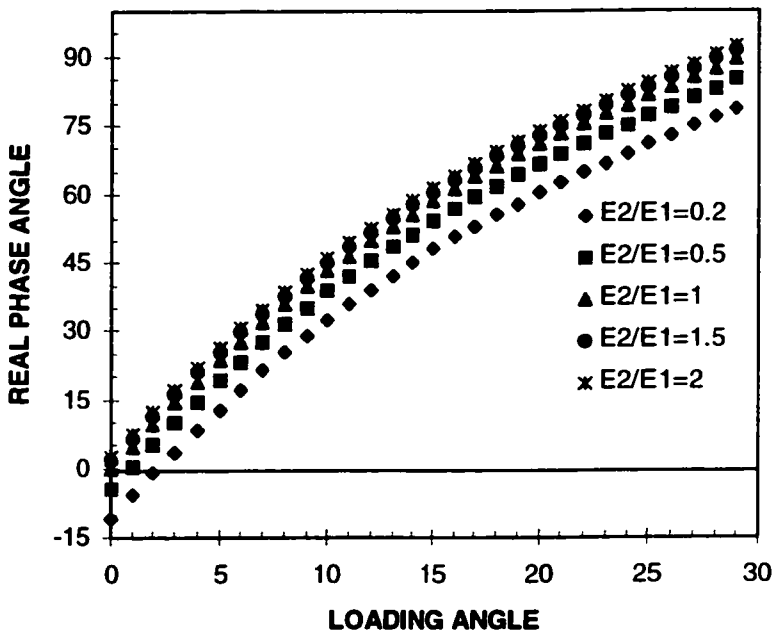

Figure 5.11 Relationships between loading angle and real phase angle for different material properties

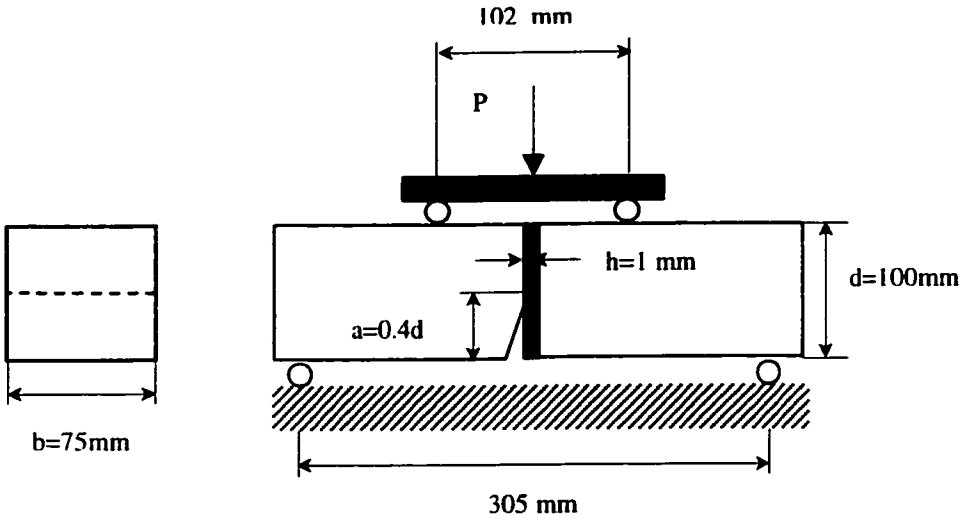

Figure 5.12 Pure bending sandwich specimen

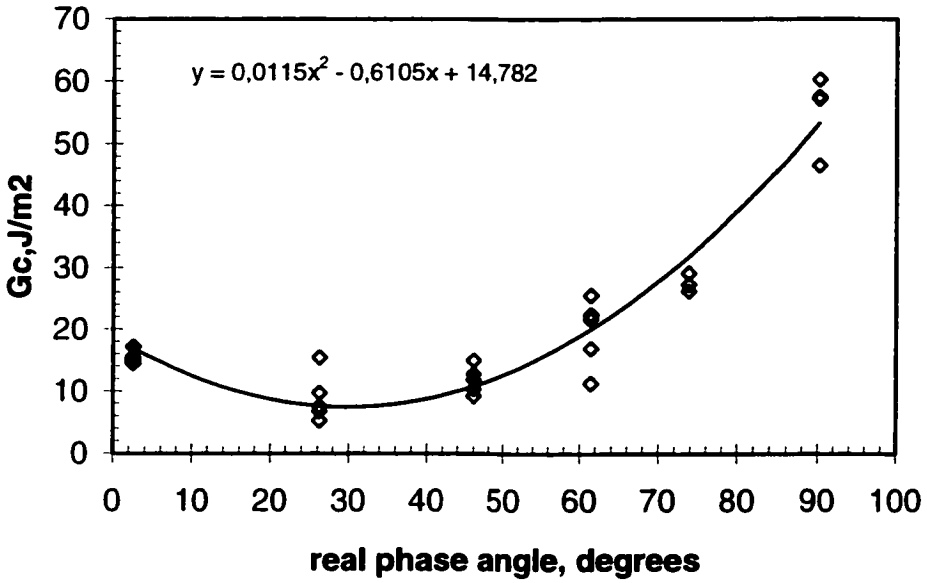

Figure 5.13 Fracture toughness curve for carbon/epoxy –concrete

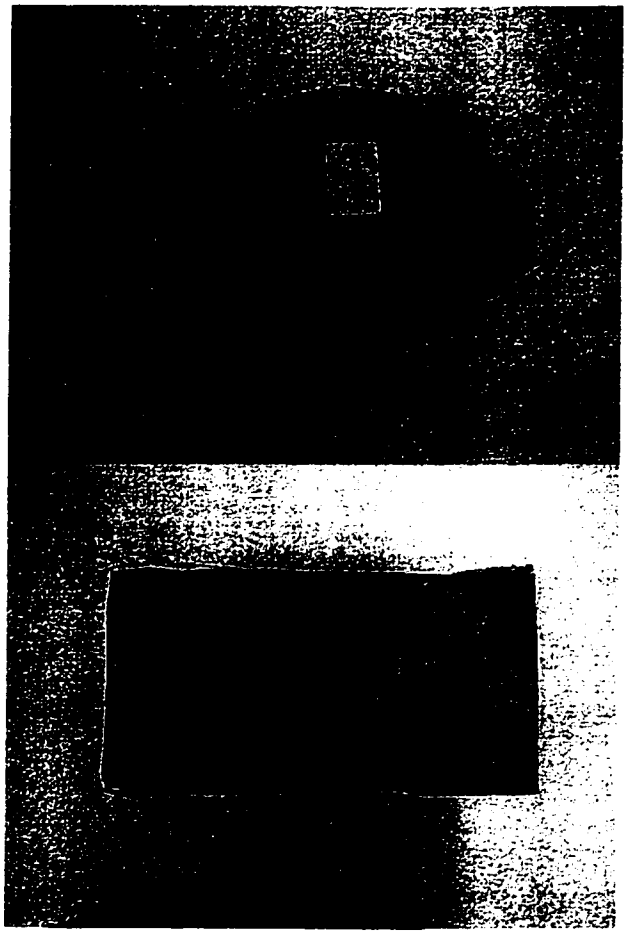

Figure 5.14 Carbon/epoxy-concrete interface failure at θ=15°

CHAPITRE 6

EFFECT OF COMPOSITE MATERIAL PROPERTIES ON THE COMPOSITE- CONCRETE INTERFACIAL RESISTANCE

Katayoun Soulati, **École Polytechnique de Montreal**

Raymond Gauvin, **École Polytechnique de Montreal**

6.1 Abstract

Composite material are bonded to reinforced concrete structures to upgrade their performance. Premature mode of failure of debonding of the composite from concrete surface prevents the structure to attain its maximum designed capacity. To understand the mechanism of debonding, the behaviour of the composite-concrete interface under mixed mode of loading is studied using sandwich specimens consisting of a thin layer of composite sandwiched between two pieces of bulk concrete. In the experimental model a Brazilian sandwich disk specimen and pure bending beam specimen are used to obtain the fracture toughness curves of glass/epoxy-concrete and carbon epoxy-concrete interface systems. The test results show that the interface resistance depends on the mechanical properties of composite and on the loading phase angle. The sensitivity of the experimental model to composite mechanical properties indicates the

effectiveness of the sandwich specimens used in this work to evaluate interface properties.

6.2 Introduction

The use of composite in infrastructure application has attracted considerable attention over the past few years. For instance, composite materials in the form of sheets or plates are bonded to reinforced concrete beams to strengthen and stiffen them. One of the major concerns in using composite materials as an external reinforcement for reinforced concrete structures is a premature mode of failure by debonding, which prevents the structure to attain its maximum designed capacity. A debonding mode of failure is brittle in nature and theoretically unpredictable. Different mechanisms of bond failure in composite strengthened RC beams were reported, which can be catagorized to two major groups; (1) peeling activated at the ends of the composite reinforcement where transfer stresses are concentrated, (2) composite-concrete interface failure. When relatively thick plates are used to strengthen reinforced concrete beams, high interface shear stresses may occur near the ends of the plates. Associated with these stresses are normal forces tending to peel off the plate. The peeling forces are relatively small and begin to have a significant effect only after interface shear failure has been initiated. This mode of failure has been studied by some authors theoretically (Oehlers and Moran, 1990, Hamoush and Ahmad, 1990, Bisby et al. 2000) and can be prevented using proper anchorage technique. On the

other hand, composite-concrete interface failure can initiate far from composite laminate ends and can originate from existing concrete tensile crack at the composite-concrete interface. The experimental results of composite strengthened reinforced concrete beams show that the bond characteristics of the composite-concrete interface are significant factors influencing the structural behavior both during the formation of flexural cracks and in the subsequent tension-stiffening phase. To increase the reliability of composite reinforcement to concrete based structures and to better understand the debonding mode of failure, it is critical to understand the behaviour of composite-concrete interface. Although many studies have been conducted to predict the behaviour of the interface between composite and concrete, the basic understanding of the interface behavior is rather limited. A mechanism of stress-strain transfer at the level of the interface and composite effective bond length have been studied by some researchers, using a number of specimen configurations or test setups. Shear stress distribution of the composite concrete bond have been investigated using single-lap shear test (Chajes, 1996, Bizindavyi and Neal, 1999), double strap (Nakaba et al., 2001, Ferrier and Hamelin, 2000, Bizindavyi et al., 2000), modified contoured double cantilever beam (CDCB) (Boyajian et al., 2000) and push part concrete test specimen (Kamel et al., 2000). The comparative parametric experimental investigations show that the bond strength and the stress distribution depends on the quality of surface treatment, composite material mechanical properties and concrete compressive strength. Experimental investigations of the influence of bond length on the strength illustrates that when the bond length increases, the failure force tends to

be increased because the apparent average bond stress decreases. However, there is a bond length beyond which no further increase in failure load can be achieved and composite failure or concrete shear failure occurs. In these investigations concrete shear failure was defined as the concrete failure close to the composite-concrete interface. The approach developed in these previous studies led to some very useful information with respect to the understanding of global bond behavior as affected by adherends mechanical properties and in evaluating the effective bond length. However the results obtained from these experimental investigations are limited to comparative studies. Also double lap and double strap joints are not inherently free of all induced peel stresses at the ends of the overlap. So there is a need to develop a methodology to determine the composite-concrete interface characteristics. Ideally such methodology would involve fracture mechanic concepts.

An experimental study on the measurement of the fracture energy of composite-concrete interface was performed by Kharbhari et al. (1996) using a modified peel test. They used the modified peel test to obtain the interfacial fracture energies associated with the composite-concrete interface, and study the effect of composite material properties and environmental effects on the interface. The interfacial composite-concrete bond quality was studied using a three point bending test modified to initiate shear failure under mode III conditions at the interface between composite and concrete (Weimer and Haupert, 2000). The crack propagation at the interface for

different types of concrete and carbon fiber reinforced (CFRP) laminate was studied and the composite-concrete interface shear resistance was reported.

Reinforced concrete beams loaded in flexure develop tensile cracks at very low load level. Composite sheets bonded to concrete surface cannot prevent cracks but lead to reduce crack width. However at all positions of a crack tip, interface is subjected to a combination of shear and normal stresses. Due to the difference in the properties of the individual materials and due to practical conditions of loading, cracking of the interface involves mix-mode of fracture effects. So our consideration in composite/concrete bonded joint is the possibility of crack growth, either within the interface or in any one of the adherends. The crack growth may be catastrophic when the fracture toughness of the interface or of one of the adherends is exceed. Because debond growth is a characteristic of bond failure, it is desirable to express the resistance to fracture in terms of debond parameters that reaches a critical value for catastrophic growth. This concepts leads to fracture mechanics of bimaterial interfaces.

The aim of this research is to investigate the effect of composite material properties on the composite-concrete interface properties by evaluation of interfacial toughness as a function of loading phase and to establish the fracture toughness curve for composite-concrete interface. The measurement of composite -concrete interface property was conducted using experimental models of sandwich specimen. Through using this

experimental models fracture toughness curves were obtained for glass/epoxy-concrete interface and for carbon/epoxy-concrete interface. It is shown that the interface properties are affected by composite material properties.

6.3 Experimental model

Composite and concrete are non homogeneous materials. Because of interaction of the several internal elements that constitute these materials, the behaviour of composite-concrete interface is complex and the state of stress at the level of interface is also complex. Therefore, to study the effects of different parameters on the overall mechanical behaviour of the interface, idealisation must be made so that relatively simple models can be constructed. The fracture mode of a bimaterial interface is mixed. Even when geometry and loading are symmetric with respect to the crack, differences between elastic properties across an interface will abrupt the symmetry. An interface crack model for a sandwich specimen is shown in figure 6.1. In these specimens a very thin layer of second material is sandwiched between two halves of the bulk of the same material. Also, as shown in figure 6.1 a pre-existing crack lies along one of the interfaces for these specimens. It was demonstrated that when the thickness of the sandwiched layer (2) is very small compared with other dimensions of the structure, the actual interface stress intensity factors at the crack tip can be obtained from the apparent mode I and mode II stress intensity factors associated with the corresponding problem for a bulk material (1) (Suo and Hutchinson, 1989). Due to

the small thickness of the composite reinforcement compare to other RC beam structural dimensions, sandwich interface crack model is recognized to be an appropriate approach to obtain the composite-concrete interface properties. Based on this approach, two types of sandwich specimen were used. Sandwich Brazilian disk specimen and pure bending sandwich beam specimen.

6.3.1 Brazilian sandwich disk specimen

Basically, a Brazilian sandwich disk specimen is a circular disk of radius R, with a centre crack of length 2a, as is shown in figure 6.2 This specimen has the diameter of the standard Brazilian specimen used to specify the tensile strength of concrete. The length of the specimen was chosen at 75 mm. This specimen was used to measure the fracture toughness of mortar-aggregate interface in (Lee and Buyukozturk, 1992), for mixed-mode fracture testing of polycrystalline ceramics in (Singh and Shetty, 1989) and for fracture toughness testing of steel-epoxy interface in (Wang and Suo, 1990). A thin layer of material 2 (one layer of composite in our case) is sandwiched between two halves disk of bulk material 1 (concrete), with a centre crack induced on one interface. In Brazilian disk specimen, mixed mode stress states ranging from pure mode I to pure mode II can be achieved by selecting the inclination angle θ of the central through crack with respect to the diametrical line of compression loading. So the loading phase is controlled by the angle θ as shown in figure 6.2. The critical strain energy release rate can be obtained with an analytical formula from the maximum

loading amplitude that the interface can sustain without decohesion and the load phase angle θ as follow:

$$G = \frac{P^2 a}{\overline{E}_1 \pi R^2 t^2}(N_I^{\ 2} + N_{II}^{\ 2}) \tag{6.1}$$

where P represents the load, R is the disk radius and t is the specimen thickness. N_I and N_{II} are non-dimensional calibration factors and are functions of the compression angles θ and the relative crack size (a/R). N_I and N_{II} are presented as fitting polynomial for (a/R)<0,3, as follow (Shah et al., 1995):

$$N_I = 1 - 4\sin^2\theta + 4\sin^2\theta(1 - 4\cos^2\theta)(a/R)^2 \tag{6.2}$$

$$N_{II} = \left[2 + (-5 + 8\cos^2\theta)(\frac{a}{R})\right]\sin(2\theta) \tag{6.3}$$

$\overline{E}_1$ is the material constant defined by the following equation for concrete:

$$\overline{E} = \frac{E}{1-\nu^2} = \frac{2G}{1-\nu} \tag{6.4}$$

where E is the modulus of elasticity, ν is the Poisson's ratio and G is the shear modulus of elasticity. The real phase angle $\hat{\psi}$ that measures the relative proportion of mode II to mode I crack opening at the interface crack tip can be calculated by:

$$\hat{\psi} = \phi + \omega \tag{6.5}$$

where ϕ measures the phase angle for the homogeneous bulk material in the absence of the thin layer:

$$\phi = \pm \tan^{-1}\left(\frac{N_{II}}{N_I}\right) = \tan^{-1}\left(\frac{K_{II}}{K_I}\right) \tag{6.6}$$

where the plus sign is for crack tip B and minus sign for crack tip A which represent both ends of the central crack opening, ω is the shift angle which defines the real phase angle at the bi-material interface crack tip (Suo and Hutchinson, 1989), ω, was obtained for our interface systems and is equal to -3.76 for glass/epoxy-concrete and 2.56 for carbon/epoxy-concrete. The interfacial fracture energy can be divided to its actual components G_I and G_{II} opening and sliding mode interfacial fracture energies:

$$G = G_1 + G_{II} \tag{6.7}$$

$$G_1 = \frac{P^2 a}{\bar{E}_1 \pi R^2 t^2} N_I^{\,2} \tag{6.8}$$

$$G_{II} = \frac{P^2 a}{\overline{E}_1 \pi R^2 t^2} N_{II}^{\ 2} \tag{6.9}$$

6.3.2 Pure bending sandwich beam specimen

The geometry of this specimen is shown in figure 6.3. The beam has the same dimension as the prisms used in standard test method for flexural strength of concrete, except it is molded in two parts so that the composite sheet can be sandwiched between two halves. A homogeneous beam specimen with a crack at mid-span on the tension side, loaded in four point bending can be used to measure mode I crack opening of a homogeneous material. Similarly to create a sandwich pure bending beam specimen, a thin layer of composite is sandwiched at mid-span while a crack is initiated along one interface in the tension side. With the presence of the thin sandwiched layer, the specimen is almost in mode I opening. In fact, it can be shown that for composite-concrete system the deviation from pure mode I is very small and critical strain energy rate can be well approximated by mode I crack opening formulation available for bulk material.

For pure bending specimen, the apparent intensity factor K_I, in the absence of the thin layer is calculated by the following equation (Tada et al., 2000):

$$K_I = f_1 \sigma_r \sqrt{\pi a} \tag{6.10}$$

where:

$$\sigma_r = \frac{6M}{bd^2} \tag{6.11}$$

Where a is the crack length, M is the applied moment in the constant moment region, b is the width of the specimen, d is the height and f_1 is a geometrical correction factor which is a function of crack length and beam width. The value of $f_1(a/b)$ can be obtained by an empirical formulas as follows:

$$f_1(a/b) = 1.122 - 1.4(a/b) + 7.33(a/b)^2 - 13.08(a/b)^3 + 14.0(a/b)^4 \tag{6.12}$$

the energy release rate of the interface in the case of a small h can be approximated by the energy release rate of the bulk, with the following relationship:

$$G = \frac{1}{\bar{E}_1}\left|k_I\right|^2 \tag{6.13}$$

6.4 Experimental procedure

6.4.1 Specimen Design and fabrication

6.4.1.1 Brazilian sandwich disk specimen

A total of 50 specimens were fabricated and tested. Concrete specimens were cast in a cylindrical plastic molds. A strip of thin stainless steel sheet (0.3x75x150mm) was placed in the diameter of the cylindrical molds to divide it in two halves. The position of the steel sheet was fixed on the sides of the cylindrical mold using adhesive. After casting, all specimens were moist-cured in a humid chamber until the time of testing. Before applying the composite to the concrete surface, the surface of the concrete was sand-blasted to remove laitance and to expose aggregates. Moist concrete semi-cylinders were left to dry in the laboratory for one day before sandblasting. The surface of concrete after sandblasting is shown in figure 6.4. The sand blasted surface is cleaned using compressed air. The surface was then primed with an epoxy primer (Sikadur Hex300 epoxy). One layer of unidirectional carbon fibre (SikaWrap 103C) and unidirectional glass fibres (SikaWrap100G) were impregnated with Sikadur Hex306 epoxy resin on a flat surface using hand lay-up technique and right after, laminated directly on the primed concrete surface. A starter crack was introduced on one interface using a strip of thin steel sheet, 0.3 mm thick. Paraffin was smeared on the steel surface and the steel strip was put in the centre area of the Brazilian disk. The two halves of the concrete cylinders were clamped together and let to cure for two weeks at ambient temperature. The relative crack size (a/R) was controlled to be 0.15. The critical crack length was chosen small enough for the calibration to be valid and large enough not to interfere with any existing irregularities in the concrete surface.

6.4.1.2 Pure bending sandwich beam specimen

It was assumed that energy absorption takes place only in fracture zone which implies that all deformation outside that zone are purely elastic. This is approximately true if the stresses are low in the major part of the beam. So a rather deep notch has been used in order to keep the maximum bending moment low for the test.

The beams were molded in two halves in wooden molds. The process of concrete cure was the same used for the Brazilian disk specimens. The composite was laminated on a primed sandblasted concrete surface using the wet handlayup technique described above. The starter crack was induced on one interface and the two halves were clamped together and let to cure in laboratory condition for two weeks before testing.

6.4.2 Materials

6.4.2.1 Concrete

One concrete mix with an average 28 days compressive strength of 35 MPa was used to mold the reinforced concrete beams in four batches. Type 10 Portland cement with no admixture was used and the maximum aggregate size was 20 mm. The ratio of cement /sand /water/aggregate in the mortar mix was 1/2 /0.5 /3 by weight. For each batch, four 152x305 mm (6x12 in) concrete cylinders were cast and tested according to ASTM C39-94 and ASTM C469-94 procedures to determine the concrete

compressive strength, modulus of elasticity and Poisson's ratio. These properties are summarized in table. 6.1 The concrete has an average cylinder compression strength of 43 MPa and an average modulus of elasticity of 37 GPa.

6.4.2.2 Composite

To measure the composite properties one layer of carbon fabric and one layer of glass fabric were respectively impregnated with epoxy using hand lay-up technique and let to cure in laboratory conditions for two weeks. The thickness of the cured lamina was measured at1 mm for both types of composite. These CFRP and GFRP laminas were tested for tensile properties according to ASTM D3039 testing procedure. The measured mechanical properties are summarized in table 6.2 Compsite Poissons' ratio were calculated with the formula presented in (Malick, 1993), taking into account fibre volume fraction and fibre and epoxy Poissons' ratio. Fibre and epoxy Poissons' ratios were obtained from (Schumusser, 1990).

6.4.2 Testing procedure

Diametrical compression test of Brazilian disk and four point bending tests of sandwiched beam were performed in laboratory conditions using servo hydraulic machine with displacement control, as illustrated in figure 6.5 The specimens were loaded under a constant slow cross head speed of 0.002 mm/sec. On the Brazilian disk

to achieve a mixed mode loading condition the angle of loading θ was ranging in steps of degrees from 5° to 29° degrees corresponding to real phase angle of 26° to 90° for carbon/epoxy-concrete interface and to real phase angle of 27° to 91° for glass/epoxy-concrete interface respectively, with a deviation of ±1° for both material systems. The relationships between angle of loading 'θ 'and real phase angle is shown in figure 6.6. The loading and displacement signals from the machine were recorded by data acquisition system connected to a PC. The load at failure were recorded and the failure mode was monitored.

It should be noted that the state of stress at the crack tip in Brazilian sandwich disk specimen at loading angle zero cannot be considered as mode I crack opening. For that reason the mode I crack opening condition is examined using pure bending sandwich specimen. In the beam specimen, with the presence of a thin composite layer the interface crack opening is not in an absolute pure mode I. However the shift angle of loading is small and corresponds to 2° for carbon/epoxy-concrete interface and 4° for glass/epoxy-concrete interface. So interface properties can be approximated by mode I crack opening formulation available for bulk material as explained in section 2-2.

6.5 Results

6.5.1 Mechanical properties of the interface

Load-displacement curves were not completely linear. The non-linearity was a result of plastic deformation and stable micro cracking of concrete before final sudden and brittle failure of the specimens. The same trend was observed for the two kinds of specimens. So, the highest value of the curve was considered as the critical failure load. The peak load P at which failure occurred was converted to fracture toughness G_c with equation 6.1. Following the relationships mentioned earlier between the angle of loading θ and the real phase angle ψ, equation 6.5, the fracture toughness curves G_c-ψ were traced for glass/epoxy-concrete interface and carbon/epoxy-concrete interface. The mode I opening is represented by the data obtained from pure bending sandwich beam specimen. The fracture toughness for other phase angles was obtained using Brazilian sandwich disk specimen.

Figure 6.7 and 6.8 show fracture toughness curves for glass/epoxy–concrete and carbon/epoxy-concrete interface system. These figures show that the interfacial toughness G_c varies with the real phase angle, $\hat{\psi}$ for both interface material systems. It can be seen that in general, the interfacial fracture energy increases with phase angle. The carbon/epoxy-concrete interface resistance is more sensitive to the phase angle variations compared to glass/epoxy concrete system. At low loading angles fracture toughness is higher for GFRP-concrete interface than CFRP-concrete, around phase angle of 70 degrees this becomes inverse but toughness stays close.

The actual component of interfacial fracture energy, G_I and G_{II} is obtained using equation 6.8 and 6.9. Figure 6.9 and figure 6.10 show the change in mode I and mode II interfacial fracture energies for the two composite systems. It is observed that mode I fracture component of interfacial fracture energy decreases linearly with phase angle for both interface systems. The variation of sliding mode II is exponential for carbon/epoxy –concrete system but it is almost linear for glass/epoxy-concrete system.

6.5.2 Mode of failure

For both types of specimen interface crack propagation occurred at the final load in a brittle and catastrophic manner. No crack propagation was observed at the level of composite- concrete interface before final rupture. The failure started always at the inserted crack tip and propagated toward the loading points. When the maximum load reached the sandwich specimen broke into two pieces in a catastrophic manner.

Figure 6.11 shows the observed failure mode of the sandwich beam specimen. Crack initiated at the crack tip propagated in the concrete and a very thin layer of concrete was separated and remained on the concrete surface. The failure mode was the same for carbon/epoxy-concrete system and glass/epoxy-concrete system.

For the Brazilian sandwich disk specimen it was observed that the fracture always initiated at the crack tip at the interface and then propagated into the bonded material.

The crack fracture trajectory depended on the phase angle of loading and moves from the interface into the bonded material as shown in figure 6.12. For both composite, the crack propagation led to composite failure when the phase angle of loading was small (5°), and shown in figure 6.13. When the angle of loading further increased, the interfacial crack, started at the interface and then propagated in concrete as shown in figure 6.14. As illustrated the thickness of the concrete increased with the phase angle of loading. Sometimes, the crack propagated at the interface on one side and mostly in the concrete on the other side as shown in figure 6.15. For the highest loading angle, 20°, an unusual phenomena was observed. For all specimen of both composite the fracture, even though it was catastrophic, appeared to have started simultaneously on both side of the steel steps, figure 6.16. However, further investigation with high speed camera or other means is recommended before reaching a final conclusion on that behaviour.

In the concrete, substrate fracture occurred in cement -aggregate interface and a concrete pieces separated from the bulk, aggregate pieces were exposed to the surface. No aggregate fracture were observed.

6.6 Conclusion

Sandwich specimen was used to measure the fracture resistance of composite-concrete interface. Using modified Brazilian sandwich disk specimen and pure bending

sandwich beam specimen, the fracture toughness curves were obtained for glass/epoxy-concrete interface and carbon/epoxy-concrete interface.

The test results indicates that the interfacial fracture toughness is a strong function of the phase angle of loading and generally increases with the loading angle. It was also observed that the composite-concrete interface resistance depends on the composite material properties. Indeed, for the same concrete and angle of loading the interfacial fracture toughness is different for the two composite-concrete systems, which demonstrates the effectiveness of this testing method in evaluation of interface properties.

At failure, the interface crack showed a tendency to enter into the concrete for both composite-concrete systems. Although it was observed that for both types of composite and a large range of angle of loading, the crack eventually propagates in concrete, the fracture toughness obtained from the experiment is different from the fracture toughness of the concrete. The difference between the fracture resistance value obtained for glass/epoxy-concrete interface and carbon/epoxy-concrete interface for the same angle of loading indicates that the crack propagates at the interface and is affected by the composite mechanical properties.

The fracture resistance measurements conducted in this study has direct applicability to the interpretation and prediction of composite-concrete interface resistance. The

value of critical fracture energy release rate obtained from this experimental model can be used in conjunction with structural analysis to design composite strengthened reinforced concrete elements against debonding mode of failure.

Due to the sensibility of these experimental models to interface properties this test is recommended for the evaluation of the effects of surface treatment and environmental conditions on composite-concrete interface behaviour.

6.7 References

Bisby LA., Green MF., Beaudoin Y., Labossiere P. (2000). FRP plates and sheets bonded to reinforce concrete beams. Advanced composite materials in bridges and structures, J.L. Humar, and A.G. Razagpur, The Canadian Society for Civil engineering, 209-216

Bizindavyi, L., Neal, K.W. (1999). Transfer lengths and bond strengths for composite bonded to concrete, Journal of composites for construction, 3, 153-160

Bizindavyi, L., Neale, K.W., Erki, M. A. (2000). Behavior of bonded FRP/concrete joints with glass fibre anchors, Advanced Composite Materials in Bridges and Structures, J. Humar, A.G. Razagpur, The Canadian Society for Civil Engineering, 719-726.

Boyajian, D.M., Davalos, J. F., Qiao, P. (2000). Development of a test specimen for FRP-concrete mode I fracture, Advanced Composite Materials in Bridges and Structures, J. Humar, A.G. Razagpur, The Canadian Society for Civil Engineering, 445-452.

Chajes, M.J., Finch, Jr. W.W., Januszka, T.F., Thomson, Jr. T.A. (1996). Bond and force transfer of composite material plates bonded to concrete, ACI structural Journal, 93, 208-17

Ferrier, E., Hamelin, P., FRP for civil engineering structure: Effects of creep in the adhesive layer, 711-18.

Hamoush S.A. and Ahmad H. (1990). Debonding of steel plate-strengthened concrete beams, Journal of Structural Engineering, 116, 356-371

Kamel A. S., Elwi A. E., Cheng J.J.R., Experimental study on the behavior of CFRP sheets bonded to concrete, Advanced Composite Materials in Bridges and Structures, J. Humar, A.G. Razagpur, The Canadian Society for Civil Engineering, 61-68

Karbhari, V. M., and Engineer, M. (1996). Investigation of bond between concrete and composite, use of a peel test, Journal of reinforced plastics and composites, 15, 208-227.

Lee, K. M., Buyukozturk, O., (1992), Fracture analysis of mortar-aggregate interfaces in concrete, Journal of engineering mechanics, 118, 2031-2047.

Malick P. K. (1993), Fiber reinforced composites materials, Manufacturing and design, M. Dekker

Nakaba, K., Kanakubo, T., Furuta, T., Youshizawa, H., (2001), Bond behaviour between fibre reinforced polymer laminates and concrete, ACI structural Journal, 98, 359-367.

Oehlers J. and Moran JP. (1990). Premature Failure of Externally plated reinforced concrete beams, Journal of Structural Engineering, 116, 978-995.

Schmueser D. W. (1990), Engineering materials handbook, testing and analysis Adhesive and sealants, Evaluating test geometries, Engineering Materials Handbook, 3. ASM International

Shah, S. P., Swartz, S. E., Ouyang, C. (1995), Fracture mechanics of concrete: Applications of fracture mechanics to concrete, rock and other quasi-brittle materials. John Wiley & sons, Inc.

Singh, D., Shetty, D.K., (1989), Fracture toughness of Polycrystalline ceramics in combined mode I and mode II loading, Journal of American Society, 72, 78-84.

Suo, Z., Hutchinson, J. W. (1989), Sandwich test specimen for measuring interface crack toughness, Material Science and Engineering, A107, 135-43.

Wang, J. S., Suo, Z. (1990), Experimental determination of interfacial toughness curves using Brazilian sandwich disk specimen. Acta metall. Mater, 38, 279-290.

Weimer, C., Haupert, F. (2000). Influence of aggregate structure on mode III interfacial fracture between concrete and CFRP, Applied composite materials, 7,183-193.

Table 6.1 Mechanical properties of concrete

Batch No.	Compressive strength, MPa	Modulus of elasticity (E), GPa	Poisson's ratio (ν)	Shear* modulus, GPa	$\overline{E} = \frac{E}{1-\nu^2}$, GPa
1	45	35.18	0.23	14.3	37.14
2	49	39.31	0.24	15.9	41.71
3	41	39.26	0.2	16.4	40.9
4	37	33.92	0.21	14	35.48
Average	43	37	0.22	15.15	38.8

*Calculated value, $G = \frac{E}{2(1+\nu)}$

Table 6.2 Mehanical properties of composites

Composite	Fibre volume fraction	Longitudinal tensile strength	E_l^*	ν	G**, GPa	$\bar{E} = \frac{E}{1-\nu^2}$
GFRP	50%	400 MPa	20 GPa	0.2	8.3	21 GPa
CFRP	50%	640 MPa	64 GPa	0.2	26.7	67 GPa

*Longitudinal modulus of elasticity

** Calculated value, $G = \frac{E}{2(1+\nu)}$

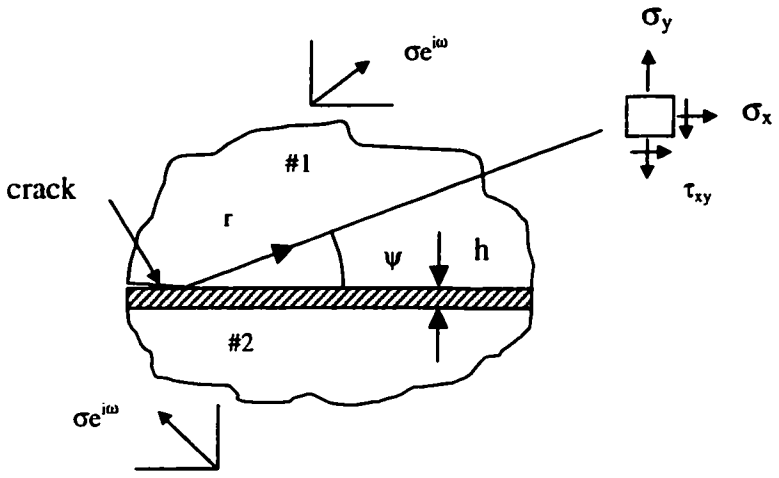

Figure 6.1 Interfacial crack in a sandwich model

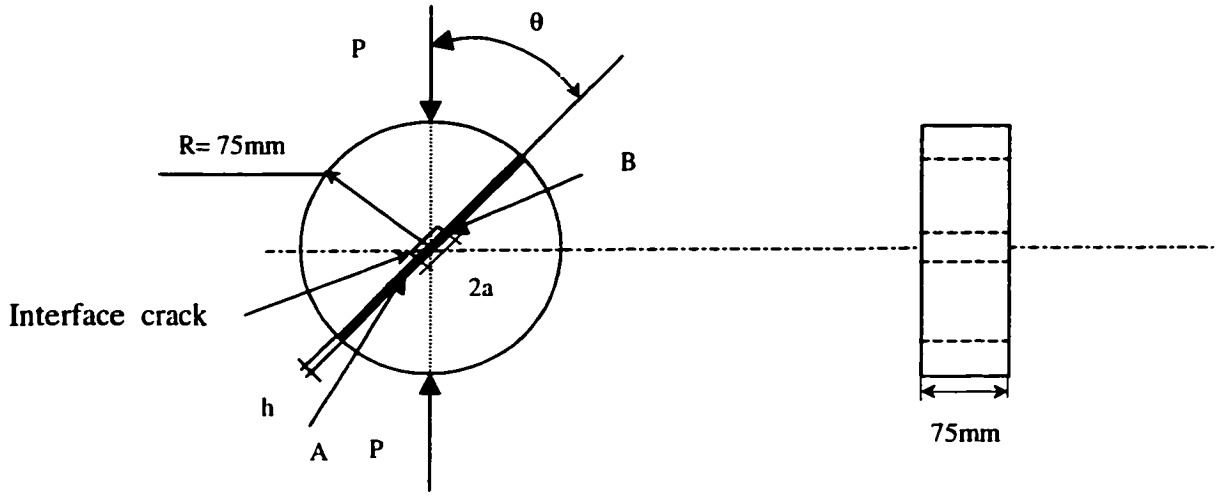

Figure 6.2 Brazilian Sandwich disk specimen in diametral compression

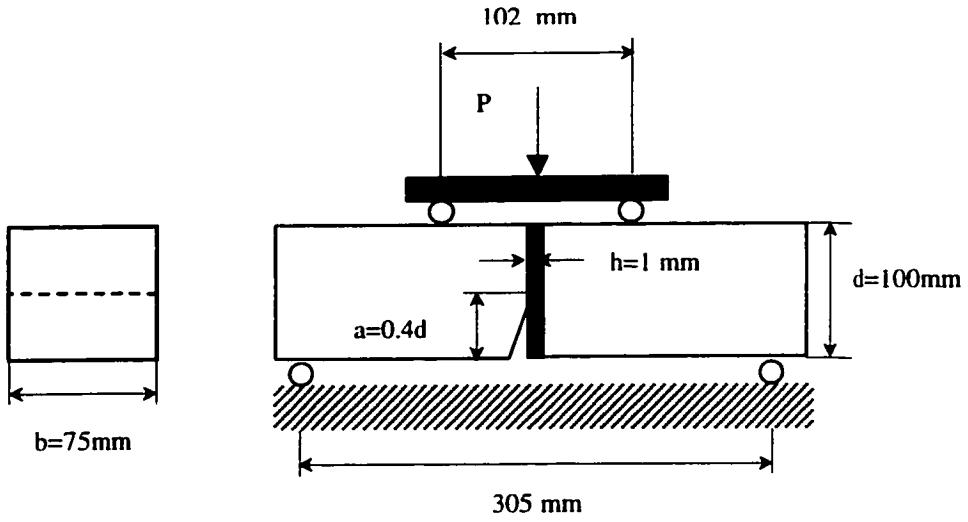

Figure 6.3 Pure bending sandwich specimen

Figure 6.4 Concrete surface after sandblasting process

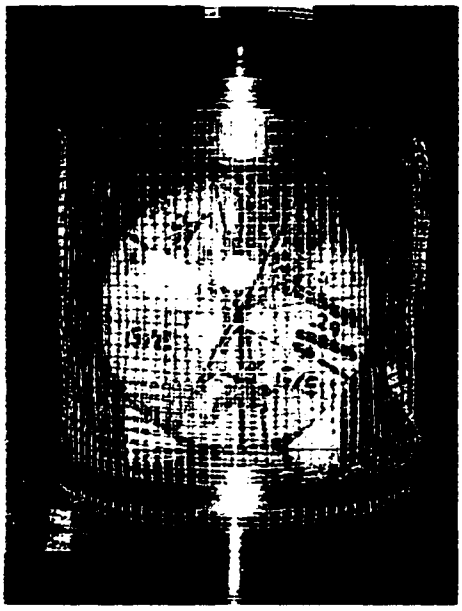

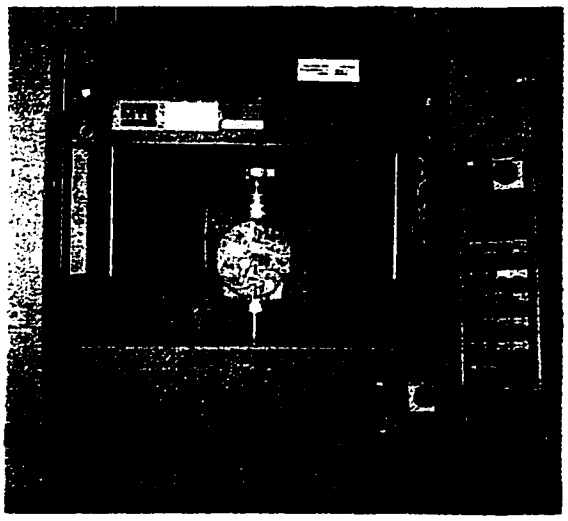

Figure 6.5 Photos of test setup for Brazilian sandwich disk specimen

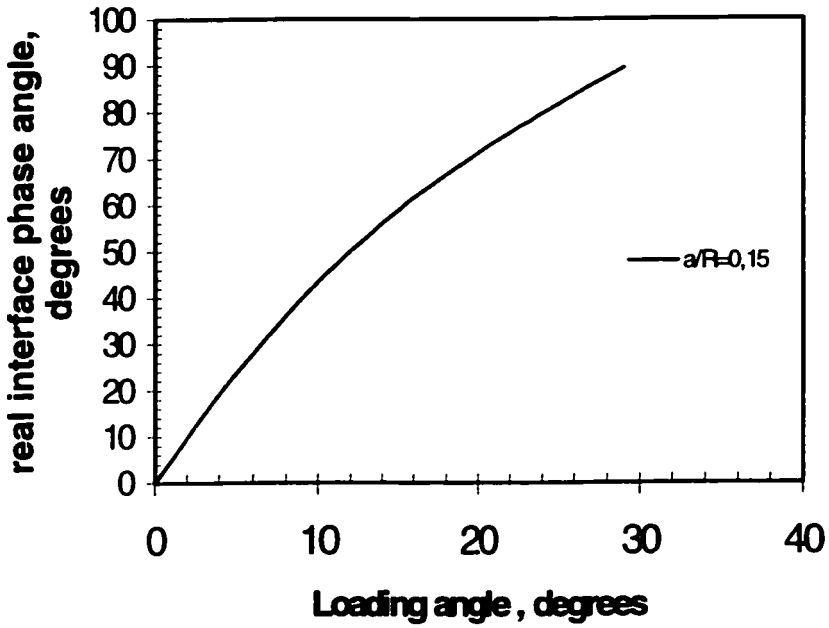

Figure 6.6 Relationships between loading angle and interface phase angle

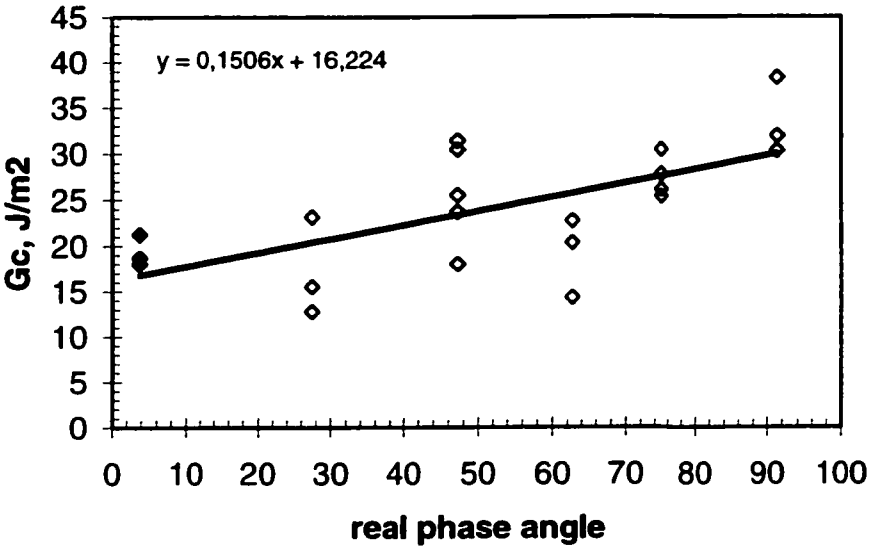

Figure 6.7 Fracture toughness curve for Glass/epoxy-concrete interface

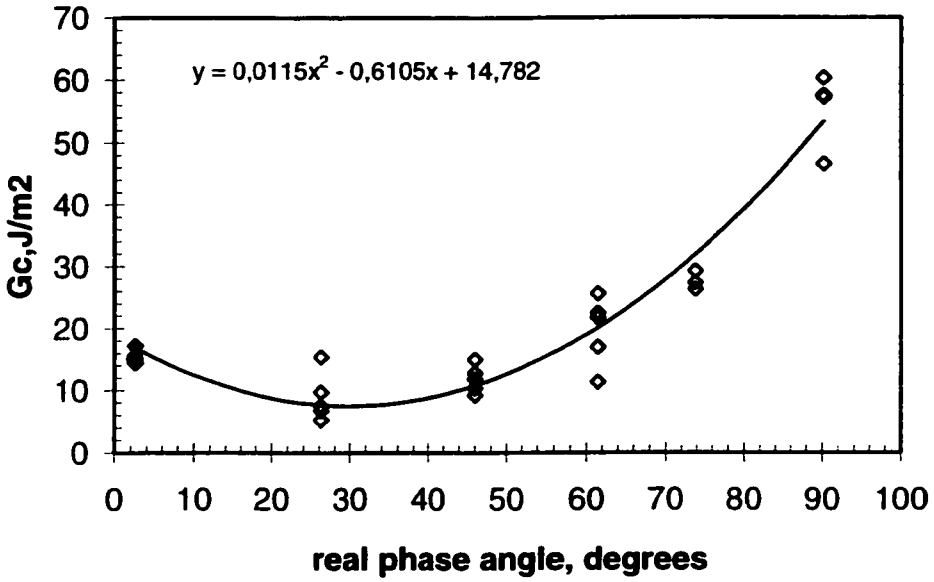

Figure 6.8 Fracture toughness curve for Carbon/epoxy-concrete interface

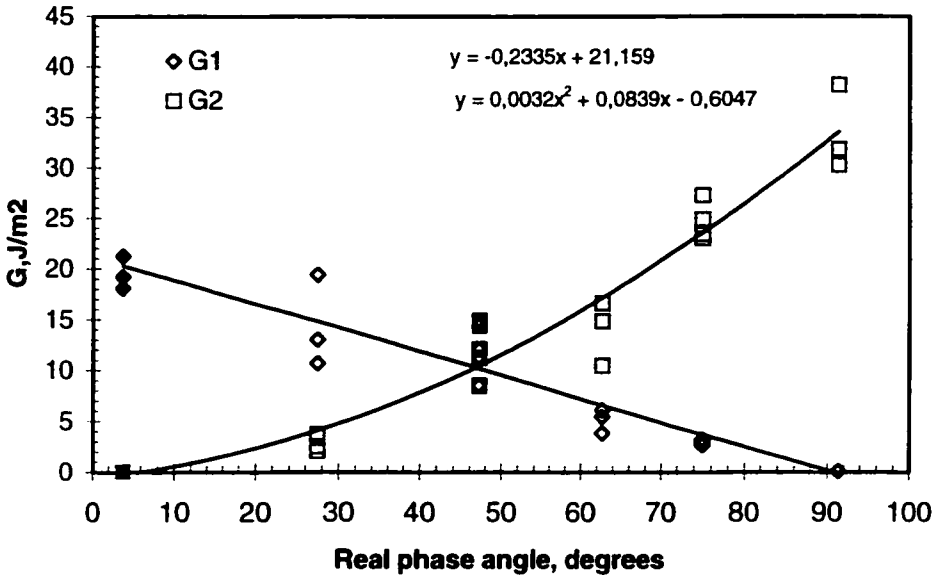

Figure 6.9 Mode I and mode II fracture toughness curves for glass/epoxy-concrete interface

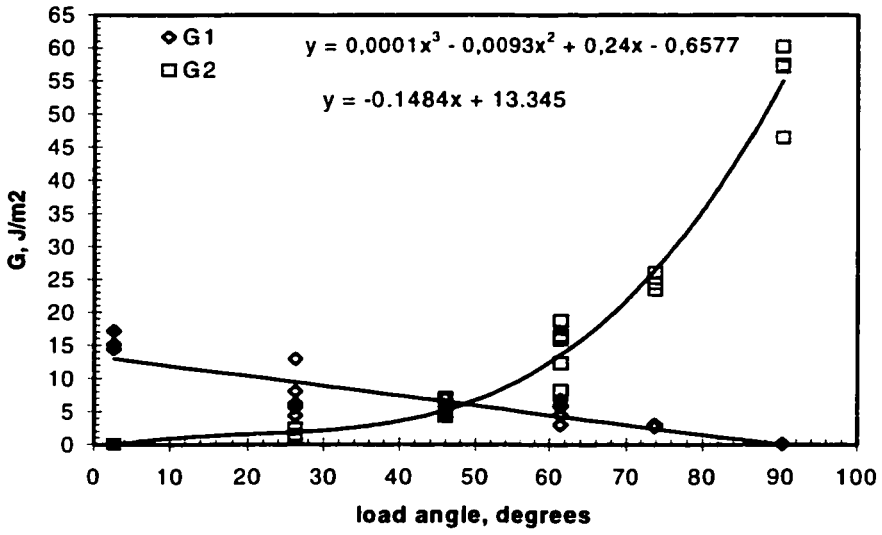

Figure 6.10 Mode I and mode II fracture toughness curves for carbon/epoxy-concrete interface

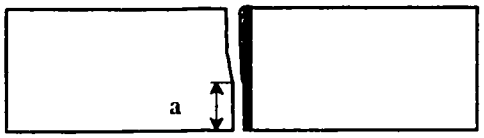

Figure 6.11 Failure of composite -concrete interface in pure bending sandwich specimen

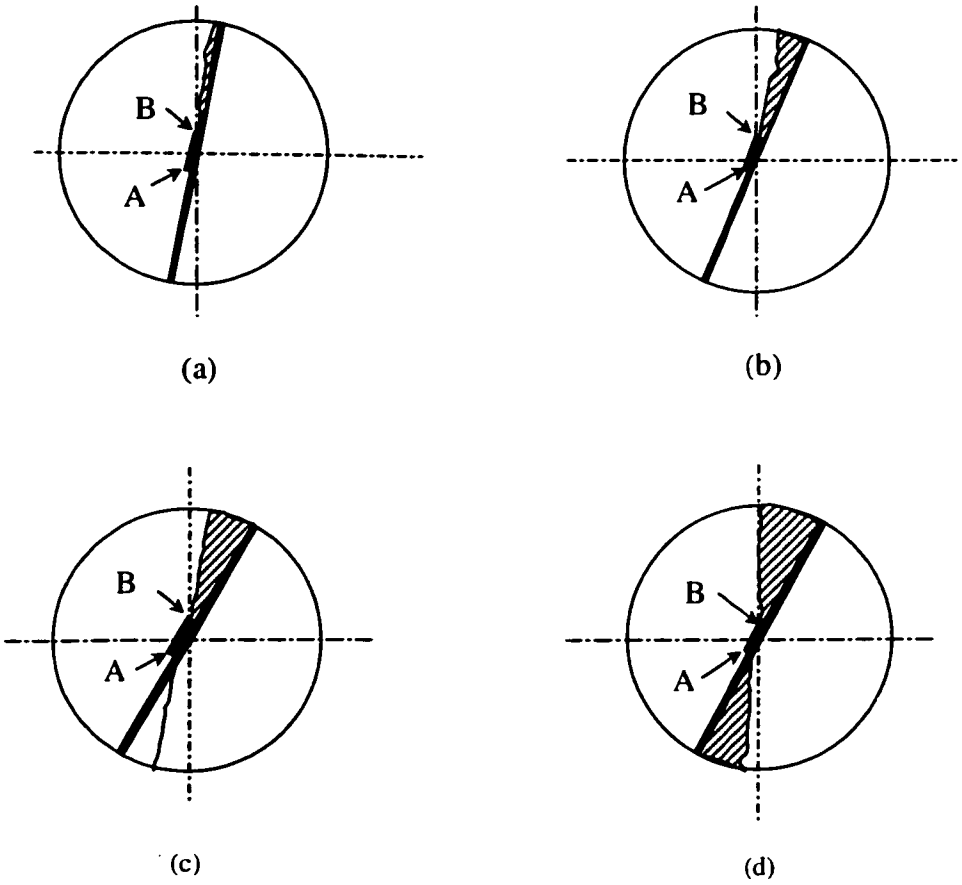

Figure 6.12 Different failure types for Brazilian sandwich disk specimen

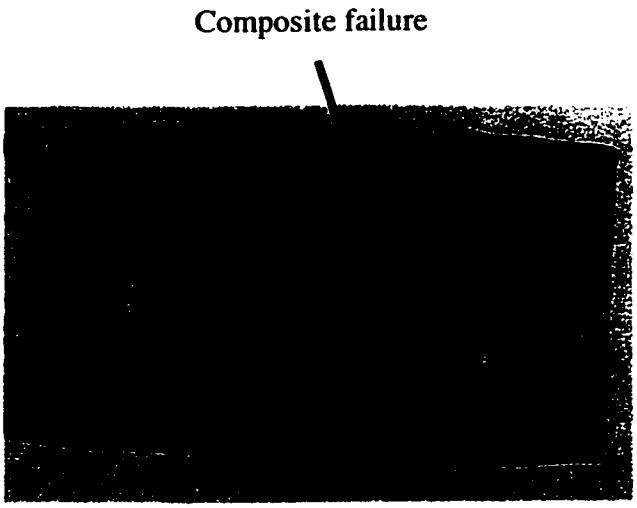

Figure 6.13 Carbon/epoxy-concrete interface fractured surface in composite, loading angle = 5°

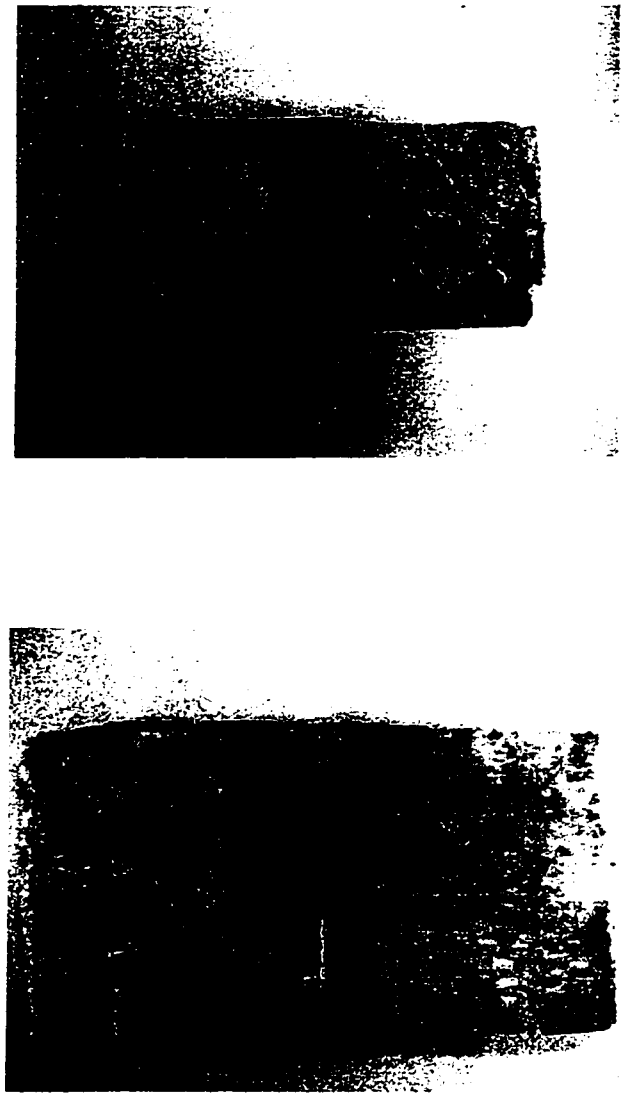

Figure 6.14 Fractured surface in composite-concrete interface:

(a) Carbon/epoxy-concrete interface, loading angle 10°

(b) Glass/epoxy –concrete interface, loading angle 10°

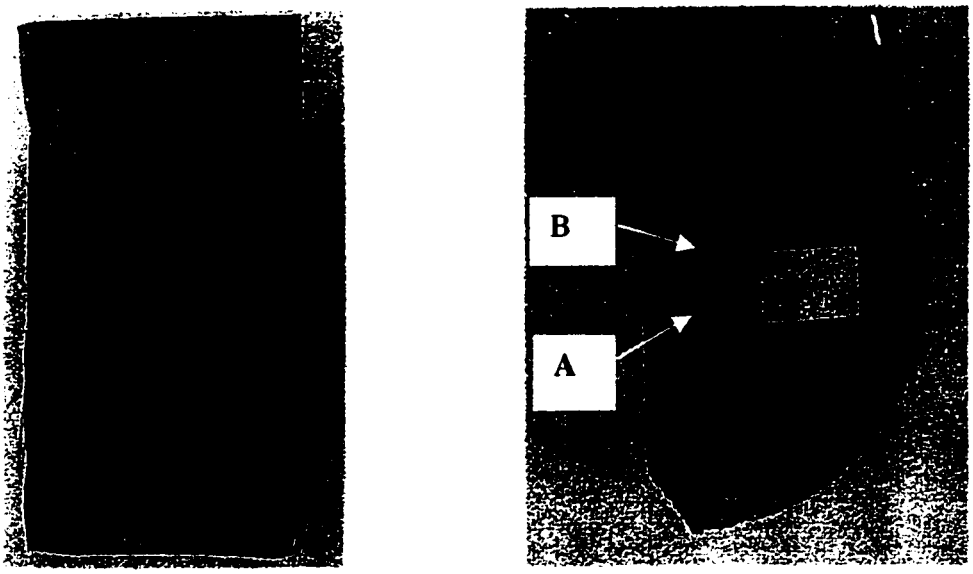

Figure 6.15 Interface crack propagation at carbon/epoxy-concrete interface

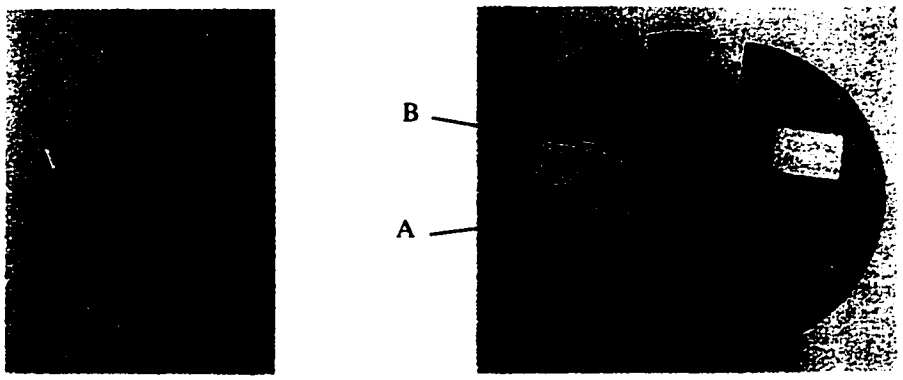

Figure 6.16 Mode II interface crack propagation at carbon/epoxy-concrete interface, loading angle θ=20°

DISCUSSION GÉNÉRALE

L'utilisation de matériaux composites pour le renforcement en flexion des poutres en béton armé est assez bien établie sur une base structurelle. Cependant, les aspects liés au choix et à l'utilisation des matériaux, aux modalités de design, aux mécanismes de rupture et à la durabilité ne sont pas toujours bien compris.

Cette thèse porte sur le mode de rupture par délaminage des poutres en béton armé renforcées par des matériaux composites et plus spécifiquement sur l'effet des propriétés des matériaux composites sur la résistance de l'interface béton-composite. D'après les principes mécaniques de la rupture de l'interface bimatière, nous suggérons une nouvelle méthode expérimentale pour mesurer les propriétés de l'interface béton-composite. Cette méthode peut être utilisée, conjointement avec l'analyse structurelle, pour concevoir des poutres de béton armé, mais semble à une rupture de délaminage.

En général, l'utilisation de matériaux composites pour fortifier les poutres en béton armé réduit la flèche et augmente la charge limite des poutres comparativement aux poutres témoins sans composite. Au chapitre 3, nous avons étudié l'effet de la rigidité structurelle du composite sur le comportement des poutres renforcées. La rigidité structurelle du composite est modifiée soit par changement du type de renfort ou par changement de l'épaisseur. Nous avons observé que la charge d'écoulement de l'acier

augmente avec la rigidité du composite, mais ces conclusions ne peuvent être transposées à la force à laquelle la rupture se produit. En effet, des ruptures prématurées peuvent survenir quand la rigidité du composite augmente. Ce mode de rupture a été observé dans les poutres renforcées au moyen de carbone-époxy, soit dans la région du moment constant ou dans celle du moment variable, mais aucun délaminage n'est survenu dans les poutres renforcées au moyen de verre-époxy. Les résultats montrent une diminution de la ductilité, exprimée par une diminution de la flèche maximale de la structure, quand la rigidité du composite augmente.

Le chapitre 4 contient les résultats des essais expérimentaux sur les poutres endommagées et subséquemment renforcées. Ces résultats montrent que l'effet de la réparation est fonction à la fois de la pré-fissuration et de la rigidité du composite. Nous observons également que les poutres réparées présentent des caractéristiques mécaniques supérieures à celles d'origine. Le degré d'endommagement ne change pas le mode de rupture, mais les poutres endommagées et subséquemment renforcées manifestent un comportement plus ductile que les poutres non endommagées et renforcées. La diffusion et la longueur des fissures de flexion dans le béton dépendent du moment appliqué et des propriétés des matériaux composites. La propriété qui influe le plus sur le comportement à court terme des poutres renforcées est la valeur de la rigidité en flexion EI. L'effet du matériau composite en changement du moment d'inertie de la section est petit. Par contre, la rigidité flexion de la poutre est plus élevée à cause de la participation du béton dans la traction entre les fissures.

Dans le chapitre 5, nous avons évalué les propriétés de l'interface béton-composite en utilisant l'approche de la mécanique de rupture. Nous y présentons une méthode expérimentale pour obtenir la ténacité de l'interface en utilisant des spécimens sandwichs. Deux sortes de spécimens sandwichs sont proposées à cette fin : le spécimen de disque brésilien et le spécimen de poutre. L'avantage du spécimen de disque brésilien est que la rupture peut être réalisée selon différentes proportions des modes I et II. Le spécimen de poutre est strictement réservé au mode I.

Au chapitre 6, nous appliquons notre méthode expérimentale pour évaluer l'effet des propriétés mécaniques du composite sur la résistance de l'interface. Les résultats d'essais montrent que la ténacité de l'interface est une fonction de l'angle de phase de chargement et qu'elle augmente généralement avec ce paramètre. La ténacité de l'interface dépend également de la rigidité du composite, même si la résine est la même pour les deux types de composites utilisés.

L'effet des propriétés du matériau composite est un facteur important. Le comportement de la poutre renforcée est non seulement contrôlé par la quantité de composite, mais aussi par les propriétés mécaniques du composite. Le composite affecte la rigidité structurelle, la fissuration du béton armé, ainsi que la résistance de l'interface béton-composite.

Pour conserver l'uniformité du joint béton-composite, l'interface doit supporter la contrainte créée par le chargement. Le délaminage du composite montre qu'en présence d'un défaut, la contrainte nécessaire pour l'initiation et la propagation des fissures est plus faible. L'étude du délaminage est reliée aux propriétés de rupture de l'interface. Les résultats expérimentaux démontrent que la rupture par délaminage ne survient pas dans une section spécifique de la poutre, mais dans les différentes régions de celle-ci. Ce mode de rupture dépend des contraintes au bout des fissures de flexion dans le béton et du taux d'énergie de déformation critique (*critical strain energy release rate*) pour la propagation des fissures d'interface, ce qu'on appelle la résistance de l'interface.

Le concept de la mécanique de rupture linéaire est utilisé pour présenter une nouvelle méthode expérimentale destinée à déterminer la ténacité de l'interface au moyen de spécimens sandwichs. Il faut cependant interpréter avec soin l'application de la mécanique de rupture linéaire à l'interface béton-composite parce que la fissure introduite initialement ne reste pas toujours dans l'interface et ne se propage pas toujours en ligne droite, mais suit un chemin quelque peu tortueux le long de l'interface. La ténacité de rupture obtenue n'est pas une propriété fondamentale, parce que le béton et le composite ne sont pas des matériaux isotropes homogènes et que le processus de rupture est compliqué par le délaminage ou l'arrêt de la fissure par un granulat à l'interface. On croit que dans un grand spécimen, quand la fissure est petite comparativement à d'autres dimensions géométriques, les effets d'hétérogénéité sont

réduits de sorte qu'on peut la considérer comme une interface bimatière à laquelle les principes de la mécanique de rupture peuvent s'appliquer. Le travail expérimental devrait être poursuivi afin d'étudier les effets de la taille des fissures dans le béton et ceux du taux de chargement.

Pour ce procédé expérimental, nous avons supposé que le niveau d'adhérence est parfait. Pour nous assurer que cette supposition puisse être appliquée en toute confiance, il est essentiel que le collage suive précisément la procédure dictée par les spécialistes. Il y a cependant lieu de noter que si les irrégularités de surface sont profondes, certaines ne seront pas complètement remplies lorsqu'on brossera ou roulera une couche primaire (*primer*) sur la surface de béton, ce qui risque d'emprisonner des vides et de former ainsi des cavités qui peuvent considérablement influer tant sur la durabilité du lien que sur la rupture de la structure.

Les éléments en béton armé sont généralement dimensionnés pour résister au-delà de la fissuration. Les fissures s'ouvrent sous charge et peuvent créer une zone de concentration de contraintes de cisaillement au bout de la fissure. Le délaminage du composite collé est donc fonction de l'état de contrainte à l'extrémité de la fissure. À cet endroit précis, les contraintes de cisaillement locales sont plus élevées que les contraintes de cisaillement moyennes agissant sur l'interface à cause du chargement. La valeur maximale de la contrainte de cisaillement supportée par l'interface ne devrait pas être considérée comme une vraie contrainte agissant sur les matériaux, mais plutôt

comme un paramètre reflétant l'intensité de la concentration de contraintes près de la fissure. La rupture de la poutre par délaminage peut survenir quand la contrainte maximale atteint une valeur critique. Cette valeur critique n'est pas nécessairement reliée à la résistance du béton, puisqu'il n'y a aucun rapport implicite entre la ténacité Kc et la résistance des matériaux.

À la section de moment constant, quand la longueur de la poutre est très grande comparativement à sa profondeur, l'ouverture de la fissure comporte deux composantes, l'une parallèle à la surface et l'autre perpendiculaire. En général, deux types de contraintes peuvent être présentes à l'interface, soit la contrainte normale et la contrainte de cisaillement. La contrainte normale résulte des effets combinés de la flexion de la structure et de la fissuration du béton. Les effets de la contrainte perpendiculaire de traction à l'interface et ceux de la faible résistance du lien béton-composite en traction s'additionnent pour diriger l'initiation et la propagation du délaminage. En termes de mécanique de rupture, le délaminage introduit au bout d'une fissure de flexion se propage en mode mixte (mode I et mode II). On peut dire, entre-temps, que dans l'encadrement de ce mécanisme, le mode I est largement dominant, bien que la participation du mode II ne puisse pas être exclue dans la propagation de la fissure de l'interface. La fissure s'ouvre plus facilement sous les contraintes de traction normales que sous les contraintes de cisaillement.

La caractérisation de l'interface par les concepts de la mécanique de rupture n'est pas suffisante pour prédire le comportement de la poutre renforcée sous charge, puisque la contrainte de cisaillement au bout de la fissure dépend non seulement de l'ouverture de la fissure, mais aussi du nombre de fissures développées dans le béton tendu, ce qui est tout à fait aléatoire. La fissuration dépend des propriétés du béton et du composite. Il est donc difficile de prévoir la position exacte du délaminage. La mise au point d'une méthode de design visant à éviter les bris catastrophiques propres au délaminage à l'interface béton-composite nécessite l'analyse simultanée de la rupture de l'interface et du comportement structurel de la poutre renforcée.

Le lien entre le comportement des poutres et celui de l'interface a pu être établi au moyen du concept d'énergie de déformation. Dans la résistance des matériaux, l'énergie de déformation d'une poutre renforcée est bien définie par la rigidité structurelle de la poutre sous charge telle que décrite par l'équation d'Euler. L'énergie critique de la rupture de l'interface peut être combinée avec l'analyse structurelle pour prévoir la déformation de la poutre au-delà de laquelle le délaminage se produit. Ceci conduit à la définition d'une perte d'énergie instable causée par le délaminage. Un tel travail nécessiterait une caractérisation plus poussée de la rigidité de la poutre renforcée et la prise en compte des effets de la fissuration et des propriétés mécaniques du composite et du béton. Le travail expérimental présenté dans cette thèse a tout de même permis de définir le phénomène et d'en identifier les principaux aspects.

L'efficacité de cette méthode de réparation est en grande partie dépendante des propriétés des matériaux qui ont été mises en évidence dans cette recherche et souligne les effets des propriétés des composites sur l'interface et le comportement structurel sous charge. L'importance de la mise au point d'un concept de design considérant les propriétés des matériaux composites a été discutée. Nous espérons que cela fournisse l'information de base pour l'introduction d'une stratégie théorique qui puisse servir à la prévention de la rupture par délaminage.

Les conditions comme l'humidité à l'interface entre le composite et le béton soulèvent le problème de la durabilité à long terme du lien. Les spécimens sandwichs proposés permettent d'évaluer l'effet de différents paramètres environnementaux sur la résistance de l'interface, ce qui constitue certainement un sujet intéressant pour une nouvelle recherche.

BIBLIOGRAPHIE

ABDALLA, H. et EL-BADRY, M.M. (1996). Deflection of concrete slabs reinforced with advanced composite materials. Advanced composite materials in bridges and structures, M.M. El-Badry, The canadian society for civil engineering, 201-208.

ADAMS, R.D. (1990). Failure strength tests and their limitations, Testing and analysis. Adhesives and sealants. Engineering materials handbook, 3. ASM International;

AL-SAIDY, A., EHSANI, M.R. et SAADATMANESH, H. (1996). Strengthening of URM walls for direct shear. Advanced composite materials in bridges and structures, M. M. El-Badry, The canadian society for civil engineering, 605-612.

ALEXANDER J.G.S. et CHENG J.J.R. (1996). Field application and studies of using CFRP sheets to strengthen concrete bridge Girders, Advanced composite materials in bridges and structures, M. M. El-Badry, The canadian society for civil engineering, 465-472.

AN, W., SAADATMANESH, H. et EHSANI, M.R. (1991). RC beams strengthened with FRP plates. II: Analysis and parametric study. Journal of Structural Engineering. 117, 3434-3455.

ARDUINI, M., D'AMBRISI, A. et Di TOMMASO, A. (1994). Shear failure of concrete beams reinforced with FRP plates. Infrastructure: New materials and methods of repair, Proceedings of the third materials engineering Conference; D. Basham,

ARDUINI, M., DI TOMMASO, A., MANFRONI et O. Nanni, A. (1996). Failure mechanisms of concrete beams reinforced with FRP flexible sheets. Advanced composite materials in bridges and structures, M. M. El-Badry, The canadian society for civil engineering, 253-260.

ATKINSON, C. et SMELSER, R.E. (1982). Combined mode fracture via the cracked Brazilian disk test, Int. J. Fract., 18, 279-291.

BANTHIA, N., YAN, C. et NANDAKUMAR, N. (1996). Sprayed fiber reinforced plastics (FRPs) for repair of concrete structures. Advanced composite materials in bridges and structures, M. M. El-Badry, The canadian society for civil engineering, 537-542.

BARTON, R. (1997). Carbon fibre``plate bonding``. Structural Survey, 15, 11-14.

BASUNBUL, I.A., AL-SULAIMANI, G.J. et BALUCH, M.H. (1990) Repaired reinforced concrete beams. ACI Materials Journal, 87, 348-354.

BAUMERT, M.E., GREEN, M.F. et ERKI, M.A.A., (1996). Review of low temperature response of reinforced concrete beams strengthened with FRP sheets. Advanced composite materials in bridges and structures, M. M. El-Badry, The canadian society for civil engineering, 565-572.

BEN CARDINO, F., SPADA, G. et SWAMY, R.N. (1998). Design to repair/up-grade RC structures: the key to a successful utilization of CFRP laminates. Sika Carbodur, Engineering Guidlines for the Use of Sika Carbodur (CFRP) Laminates for Structural Strengthening of Concrete Structures. Sika Canada Inc.

BHUTTA, S.A. (1993), Analytical modeling of hybride composite beams. MSc Thesis, Virginia Polytechnic Institute and State University, USA.

BHUTTA, S.A. et AL-QADI, I.L. (1994). Hybrid composite beams: Analytical modeling. Infrastructure: New materials and methods of repair, Proceedings of the third materials engineering conference, K Basham.

BHUTTA, S.A. et QADI, I.L. (1993). Using carbon fibre reinforced polymers to rehabiliate civil engineering structures: An review. Virginia Polytechnique Institute and State University, IIK7-IIK13, USA.

BISBY, L.A., GREEN, M.F., BEAUDOIN, Y. et LABOSSIERE, P. (2000). FRP plates and sheets bonded to reinforce concrete beams. Advanced composite materials

in bridges and structures, J.L. Humar, et A.G. Razagpur, The Canadian Society for Civil engineering, 209-216.

BIZINDAVYI, L., NEALE, K.W. (1999). Transfer lengths and bond strengths for composite bonded to concrete, Journal of composites for construction, 3, 153-160.

BONANCCI, J.F. (1996). Strength, failure mode and deformability of concrete beams strengthened externally with advanced composites, Advanced composite materials in bridges and structures, M. M. El-Badry, The canadian society for civil engineering, 419-426.

BONACCI, J.F. et MAALEJ, M. (2001). Behavioural trends of RC beams strengthened with externally bonded FRP. J. Composites for Construction, 5(2), 102-13.

BOYAJIAN, D.M., DAVALOS, J. F. et QIAO, P. (2000). Development of a test specimen for FRP-concrete mode I fracture, Advanced Composite Materials in Bridges and Structures, J. Humar et A.G. Razagpur, The Canadian Society for Civil Engineering, 445-452.

BROWN, J.H. (1972). Measuring the fracture toughness of cement paste and mortar.

Magazine of Concrete Research. 24,

BUYUKOZTURK, O. et HEARING, B. (1998). Failure behavior of precracked concrete beams retrofitted with FRP. J. composites for construction. 2(3), 138-144.

CAO, H.C. et EVANS, A.G. (1989). Experimental study of the fracture resistance of bimaterial interfaces. Mechanics of Materials, 295-304.

CHAJES, M.J., FINCH, W.W., JANUSKA, T.F. et THOMSON, T.A. (1996). Bond and force transfer of composite material plates bonded to concrete. ACI Structural Journal, 93, 208-217.

CHAJES, M.J., MERTA, D.R., THOMSON, JR T.A. et FARSHMAN, C.A. (1994). Durability of composite material reinforcement. Infrastructure: New materials and methods of repair, Proceedings of the third materials engineering conference, K. Basham,

CHAJES, M.J., THOMSON, T.A. et FARCHMAN, C.A. (1995). Durability of concrete beams externally reinforced with composite fabrics. Construction and Building Materials, 9, 141-148.

CHAJES, M.J., THOMSON, T.A., JANUSZKA, T.F. et FINCH, W.W. (1994).

Flexural strengthening of concrete beams using externally bonded composite materials. Construction and Building Materials, 8, 191-201.

CHARALAMBIDES, P.G., LUND, J., EVANS, A.G. et MCMEEKING, R.M. (1989). A test specimen for determining the fracture resistance of bimaterial interfaces. Journal of Applied Mechanics. 56, 77-82.

CHARBERT, A., LUYCKX, J., BASTIEN, J. et PICARD, A. (1996). The strengthening of structural concrete with an aramid woven fibre/epoxy resin composite. Advanced composite materials in bridges and structures, M. M. El-Badry, The canadian society for civil engineering, 443-448.

DEBLOIS, M., PICARD, A. et BEAULIEU, D. (1992). Renforcement de poutres en béton armé a l'aide de matériaux composites: études théorique et expérimentale. Advanced composite materials in bridges and structures, Labossiere et K.W. Neale,

DEMERS, M., HÉBERT, D., GAUTHIER, M. LABOSSIERE, P. et NEALE, K.W. (1996), The strengthening of structural concrete with an aramid woven fibre/epoxy resin composite. Advanced composite materials in bridges and structures, M. M. El-Badry, The canadian society for civil engineering, 435-442.

DIMAS J.V., EHSANI, M.R. et SAADATMANESH, H. (1996). Strengthening of R/C beams in a nuclear power plant. Advanced composite materials in bridges and structures, M.M. El-Badry, The canadian society for civil engineering, 613-620.

DJELAL, C., DAVID, E. et BUYLE-BODIN, F. (1996). Utilisation de plaque en composite pour la reparation de poutres en béton armé endomaggées, Advanced composite materials in bridges and structures. M.M. El-Badry, The canadian society for civil engineering, 581-588.

DUNDURS, A.H. (1965). A crack between dissimilar media. Journal of Applied Mechanics Trans. ASME, 32:400-402.

EL-ATTAR et EL-BAR, A. (1994). Flexural response of FRP reinforced concrete strucures. Infrastructure: New materials and methods of repair, Proceedings of the third materials engineering conference, K. Basham, 583-591.

EVANS, A.G. et HUTCHINSON, J.W. Effects of non-planarity of the mixed mode fracture resistance of bimaterial interfaces. Acta Metall., 37.

FANNING P.J. et KELLY, O. (2001). Ultimate response of RC beams strengthened with CFRP plates. J. composites for Construction, 5, 122-127.

GEMERT, D.V. Force transfer in epoxy bonded steel/concrete joint. International Journal of Adhesion and Adhesives, 1, 67-72.

GHANI RAZAGHPOUR A. et MIR MAZHER A. (1996). Ductility and strength of concrete beams externally reinforced with CFRP sheets. Advanced composite materials in bridges and structures, M.M. El-Badry. The canadian society for civil

engineers, 505-518.

GRACE, N.F., SAYED, G.A., SOLIMQAN, A.K. et SALEH, K.R. (1999) Strengthening reinforced concrete beams using fiber reinforced polymer (FRP) laminates, ACI Struct. J., 96, 865-875.

HAMOUSH, S.A. et AHMED, S.H. (1990). Debonding of steel plate-strengthened concrete beams. J. of Struct. Engng., 116, 356-371.

HOA, S.V., XIE, M. et XIAO, X.R. (1996). Repair of steel reinforced concrete with carbon/epoxy composites, Advanced composite materials in bridges and structures, M. M. El-Badry, The canadian society for civil engineers. 573-580.

HUSSAIN, M., SHARIF, A.M., BASUNBUL, I.A., BALUCH, M.H. et AL. SULAIMANI, J. (1995), Flexural behavior of precracked reinforced concrete beams strengthened externally by steel plates. ACI Structural Journal, 28, 14-22.

HUTCHINSON, A.R. et RAHIMI, H. (1993). Behavior of reinforced concrete beams externally bonded fibre reinforced plastics. Proc. 5th Int. Conf. on Structural faults and repair, M.C. Ford, Engineering Technics Press.

HUTCHINSON, A.R. et RAHIMI, H. (1996). Flexural strengthening of concrete

beams with externally bonded FRP reinforcement. Advanced composite materials in bridges and structures, M. M. El-Badry, The canadian society for civil engineers.

ISIS CANADA, (2000), Strengthening reinforced concrete structures with externally-bonded fiber reinforced polymers, ISIS CANADA.

KAMEL, A.S., ELWI, A.E. et CHENG, J.J.R., (2000), Experimental study on the behavior of CFRP sheets bonded to concrete, Advanced Composite Materials in Bridges and Structures, J. Humar et A.G. Razagpur, The Canadian Society for Civil Engineering, 61-68.

KARBHARI, V.M. et ENGINEER, M. (1996). Investigation of bond between concrete and composite, use of a peel test, J. reinforced plastics and composites, 15, 208-227.

KARBHARI, V.M. et SEIBLE, F. (2000), Fiber reinforced composites-Advanced material for renewal of civil infrastructure, Applied Composite Materials, 7, 95-124.

JOHNSON, R.P., TAIT C.J. et TAIT, C.J. (1981). The strength in combined bending and tension of concrete beams with externally bonded reinforcing plates. Building and Environment. 16, 287-298.

JONES, R., SWAMY, R.N. et ANG, T.H. (1982). Under- and over-reinforced concrete beams with glued steel plates. International Journal of Cement Composite and Light Weight Concrete. 1, 19-32.

JONES, R., SWAMY, R.N. et CHARIF, A. (1988). Plate separation and anchorage of reinforced concrete beams strengthened by epoxy-bonded steel plates. The Structural Engineer. 66,

KARAM, G. N. (1992). Optimal design for prestressing with FRP sheets in structural members. Advanced composite materials in bridges and structures, K.W. Neale et P. Labossiere,

KARBHARI, V.M. (1997). On the use of composites for bridge strengthening and rehabiliation-Manufacturing and durability. Practical solutions for bridge strengthening and rehabiliation, BSAR II, Kansas City, USA.

KARBHARI, V.M. et ENGINEER, M. (1995). Assessment of interfacial fracture energy between concrete and glass reinforced composites. Journal of Materials Science Letters, 14, 1210-1213.

KARBHARI, V.M., ENGINEER, M., (1996). Investigation of bond between concrete and composite: Use of a peel test. Journal of Reinforced Plastics and Composites, 15, 208-227.

LANE, J.S., LEEMING, M.B., DARBY, J.J. et LUCKE, P.S. (1998). Field testing of 18m post-tensioned concrete beams strengthened with CFRP plates. Sika Carbodur, Engineering Guidlines for the Use of Sika Carbodur(CFRP) Laminates for Structural Strengthening of Concrete Structures. Sika Canada Inc.

LEE, K.M. et BUYUKOZTURK. O. (1992). Fracture analysis of mortar-aggregate interfaces in concrete. J. Engng Mechanics., 118, 2031-2046.

LEE, Y.J., BOOTHBY, T.E., BAKIS, C.E. et NANNI, A. (1999). Slip modulus of FRP sheets bonded to concrete, J. Composites for construction, 3(4), 161-167.

LEUNG, C.K.Y. (2001). Delamination failure in concrete beams retrofitted with a bonded plate. J. Mat. Civil Engng., 13(2), 106-113.

LIECHTI, K.M. (1990). Fracture testing and failure analysis, Testing and analysis. Adhesives and sealants. Engineering materials handbook. 3. ASM International.

LIECHTI, K.M. et KNAUSS, W.G. (1982). Crack propagation at material interfaces: II experiments on mode interaction. Experimental Mechanics, 383-391.

LIMBERGER, E. et VIELHABER, J. (1996). Experimental investigations on the behavior of CFRP-prepreg strengthened structural RC elements. Advanced composite

materials in bridges and structures, M. M. El-Badry, The canadian society for civil engineers, 597-604.

MALEK, A.M., SAADATMANESH, H., EHSANI, M.R., (1996). Shear and normal stress concenterations in RC beams strengthened with FRP plates. Advanced composite materials in bridges and structures, M. M. El-Badry, The canadian society for civil engineers, 629-637.

MALICK, P.K. (1993). Fiber reinforced composites materials : Manufacturing and design. Marcel Dekker.

MCDONALD, M.D. et CALDER, A.J.J. (1982). Bonded steel plating for strengthening concrete structures. Int. J. Adhesionn and Adhesives. 119-127.

MC KENNA, J.K. et ERKI, M.A. (1994). Strengthening of reinforced concrete flexural members using externally applied steel plates and fibre composite sheets- a survey. Canadian Journal of Civil Engineering, 21, 16-24.

MEIER, U., KAISER, H. (1981). Strengthening of structure with CFRP laminates. Advanced composite materials in Civil Engineering structures, Proceedings of ASCE specialty Conference , Iyer L. and Sen R., American Society of Civil Engineers.

MEIER, U. et KAISER, H. (1991). Strengthening of structures with CFRP laminates. Proceedings of the specialty conference on advanced composites materials in civil engineering structures, 224-232.

MEIER, U. (1992). Carbon fibre-reinforced polymers: Modern materials in bridge engineering. Structural Engineering International, 1, 7-12.

MEIER, U. (1998). Developement of composite strip bonding technique for the post-strengtheing of structure. Sika Carbodur, Engineering Guidlines for the Use of Sika Carbodur (CFRP) Laminates for Structural Strengthening of Concrete Structures. Sika Canada.

MEIER, U. (2000). Composite materials in bridges repair. Applied Composite Materials, 7, 75-94.

MEIER, U., DEURING, M., MEIER, H. et SCHWEGLER, G. (1992). Strengthening of structures with CFRP laminates: Research and applications in Switzerland. Advanced composite materials in bridges and structures, K. W Neale. and P. Labossiere, The canadian society for civil engineers, Quebec, Canada.

MUKHOPADHYAYA, P. et SWAMY, N. (2001). Interface shear stress: A new design criterion for plate debonding. J. composite Const., 5, 35-43.

NAKABA, K., KANAKUBO, T., FURUTA, T. et YOUSHIZAWA, H. (2001). Bond behaviour between fibre reinforced polymer laminates and concrete, ACI structural Journal, 98, 359-367.

NANNI, A. (1993). FRP- Reoinforced plastic(FRP) Reinforcement for Concrete Structures. Properties and Application, A. NANNI, Elsvier.

NEUBAVER, U. et ROSTASY, F.S. (1997). Design aspects of concrete structures strengthened with externally bonded CFRP-plates, Structural faults and repair, 2, 109-118.

NEWMAN, K. et NEWMAN, J.B. (1969). Failure theories and design creteria for plain concrete. Structure, solid mechanics and engineering design. Proceeding of civil engineering materials conference, part1&2, Southampton.

NITEREKA, C. et NEALE, K.W. (1999). Analysis of reinforced concrete beams strengthened in flexure with composite laminates. Can. J. Civ. Engng., 26 , 646-54.

NGUYEN, D.N., CHAN, T.K. et CHEONG, H.K. (2001). Brittle failure and bond development length of CFRP-concrete beams. J. of composites for construction, 5(1), 12-17.

OEHLERS, D.J. (1988). Reinforced concrete beams with steel plates glued to their soffits; prevention of plate separation induced by flexural peeling. Report. Departement of Civil Engineering, The University of Adelide, Australia.

OEHLERS, D.J. et MORAN, J.P. (1990). Premature failure of externally plated reinforced concrete beams. J. Struct. Engng., 116, 978-995.

OJDROVIC, R.P. et PETROSKI, H.J. (1987). Fracture behavior of notched concrete cylinder. J. Engng. Mechanics, 113, 551-1564.

PICARD, A., MASSICOTTE, B. et BOUCHER, E. (1995). Strengthening of reinforced concrete beams with composite materials: theoretical study. Composite Structures. 31, 63-75.

PILLAI, S.U. et KIRK, D.W. (1983). Reinforced concrete design in Canada. Mc Graw-Hill, Ryerson Ltd.

RAHMAN, A.H. et TAYLOR, D.A. (1992). Deflections of FRP-reinforced slabs: A finite element study. Advanced composite materials in bridges and structures; K.W. Neale et P. Labossiere, Sherbrook, Quebec, Canada.

RAZAGPUR, A.G., ALI, MM. (1996), Ductility and strength of concrete beams externally reinforced with CFRP sheets. Advanced composite materials in bridges and structures, 505-512.

RICE, J.R. (1988). Elastic fracture concepts for interfacial cracks. J. Applied Mechanics Trans. 55, 98-103.

RITCHIE, P.A., THOMAS, D.A., LU, L. et CONNELLY, G.M. (1991). External reinforcement of concrete beams using fibre reinforced plastics. ACI Struct. J., 88, 490-500.

ROBERTS, T.M., HAJI-KAZEMI, H. (1989). Theoretical study of the behavior of reinforced concrete beams strengthened by externally bonded steel plates. Proc. Instn. Engrs, Part 2. 87, 651-663.

ROSS, C.A., JEROME, D.M., TEDESCO, J.W. et HUGHES M.L., (1999), Strengthening of reinforced concrete beams with externally bonded composite laminates. ACI Struct. J. 96(2), 212-220.

ROSTASY, F.S., HANKERS, C. et RANISCH, E.H. (1992). Strengthening of R/C and P/C structures with bonded FRP plates. Advanced composite materials in bridges and structures, K. W. Neale. and P. Labossiere, Canada.

ROSTASY, F.S. (1993). Strengthening of R/C and P/C structures with bonded steel and FRP plates, Proc. 5th Int. Conf. on Structural Faults and Repair, 2, Engineering Technics Press, 217-224.

SAADATMANESH, H. et EHSANI, M.R. (1990). Fibre composite plates can strengthen beams. Concrete International. 65-71.

SAADATMANESH, H. et EHSANI, M.R. (1991). RC beams strengthened with GFRP plates. I: Experimental study. J. Struct. Engng. 117, 3417-3433.

SAADATMANESH, H. et Malek, A.M. (1998). Design guidelines for flexural strengthening of RC beams with FRP plates. J. composites for construction, 2

SATO, Y., UEDA, T. et KAKUTA, Y. (1996). Shear reinforcing effect of carbon fibre sheet attached to side of reinforced concrete beams, Advanced composite materials in bridges and structures, M. M. El-Badry, The canadian society for civil engineers, 621-628.

SCHMUESER, D.W., (1990). Engineering materials handbook, testing and analysis. Adhesive and sealants. Evaluating test geometries. Engineering materials Handbook, 13. ASM International.

SHAH, S. P., SWARTZ, S. E. et OUYANG, C. (1995), Fracture mechanics of concrete: Applications of fracture mechanics to concrete, rock and other quasi-brittle materials, John Wiley & Sons, Inc.

SHARIF, A., AL-SULAIMANI, G.J., BASUNBUL, I.A., BALUCH, M.H. et GHALEB, B.N. (1994). Strengthening of initially loaded reinforced concrete beams using FRP plates. ACI Struct. J. 91, 160-168.

SHARPE, L.H. (1990). Adhesive and sealants. Fundamentals of adhesive and sealant technology overview, Adhesive technology. Engng. materials handbook. 3, ASME International.

SIERAKOWSKI, R.L., ROSS, C.A., TEDESCO, J.W. et HUGHES, M.L. (1994). Concrete beams with externally bonded carbon fibre reinforced plastic (CFRP) strips Infrastructure: New materials and methods of repair, Proceedings of the third materials engineering conference, K. Basham.

SIKA CANADA INC. (1998). Sika Carbodur, Engng. guidelines for the use of CarboDur (CFRP) laminates for structural strengthening, first edition.

SINGH, D. et SHETTY, D.K. (1989). Fracture toughness of Polycrystalline ceramics in combined mode I and mode II loading, J. American Society, 72, 78-84.

SPADEA, G., BENCARDINO, F. et SWAMY, R.N., (1998), Structural behavior of composite RC beams with externally bonded CFRP. J. Composites Construction, 2(3), 132-137.

SPADEA, G., BENCARDINO, F. SWAMY, R.N. et MUKHOPADHYAYA, P. (2000). Design against premature debonding and brittle behavior the key to structural integrity with FRP bonded structural strengthening, Advanced composite materials in bridges and structures, J. L. Humar et A. G. Razagpur, 15-18.

STEINER, W. (1996). Strengthening of structures with CFRP strips, Advanced composite materials in bridges and structures. Advanced composite materials in bridges and structures, M. M. El-Badry, The canadian society for civil engineers. 407-417.

SUO, Z. et HUTCHINSON, J.W. (1989). Sandwich test specimen for measuring interface crack toughness. Material Science and Engineering, A107, 135-143.

SWAMY, R.N., JONES, R. et CHARIF, A. (1989). The effect of external plate reinforcement on the strengthening of structurally damaged RC beams. The Structural Engineer. 67. 45-56.

SWAMY, R.N., JONES, R. et BLOXHAM, J.W., (1987). Structural behavior of reinforced concrete beams strengthened by epoxy-bonded steel plates. The Structural Engineers. 65. 59-68.

SWAMY. R.N., LYNSDALE C.J., MUKHOPADHYAYA, P. (1996). Effective strengthening with ductility: use of externally bonded plates of non-metallic composite materials. Advanced composite materials in bridges and structures, M. M. El-Badry, The canadian society for civil engineers. 481-488.

TADA, H., PARIS, P.C. et IRWIN, G.R. (2000). The stress analysis of cracks handbook, The American Society of Mechanical Engineers.

TALJSTEN, B., Strengthening of concrete structures with CFRP-sheets applications and full scale tests in Sweden. (2000). Advanced composite materials in bridges and structures, J. Humar et A.G. Razaghpur, 513-520.

TASNON, M., MISSIHOM, M. et GÉRIN-LAJOIE, G. (1996). Restoration of building facades with composite materials. Advanced composite materials in bridges and structures, M. M. El-Badry, The canadian society for civil engineers, 589-596.

TENG, J.G., LAM, L., CHAN, W. et WANG, J. (2000). Retrofitting of deficient RC cantilever slabs using GFRP strips. J. composites for construction, 4(2), 75-84.

TRIANTAFILLO, T.C., DESKOVIC, N. et DEURING, M. (1992). Strengthening of concrete structures with prestresses fibre reinforced plastic sheets. ACI Structural Journal, 89, 235-244.

TRIANTAFILLOU, T.C. et DESKOVIC, N. (1991). Innovative prestressing with FRP sheets: Mechanics of short-term behavior. Journal of Engineering Mechanics, 117, 1652-1672.

TRIANTAFILLOU, T.C. et PLEVRIS, N. (1981) Post-strengthening of R/C beams with epoxy- bonded fibre composite materials. L Iyer. and N. Sen, Advanced composite materials in civil engineering structures, American Society of Civil Engineers.

TRIANTAFILLOU, T.C. et PLEVRIS, N. (1992). Strengthening of RC beams with epoxy-bonded fibre-composite materials. Materials and Structures. 25, 201-211.

TRIPI, J.M., BAKIS, C.E., BOOTHBY T.E. et NANNI, A. (2000). Deformation in concrete with external CFRP sheet reinforcement. J. composites for construction, 4(2), 85-94.

VARASTEHPOUR, H. et HAMELIN, P. (1996). Experimental study of RC beams strengthened with CFRP plate. Advanced composite materials in bridges and structures, M. M. El-Badry, The canadian society for civil engineers, 555-563.

WALSER, R. et STEINER, W. (1998). Strengthening a bridge with advanced materials. Sika Carbodur, Engineering Guidlines for the Use of Sika Carbodur (CFRP) Laminates for Structural Strengthening of Concrete Structures, Sika Canada Inc.

WANG, J.S. et SUO, Z. (1990). Experimental determination of interfacial toughness curves using Brazil-Nut sandwiches. Acta Metall. Mater. 38, 279-290.

WEIMER, C., HAUPERT, F. (2000). Influence of aggregate structure on mode III interfacial fracture between concrete and CFRP, Applied composite materials, 7,183-193.

WIGHT, R.G., GREEN, M.F. et ERKI, M.A. (1996). Wight R. G., Green M. F. and Erki M. A. Post-strengthening prestresses concrete beams with prestressed FRP sheets. Advanced composite materials in bridges and structures, M. M. El-Badry, The canadian society for civil engineers. 449-456.

ZIRABA, Y.N., BALUCH, M.H., BASUNBUL, I.A., SHARIF, A.M., AZAD, A.K. et AL-SULAIMANI, J. (1994). Guidlines toward the design of reinforced concrete beams with external plates, ACI Structural Journal, 91,